REPORT ITU-R BO.2071

System parameters of BSS between 17.3 GHz and 42.5 GHz and associated feeder links

(2006)

1 Introduction

Working Party 6S has identified the need to assemble system parameters and system characteristics for the BSS bands between 17.3 GHz and 42.5 GHz and associated feeder links. For that purpose, a Report had been developed on the basis of inputs to ITU-R. An example of the parameters is shown as follows:

a) Service requirements
   – service description, service objective, service availability, bit rate, etc.

b) Feeder-link parameters
   – feeder-link frequency, earth station e.i.r.p., feeder-link transmitting parameters, etc.

c) Modulation, link parameters
   – bandwidth, modulation, coding, polarization, sharing criteria, etc.

d) Satellite parameters
   – satellite e.i.r.p. (pfd), transmitting antenna pattern, etc.

e) Receiver parameters
   – receiving antenna diameter, antenna pattern, etc.

Further contributions are invited for future updates of this Report, which may eventually serve in establishing system parameters of BSS services operating above 17 GHz, including the associated feeder links.

Note that for the specific problem of rain mitigation techniques in the noted bands, WP 6S developed Recommendation ITU-R BO.1659 – Mitigation techniques for rain attenuation for BSS systems in frequency bands between 17.3 GHz and 42.5 GHz.

The BSS systems in the frequency bands between 17.3 GHz to 42.5 GHz have the possibility to deliver wideband RF digital multiprogramme services, which may consist of SDTV, HDTV, audio and data programmes. In addition, it is also possible to implement interactive multimedia and on-demand services. To facilitate the introduction of BSS in the bands, WP 6S/RG 9 was established to carry out studies on applicable technologies to improve service availability against rain attenuation, and on outlining necessary BSS system characteristics.

In the Radio Regulations, the band 17.3-17.8 GHz in Region 2 and the band 21.4-22.0 GHz in Regions 1 and 3 are allocated to BSS as of 1 April 2007.

Appendix 1 to Annex 1 to this Report contains examples of system parameters of BSS systems and their associated feeder links in frequency bands 17.3-17.8 GHz and 24.75-25.25 GHz, which are allocated for BSS feeder links in Region 2.

The system parameters given in Table 1 are based on information supplied by Canada in accordance with Appendix 4 of the Radio Regulations (RR). The system parameters given in Table 2 are based on information supplied by the United States of America. Using the system parameters provided in Table 1 and information provided in ETSI DVB-S.1 standard (version EN 301 210 V1.1.1) as the minimum satellite system link performance requirements, Appendix 2 to Annex 1 contains a study on the impact of satellite separation on system performance of typical BSS systems. Utilizing the same methodology as provided in Appendix 2, Appendix 3 to Annex 1 re-examines the impact of satellite separation on system performance for BSS systems using information provided in ETSI DVB-S.2 standard (version EN 302 307 V1.1.1). However, it should be noted that it was assumed in these studies that the downlink and uplink e.i.r.p.s (of both the wanted and interfering networks) were scaled with the *C*/*N* threshold for the type of modulation used regardless of whether the capability exists for both networks. This has simply been done for comparison purposes to illustrate the effect of the type of modulation employed. The actual Appendix 4 of the RR data filed for each network and Article 21 pfd limits will ultimately determine the maximum downlink e.i.r.p. regardless of the *C*/*N* threshold for the type of modulation used. The feasibility of using higher order modulation techniques (e.g. higher than 8-PSK) over satellite links remains to be proven in practice.

Annex 2 to this Report shows study results for 21 GHz band broadcasting satellites based on input documents to WP 6S. Measured downlink receiving earth station antenna patterns are shown in § 2. Some examples of BSS systems utilizing the locally-variable e.i.r.p. systems in the 21 GHz band are introduced in § 3.

In § 4, a study of antenna radiation pattern of a variable e.i.r.p. broadcasting-satellite system in the 21 GHz band is described. Section 5 shows a study result of interference from the locally variable e.i.r.p. satellite systems into a conventional satellite system. Section 6 deals with methodology to evaluate unwanted emission from 21 GHz band BSS. Finally, a transmission scheme utilizing the receiver with a storage function is described in § 7.

Annex 1

System parameters of unplanned BSS systems and associated feeder links in frequency bands 17.3-17.8 GHz and 24.75-25.25 GHz

Appendix 1 to Annex 1

Examples of system parameters of unplanned BSS systems and associated feeder links in frequency bands 17.3-17.8 GHz and 24.75-25.25 GHz

Table 1 contains an example summary of the Canadian coordination information submitted to BR (CAN-BSS-95). The system plans to provide TV broadcasting and interactive multimedia services. Furthermore, coordination information submitted by another Region 2 country for providing broadcast services is included in the third column, titled “Other”, of the Table.

TABLE 1

System characteristics

		CAN-BSS-95	Other
Orbit		GEO	GEO
Position		95.0° W	101.0° W
Frequency	Uplink	24.75-25.25 GHz	24.75-25.25 GHz
	Downlink	17.3-17.8 GHz	17.3-17.8 GHz
Broadcast			
Coverage		North America	North America
Assigned channel bandwidth		25 MHz	25-500 MHz
Uplink			
Satellite receive antenna gain		35 dBi	49.4 dBi
E.S. transmit antenna size		5.6 m, 3.5 m	5-13 m
E.S. transmit antenna gain (maximum)		61.1 dBi, 57.0 dBi	60.5-68.8 dBi
Receiving satellite system noise temperature		730 K	810 K
E.S. transmit antenna pattern		AP 4 A, B, C, D, φ parameters: 29, 25, 32, 25, 7°	Rec. ITU-R S.465
Polarization		Circular left	Circular left
Maximum power supplied to the input of E.S. transmitting antenna		22.2 dBW	21.2-29.5 dBW
Downlink			
Satellite transmit antenna gain		35 dBi	49.4 dBi
E.S. receive antenna size		0.45-1.4 m	0.45-1.2 m
E.S. receive antenna gain		36.1-46.0 dBi	36.5-45.0 dBi
Polarization		Circular right	Circular right
E.S. receive noise temperature		170 K	140 K
E.S. receive antenna pattern		(see Attachment 1 to Appendix 1)	Rec. ITU-R S.465
Maximum power supplied to the input of satellite transmitting antenna		22.2 dBW	14.8-19.1 dBW
E_b/N_0		6.5 dB	No info.
C/N threshold		6.6 dB	No info.
Required C/N (clear-sky)		9.0 dB	Uplink 17.4 dB, Downlink 6-17.6 dB
Multimedia (CAN-BSS-95 only)			
Forward link			
Coverage		Visible earth	
Channel bandwidth		25 MHz	
Uplink			
Satellite receive antenna gain		44.5 dBi	
E.S. transmit antenna size		5.6 m, 3.5 m	

TABLE 1 (*continued*)

	CAN-BSS-95	Other
E.S. transmit antenna gain (maximum)	61.1 dBi, 57.0 dBi	
Receiving satellite system noise temperature	730 K	
E.S. transmit antenna pattern	AP 4 A, B, C, D, φ parameters: 29, 25, 32, 25, 7°	
Polarization	Circular left	
Maximum power supplied to the input of E.S. transmitting antenna	18.0 dBW	
Downlink		
Satellite transmit antenna gain	44.5 dBi	
E.S. receive antenna size	0.45-1.4 m	
E.S. receive antenna gain	36.1-46.0 dBi	
Polarization	Circular right	
E.S. receive noise temperature	170 K	
E.S. receive antenna pattern	(see Attachment 1 to Appendix 1)	
Maximum power supplied to the input of satellite transmitting antenna	21.0 dBW	
E_b/N_0	6.5 dB	
C/N threshold	6.6 dB	
Required C/N (clear-sky)	11.0 dB	
Return link		
Coverage	Visible earth	
Channel bandwidth	55 MHz, 113 MHz	
Uplink		
Satellite receive antenna gain	44.5 dBi	
E.S. transmit antenna size	0.45-1.4 m	
E.S. transmit antenna gain (max)	39.2-49.1 dBi	
Receiving satellite system noise temperature	730 K	
E.S. transmit antenna pattern	Rec. ITU-R S.465	
Uplink polarization	Circular left, circular right	
Maximum power supplied to the input of E.S. transmitting antenna	36.4 dBW, 39.7 MHz	
Downlink		
Satellite transmit antenna gain	44.5 dBi	
E.S. receive antenna size	5.6 m, 3.5 m	
E.S. receive antenna gain	58.0 dBi, 54 dBi	
Downlink polarization	Circular right, circular left	
E.S. receive noise temperature	185 K	
E.S. receive antenna pattern	AP 4 A, B, C, D, φ parameters: 29, 25, 32, 25, 7°	
Maximum power supplied to the input of satellite transmitting antenna	21.2 dBW	

TABLE 1 (*end*)

	CAN-BSS-95	**Other**
E_b/N_0	6.5 dB	
C/*N* threshold	6.6 dB	
Required *C*/*N* (clear-sky)	10.0 dB	

Table 2 contains parameters of another example system that could operate in the 17.3-17.8 GHz and 24.75-25.25 GHz bands. The system has a reconfigurable "bent-pipe" payload capable of providing TV broadcasting services using fixed beams over North and South America, respectively, or a steerable beam over North America.

TABLE 2

Additional system characteristics

		HDBSS-A (NAF)	**HDBSS-A (SAF)**	**HDBSS-A (NAS)**
Orbit		GEO	GEO	GEO
Position		67.5° W	67.5° W	67.5° W
Frequency	Uplink	24.75-25.25 GHz	24.75-25.25 GHz	24.75-25.25 GHz
	Downlink	17.3-17.8 GHz	17.3-17.8 GHz	17.3-17.8 GHz
Coverage		North America	South America	North America
Assigned channel bandwidth		24 MHz	24 MHz	48 MHz
Uplink				
Satellite receive antenna gain		37 dBi	34.2 dBi	46.1 dBi
E.S. transmit antenna size		6-11 m	6-11 m	6-11 m
E.S. transmit antenna gain (maximum)		61.1-67 dBi	61.1-67 dBi	61.1-67 dBi
Receiving satellite system noise temperature		815 K	815 K	865 K
E.S. transmit antenna pattern		Rec. ITU-R S.465	Rec. ITU-R S.465	Rec. ITU-R S.465
Polarization		Circular left/ circular right	Circular left	Circular left
Maximum power supplied to the input of E.S. transmitting antenna		13.5-20 dBW	13.5-20 dBW	13.5-20 dBW
Downlink				
Satellite transmit antenna gain		34.5 dBi	30.9 dBi	46.1 dBi
E.S. receive antenna size		0.45-1.8 m	0.45-1.8 m	0.45-1.8 m
E.S. receive antenna gain		36.1-48.1 dBi	36.1-48.1 dBi	36.1-63.9 dBi
Polarization		Circular right circular left	Circular right	Circular right

TABLE 2 (*end*)

	HDBSS-A (NAF)	HDBSS-A (SAF)	HDBSS-A (NAS)
E.S. typical G/T	12.3-24.3 dB/K	12.3-24.3 dB/K	12.3-24.3 dB/K
E.S. receive antenna pattern (For off axis angles up to 20°)	Rec. ITU-R S.465 Rec. ITU-R S.580	Rec. ITU-R S.465 Rec. ITU-R S.580	Rec. ITU-R S.465 Rec. ITU-R S.580
Maximum power supplied to the input of satellite transmitting antenna	21.1 dBW, 23.7 dBW	21.1 dBW, 23.7 dBW	18.6 dBW
E_b/N_0	2.9 dB	2.9 dB	4.9 dB
C/N threshold	4.1 dB	4.1 dB	8.9 dB
Required C/N (clear-sky)	5.6 dB	5.6 dB	10.4 dB

Attachment 1 to Appendix 1

Reference receiving antenna pattern

Antenna pattern:

$$G_{co}(\varphi) = G_{max} = 2.5 \times 10^{-3}\left(\frac{D}{\lambda}\varphi\right)^2 \quad \text{for } 0 \le \varphi < \varphi_m \quad \text{where } \varphi_m = \frac{\lambda}{D}\sqrt{\frac{G_{max} - G_1}{0.0025}}$$

$$G_{co}(\varphi) = G_1 = 29 - 25\log_{10}\varphi_r \quad \text{for } \varphi_m \le \varphi < \varphi_r \quad \text{where } \varphi_r = 95\frac{\lambda}{D}$$

$$G_{co}(\varphi) = 29 - 25\log_{10}\varphi \quad \text{for } \varphi_r \le \varphi < 7°$$

$$G_{co}(\varphi) = 7.9 \text{ dBi} \quad \text{for } 7° \le \varphi < 9.2°$$

$$G_{co}(\varphi) = 32 - 25\log_{10}\varphi \quad \text{for } 9.2° \le \varphi < 48°$$

$$G_{co}(\varphi) = -10 \text{ dBi} \quad \text{for } 48° \le \varphi < 180°$$

where:

G_{co}: co-polar gain (dBi)

G_{max}: maximum isotropic gain of the antenna (dBi)

φ: off-axis angle (degrees)

D antenna diameter (m)

λ: wavelength (m).

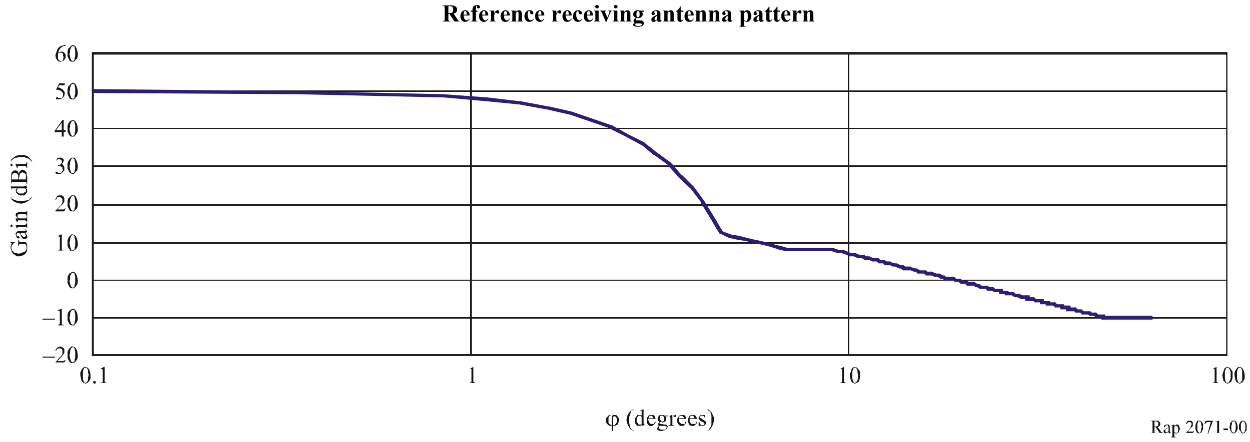

Appendix 2
to Annex 1

A study of orbital separation requirements for the unplanned BSS and associated feeder links in frequency bands 17.3-17.8 GHz and 24.75-25.25 GHz

1 Introduction

This Appendix examines the impact of satellite separation (intersystem interference) on system performance of typical BSS systems operating in frequency bands 17.3-17.8 GHz and 24.75-25.25 GHz.

2 Methodology

The system performance is represented by the system margin, which is defined as:

$$\text{System margin} = \left(\frac{C}{N+I}\right)_{system,faded} - \left(\frac{C}{N}\right)_{threshold}$$

where:

$\left(\frac{C}{N+I}\right)_{system,faded}$: overall system $\left(\frac{C}{N+I}\right)$ with uplink availability of 99.95% of the year and the downlink availability of 99.8% of the year

$$\left(\frac{C}{N}\right)_{threshold} = \frac{E_b}{N_0} + 10\log\left(\frac{R_b}{BW}\right)$$

$$= \frac{E_b}{N_0} + 10\log\left(\frac{BW \cdot ML \cdot FEC \cdot RS}{BW \cdot BWF}\right)$$

$$= \frac{E_b}{N_0} + 10\log\left(\frac{ML \cdot FEC \cdot RS}{BWF}\right)$$

and

R_b: bit rate (Mbit/s)

BW: channel bandwidth (MHz)

ML: modulation level, e.g. 2 for QPSK and 3 for 8-PSK

FEC: FEC rate

RS: Reed-Solomon coding rate

BWF: bandwidth shaping factor (roll-off factor).

The analysis was performed for two types of interfering systems: homogeneous and inhomogeneous. For the inhomogeneous case, interfering systems with different modulation schemes from the wanted system were examined. Both QPSK and 8-PSK modulation schemes were examined using different FEC rates in order to assess the sensitivity of the satellite separation requirements on these parameters.

2.1 Assumptions

The system characteristics used in the analysis are listed in Attachment 1 to Appendix 2. They are largely based on the attachment to Annex 11 of the March 2003 WP 6S Chairman's Report. The analysis was carried out on the following assumptions:

a) The interfering satellites are located with equal spacing on both sides of the wanted satellite. Both first and second adjacent interfering satellites were assumed. Co-coverage is assumed for wanted and interfering satellites.

b) Recommendation ITU-R P.618-8 was used to calculate propagation attenuation. The uplink availability is assumed to be 99.95% of the year and the downlink availability is assumed to be 99.8% of the year; this results in an overall system availability of 99.75% of the year.

c) Recommendation ITU-R BO.1212 was used to calculate the total interference.

d) The receiving earth station is located in rain climatic zone "M". (Rain rate = 72.4 mm/h exceeded for 0.01% of the average year.)

e) The wanted and interfering uplink earth stations were assumed to be in the same location, as this represents the worst-case scenario.

f) The minimum required link performance is obtained from ETSI standard EN 301 210 V1.1.1. (DVB; Framing structure, channel coding and modulation for DSNG and other contribution applications by satellite.)[1]

[1] It is noted that ETSI standard EN 301 210 V.1.1.1 will be updated in the near future. Pending on the updated values, the results presented in this document might be changed.

3 Results

3.1 Homogeneous model for interfering system based on wanted system

Case 1: using QPSK modulation

Analysis was performed to examine the relationship between system performance and satellite spacing for one pair and two pairs of interfering satellites. It is assumed that an FEC rate of 3/4 is used. The results of the analysis are shown in Fig. 1.

FIGURE 1

System margin vs. satellite spacing for system using QPSK

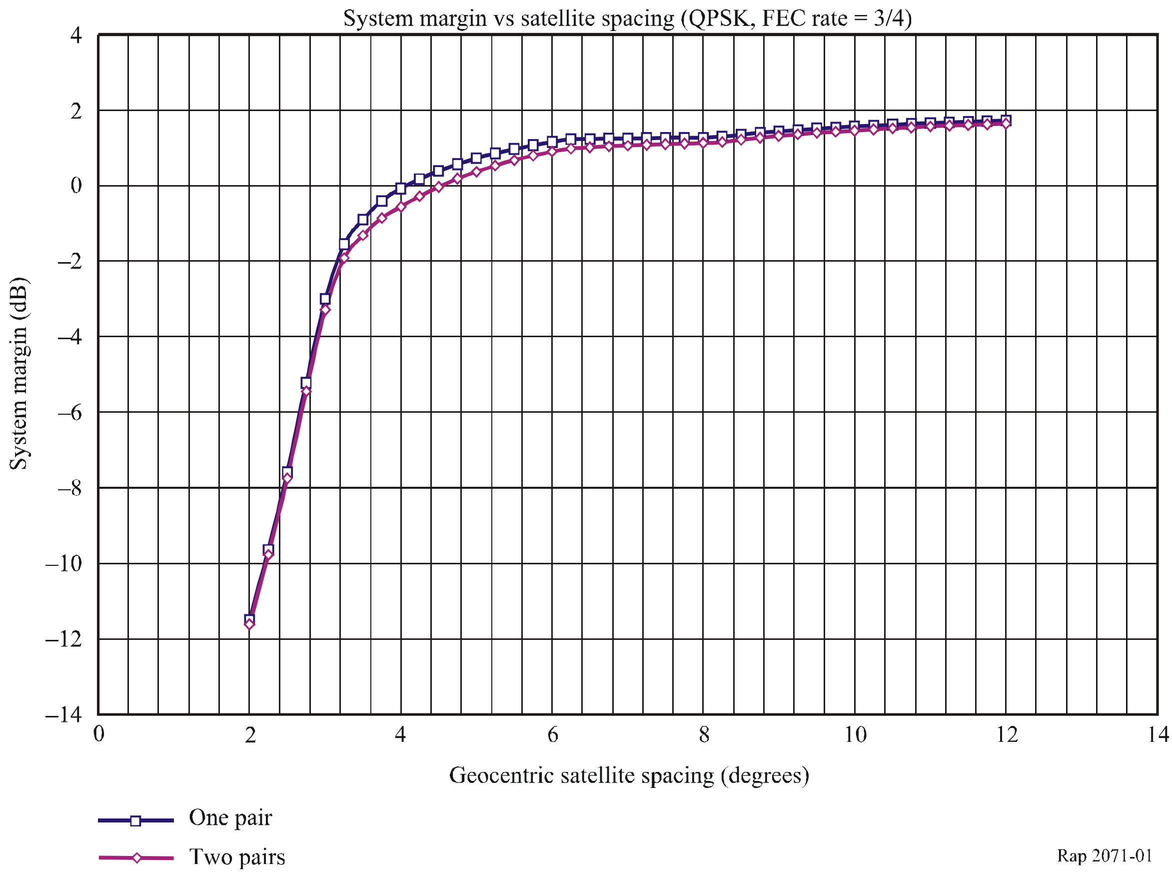

In order to study the effect of FEC rate on the system performance, an analysis was performed to determine the relationship between system margin and satellite spacing for systems with various FEC rates. Figure 2 shows the analysis results, which are based on two pairs of interfering satellites.

FIGURE 2

System margin vs. satellite spacing for various FEC rates

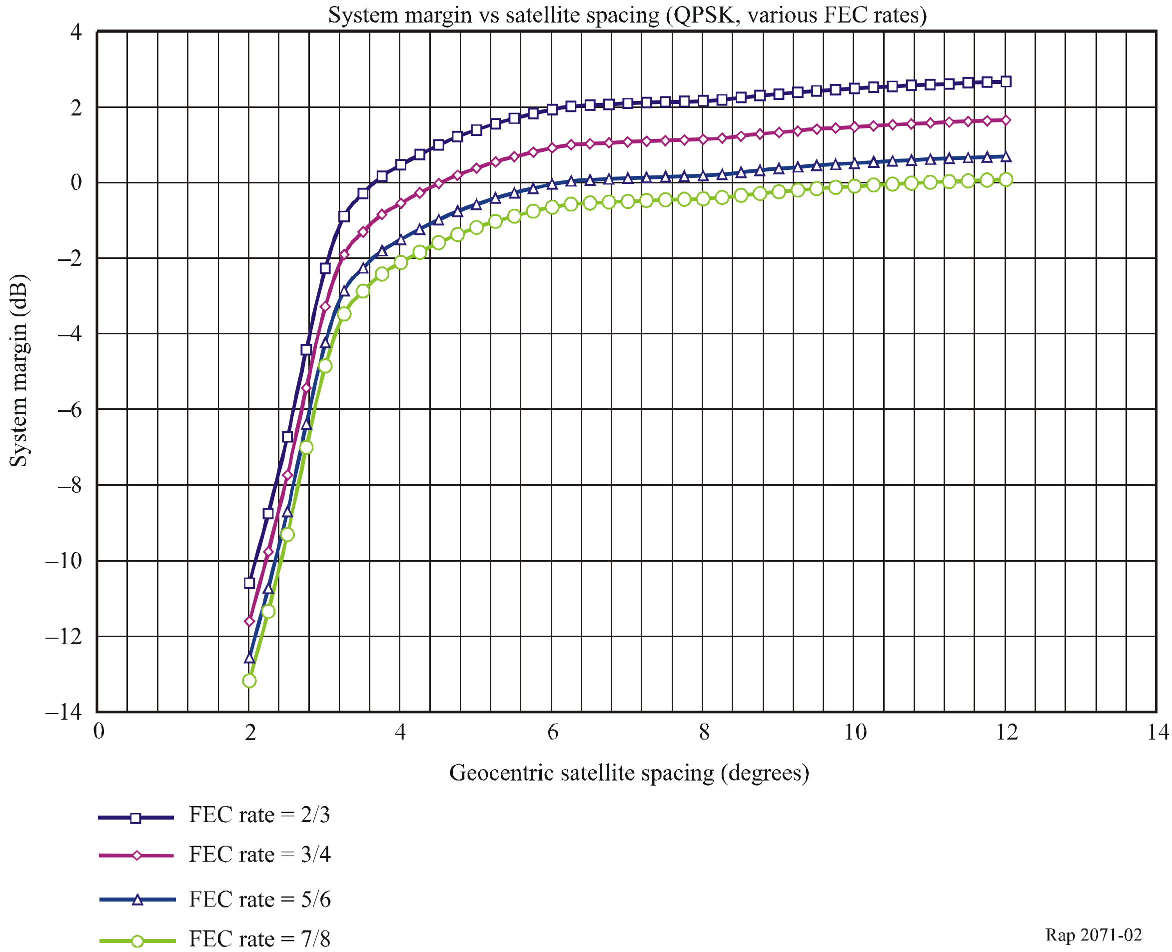

Case 2: using 8-PSK modulation

A similar analysis was performed for systems using 8-PSK modulation and an FEC rate of 2/3. It is expected that, due to change in the modulation scheme, the transmitting satellite power (downlink power) and the transmitting earth station power (uplink power) have to be increased. It is determined that the $(C/N)_{threshold}$ of the 8-PSK system is 3.66 dB higher than that of the QPSK system; therefore, an increase of 3.66 dB is applied to the uplink and downlink powers of the 8-PSK system. Figure 3 shows the relationship between system performance and satellite spacing for a system using 8-PSK modulation.

FIGURE 3

System margin vs. satellite spacing for system using 8-PSK

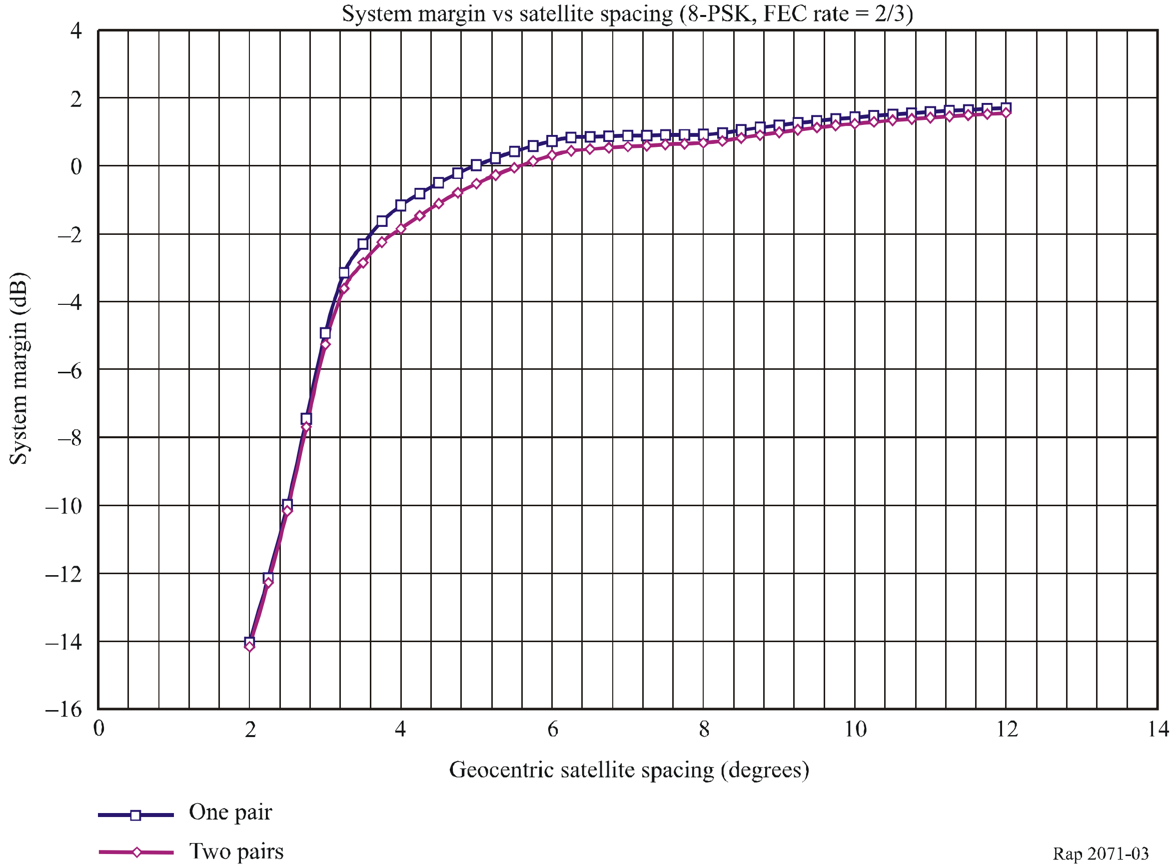

3.2 Inhomogeneous model for interfering system based on different modulation schemes

To further study the effect of different modulation schemes on the system performance, analysis was performed for an inhomogeneous model involving systems using QPSK and 8-PSK. It is assumed that the QPSK systems possess the characteristics of the QPSK system in Case 1 of § 3.1 and the 8-PSK system possesses the characteristics of the 8-PSK system in Case 2 of § 3.1.

Case A: wanted system uses 8-PSK and interfering systems uses QPSK

Figure 4 shows the relationship between system performance and satellite spacing for one pair and two pairs of interfering satellites.

FIGURE 4

System margin vs. satellite spacing for 8-PSK interfered by QPSK

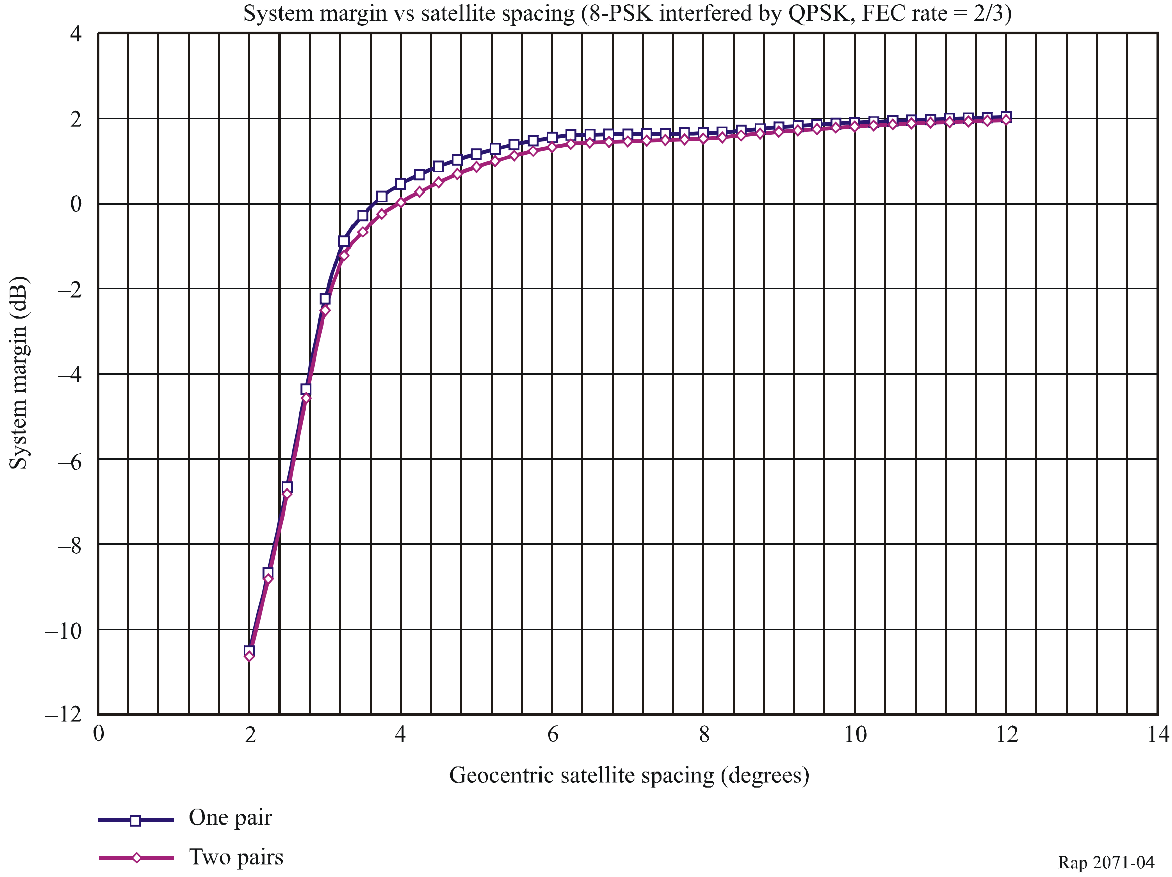

Case B: wanted system uses QPSK and interfering systems uses 8-PSK

Figure 5 shows the relationship between system margin and satellite spacing for various FEC rates. The results are shown for two pairs of interfering satellites.

4 Conclusion

Based on the system characteristics given in Attachment 1 to Appendix 2, this Report studies the impact of satellite separation (intersystem interference) on system performance of typical BSS systems operating in frequency bands 17.3-17.8 GHz and 24.75-25.25 GHz. The results of the study are summarized in Table 3.

FIGURE 5

System margin vs. satellite spacing for QPSK interfered by 8-PSK

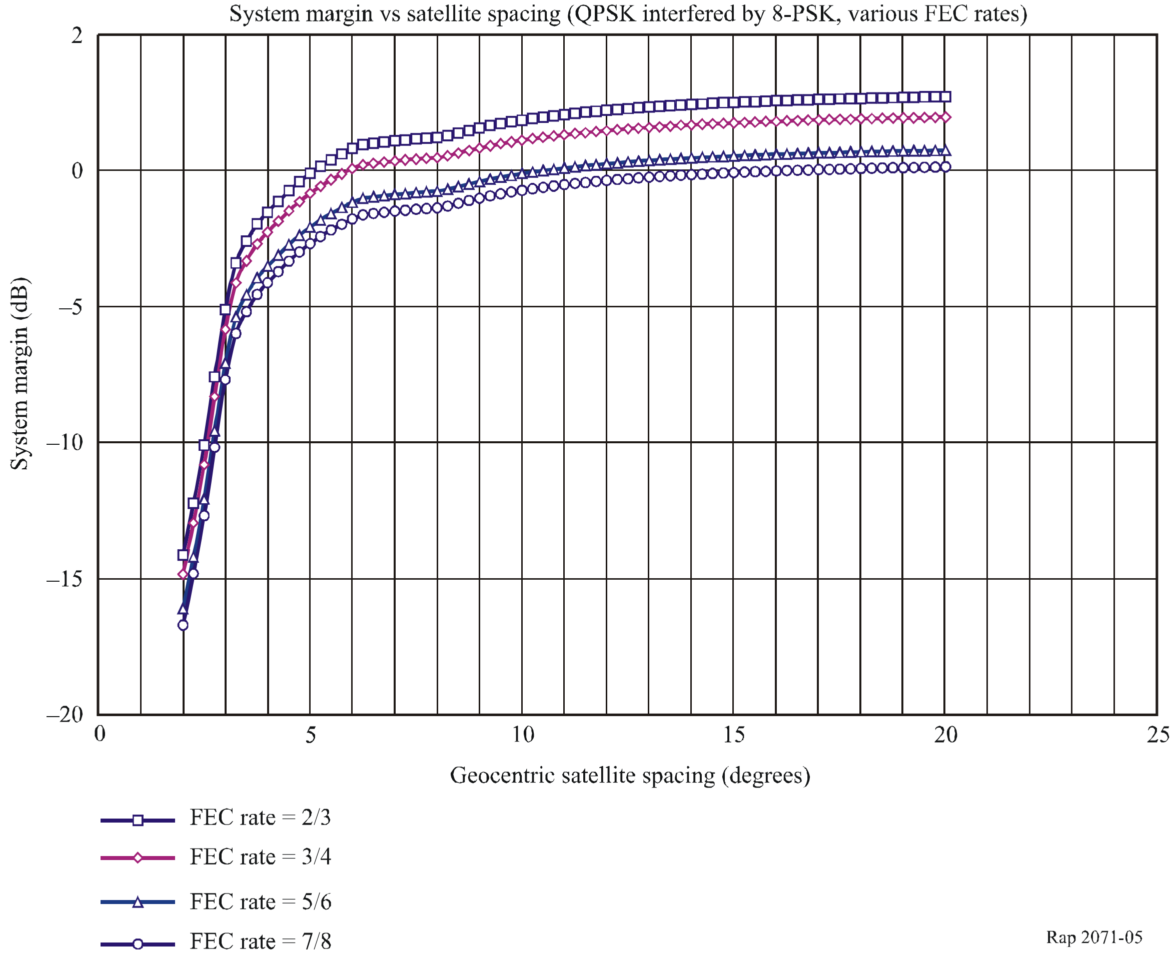

TABLE 3

	Increase in uplink and downlink power (dB)	Satellite spacing to achieve 0 dB system margin (degrees)
Homogeneous interfering model		
QPSK with FEC rate = 2/3	0	3.66
QPSK with FEC rate = 3/4	0	4.54
QPSK with FEC rate = 5/6	0	6.15
QPSK with FEC rate = 7/8	0	11.1
8-PSK with FEC = 2/3	3.66	5.57
Inhomogeneous interfering model		
QPSK with FEC rate = 2/3 interfered by 8-PSK	0	5.13
QPSK with FEC rate = 3/4 interfered by 8-PSK	0	5.96
QPSK with FEC rate = 5/6 interfered by 8-PSK	0	10.7
QPSK with FEC rate = 7/8 interfered by 8-PSK	0	17.25
8-PSK with FEC rate = 2/3 interfered by QPSK	3.66	3.97

Attachment 1
to Appendix 2

System characteristics

	Wanted	Interfering 1	Interfering 2
Sat. longitude (W: −ve)	–95°	–99°	–103°
Channel bandwidth	25 MHz		
Uplink			
E.S. Tx pointing loss	0.5 dB		
Sat. Rx antenna gain	35 dBi		
Rx Sat system noise temp	730 K		
Availability	≥ 99.95%		
E.S. latitude	43.67°		
E.S. longitude	–79°		
Frequency	25 GHz		
Polarization	Circular		
E.S. Tx antenna size	5.6 m		
E.S. Tx power	22.2 dBW		
Combiner loss to antenna	2 dB		
E.S. Tx antenna gain	61.48 dBi		
E.S. Tx antenna pattern (co-pol)	AP 4 A, B, C, D, φ coefficients: 29, 25, 32, 25, 7°		
E.S. Tx antenna pattern (x-pol)	AP 4 A, B, C, D, φ coefficients: 19, 25, 32, 25, 7°		
Downlink			
E.S. latitude	29.7°		
E.S. longitude	–95.3°		
E.S. receive antenna size	0.45 m		
E.S. Rx antenna gain	36.49 dBi		
E.S. Rx noise temperature	170 K		
E.S. Rx antenna pattern co-pol	Refer to Annex 11 6S/349		
E.S. Rx antenna pattern x-pol	ITU-R BO.1213		
E.S. pointing loss	0.5 dB		
Availability	≥ 99.8%		
Type of modulation	QPSK		
BW shaping factor	1.35		
FEC rate	0.75		
RS coding	RS-188/204		
Frequency	17.55 GHz		
Polarization	Circular		
Sat. Tx power	22.2 dBW		
Sat Tx antenna gain	35 dBi		
Combiner losses to antenna	1 dB		

Attachment 2
to Appendix 2

Error performance requirements[2]

Modulation	Inner code rate	Spectral efficiency (bit/symbol)	Modem implementation margin (dB)	Required E_b/N_0 (Note 1) for BER = 2×10^{-4} before RS QEF after RS (dB)
QPSK	1/2	0.92	0.8	4.5
	2/3	1.23	0.8	5.0
	3/4	1.38	0.8	5.5
	5/6	1.53	0.8	6.0
	7/6	1.61	0.8	6.4
8-PSK (optional)	2/3	1.84	1.0	6.9
	5/6	2.30	1.4	6.9
	8/9 (Note 3)	2.46	1.5	9.4
16-QAM (optional)	3/4 (Note 3)	2.76	1.5	9.0
	7/6	3.22	2.1	10.7

NOTE 1 – The figures of E_b/N_0 are referred to the useful bit-rate R_u (188 byte format, before RS coding) (so takes account of the factor 10 log 188/204 ≅ 0.36 dB due to the Reed-Solomon outer code) and include the modem implementation margins. For QPSK the figures are derived from EN 300 421.

For 8-PSK and 16-QAM, modem implementation margins which increase with the spectrum efficiency are adopted to cope with the larger sensitivity associated with these schemes.

NOTE 2 – Quasi-error-free (QEF) means approximately less than one uncorrected error event per hour at the input of the MPEG-s demultiplexer. Other residual error rate targets could be defined for "contribution quality" transmissions. The bit error ratio (BER) of 2×10^{-4} before RS decoding corresponds approximately to a byte error ratio between 7×10^{-4} and 2×10^{-3} depending on the coding scheme.

NOTE 3 – 8-PSK 8/9 is suitable for satellite transponders driven near saturation, while 16-QAM 3/4 offers better spectrum efficiency for quasi-linear transponders, in FDMA configuration.

---

2 Table 5 from ETSI standard EN 301 210 V1.1.1. (DVB; Framing structure, channel coding and modulation for DSNG and other contribution applications by satellite.)

Appendix 3
to Annex 1

A further study of orbital separation requirements for BSS and associated feeder links in frequency bands 17.3-17.8 GHz and 24.75-25.25 GHz

1 Introduction

Using the same methodology as provided in Appendix 2 to Annex 1, this Appendix re-examines the impact of satellite separation on system performance for BSS systems using information provided in ETSI DVB-S.2 standard (Version EN 302 307 V1.1.1), http://webapp.etsi.org/WorkProgram/Report_WorkItem.asp?WKI_ID=19738.

2 Assumptions

The system characteristics used in the original analysis are listed in Appendix 2 to Annex 1. This analysis was carried out with the following new assumptions, which are obtained from the ETSI standard:

1 FEC encoding:

- Inner code: LDPC
- Outer code: BCH
- Frame length: 64 800 bits.

In this study, the inner code rate will be referred to as FEC rate. Please see Attachment 1 to Appendix 3 for a list of coding parameters.

2 Symbol rate: 27.5 MBd

3 Bandwidth: 35.75 MHz

4 Satellite transponder: dynamic pre-distortion with phase noise

5 In this study, the system uplink and downlink transmit powers are assumed to be the same value.

It should be noted that the draft ETSI DVB-S.2 standard gives error performance in terms of an ideal E_b/N_0, hence when calculating the link budgets an allowance needs to be included, represented as C/N degradation, to account for satellite channel impairments. In the ETSI standard, examples of satellite channel impairments were provided based on computer simulations using realistic satellite channel models. In this study, C/N degradation is taken into account as the modem implementation margin. The required E_b/N_0 is therefore calculated as:

$$\text{Required } E_b/N_0 = \text{Ideal } E_b/N_0 + \text{Modem implementation margin}$$

Please refer to Table 6 which lists the system error performance requirements with their corresponding $\left(\frac{C}{N}\right)_{threshold}$ values.

Furthermore, the ETSI DVB-S.2 standard contains two unconventional APSK modulation schemes, which are described below:

16-APSK:

The I/Q constellation diagram representing 16-APSK modulation is composed of two concentric rings of uniformly spaced 4 and 12-PSK points, respectively in the inner ring of radius R_1 and outer ring of radius R_2.

FIGURE 6

16-APSK signal constellation

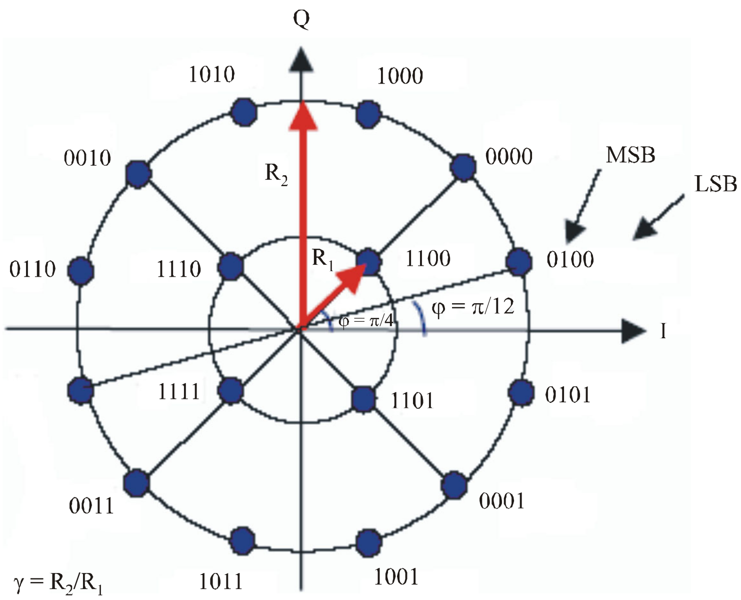

Rap 2071-06

32-APSK:

The I/Q constellation diagram representing the 32-APSK modulation is composed of three concentric rings of uniformly spaced 4, 12 and 16-PSK points, respectively in the inner ring of radius R_1, the intermediate ring of radius R_2 and the outer ring of radius R_3.

FIGURE 7

32-APSK signal constellation

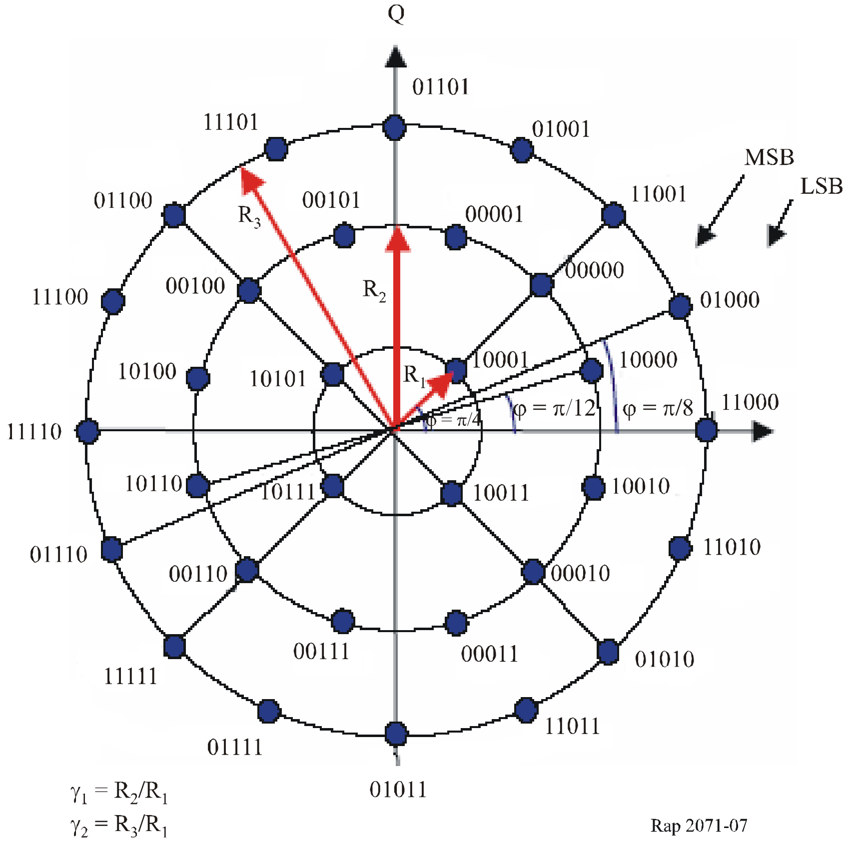

3 Results

3.1 Homogeneous model for interfering system based on wanted system

This section analyses the relationship between system performance and satellite spacing for one and two adjacent pairs of interfering satellites. The results are shown in Figs. 8, 10 and 12. The system parameters were appropriately adjusted to limit the maximum orbital spacing requirement between satellites of 20°.

3.1.1 Case 1: using QPSK modulation

An FEC rate of 3/4, and a QPSK modulation scheme were used.

FIGURE 8

System margin vs. satellite spacing for system using QPSK

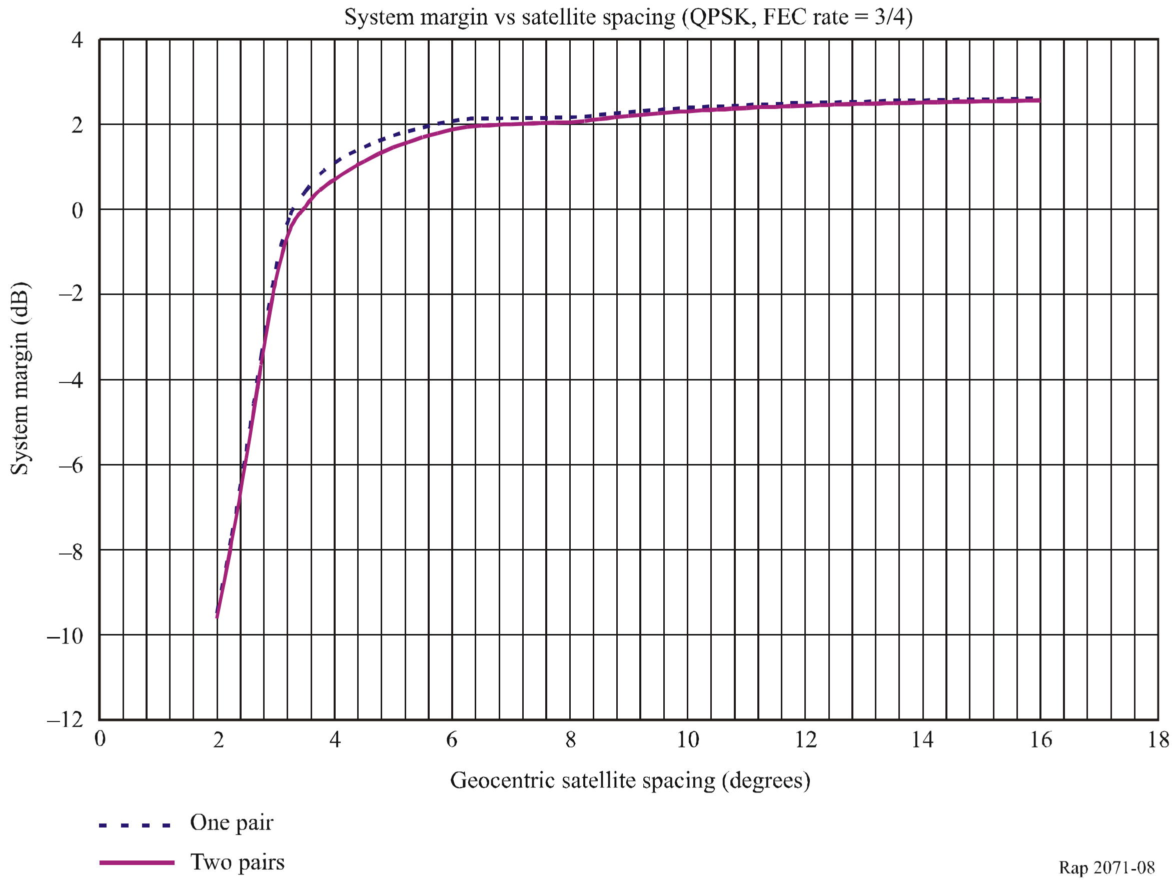

In order to study the effect of FEC rate on the system performance, analysis was performed to determine the relationship between system margin and satellite spacing for systems with various FEC rates. Figure 9 shows the analysis results.

FIGURE 9

System margin vs. satellite spacing for various FEC rates

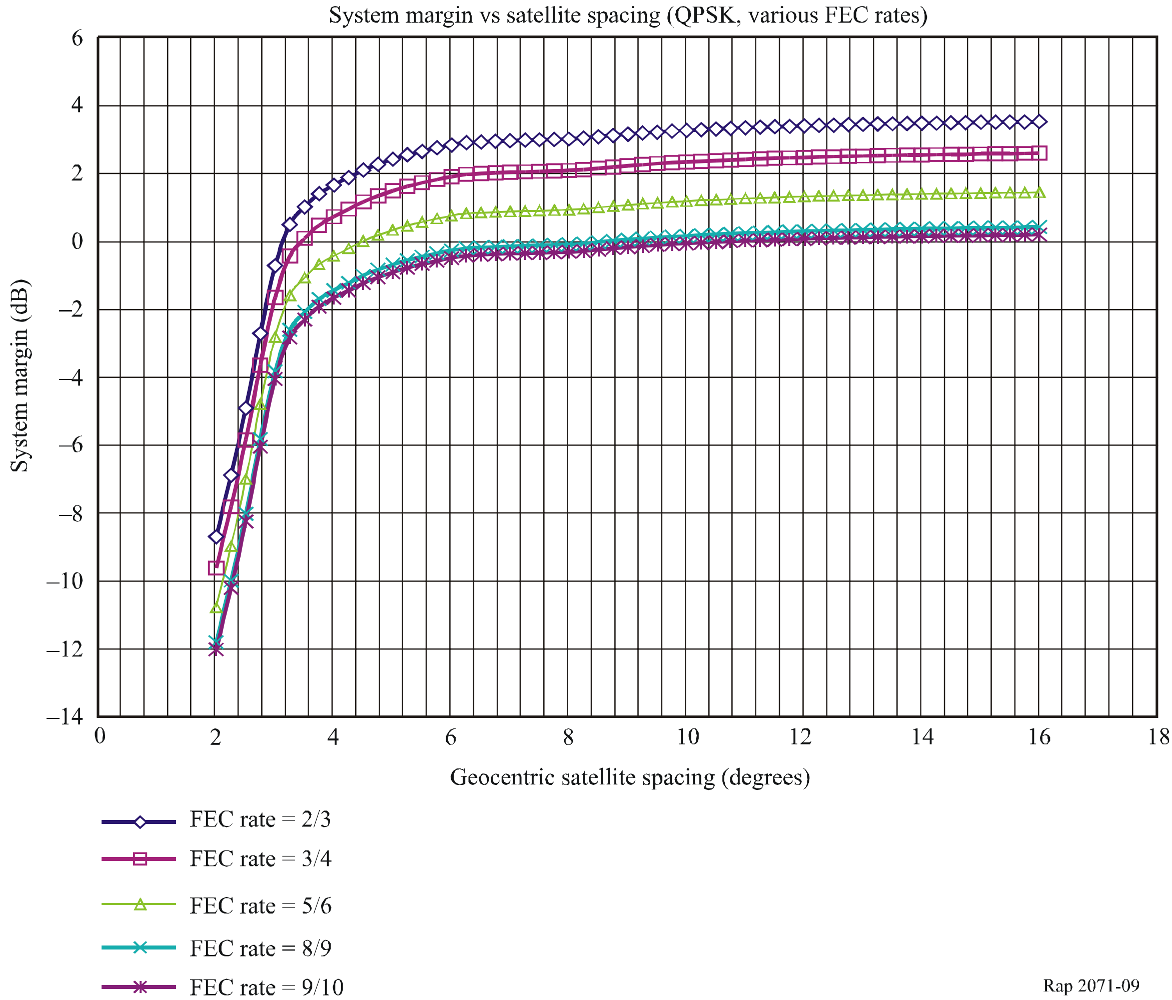

3.1.2 Case 2: using 8-PSK modulation

A similar analysis to that of Case 1 was performed for systems using 8-PSK modulation and an FEC rate of 2/3. Due to the higher $(C/N)_{threshold}$ values resulting from the higher modulation level and maintaining the same receive earth station figure-of-merit, the transmit satellite power (downlink power) and the transmit earth station power (uplink power) have to be increased.

It is determined that the $(C/N)_{threshold}$ of an 8-PSK system is 3.75 dB higher than that of the QPSK system; therefore, an increase of 3.75 dB is applied to both the uplink and downlink powers of the 8-PSK system. Figure 10 shows the relationship between system performance and satellite spacing for a system using 8-PSK modulation, and Fig. 11 shows the effect of FEC rate on the system performance.

Figure 11 shows that for FEC rates of 8/9 and 9/10, the system margin will always be less than 0 dB. Therefore, an additional increase in uplink and downlink powers is needed. For an FEC rate of 8/9, an increase of 1.74 dB is necessary to have 0 dB system margin at 20° satellite spacing. For an FEC rate of 9/10, the transmit power increase is 2.19 dB.

FIGURE 10

System margin vs. satellite spacing for system using 8-PSK

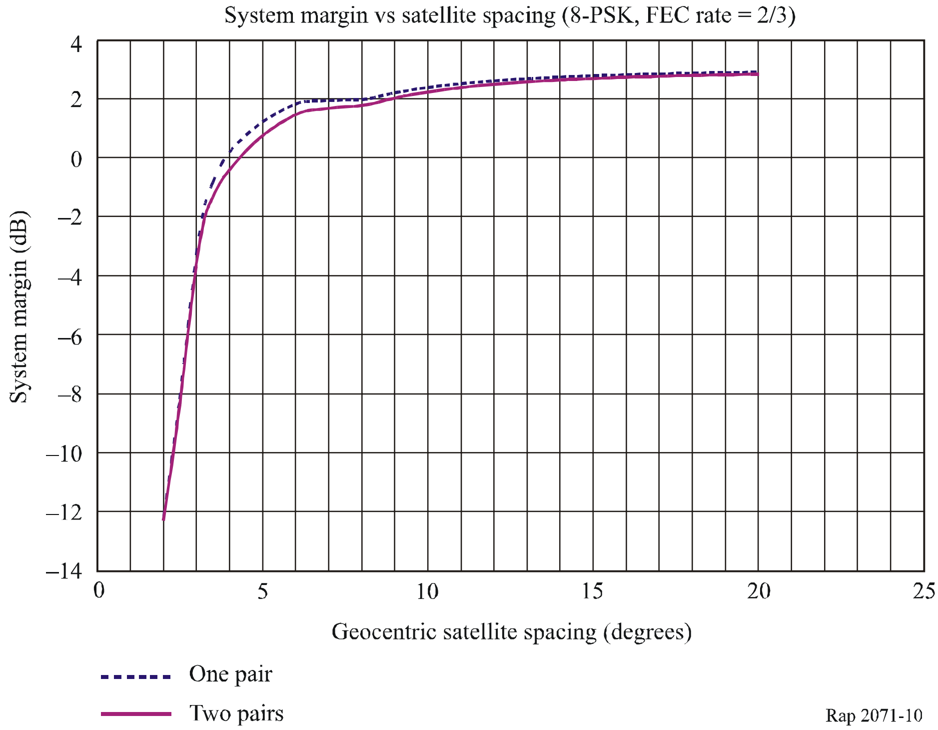

FIGURE 11

System margin vs. satellite spacing for various FEC rates

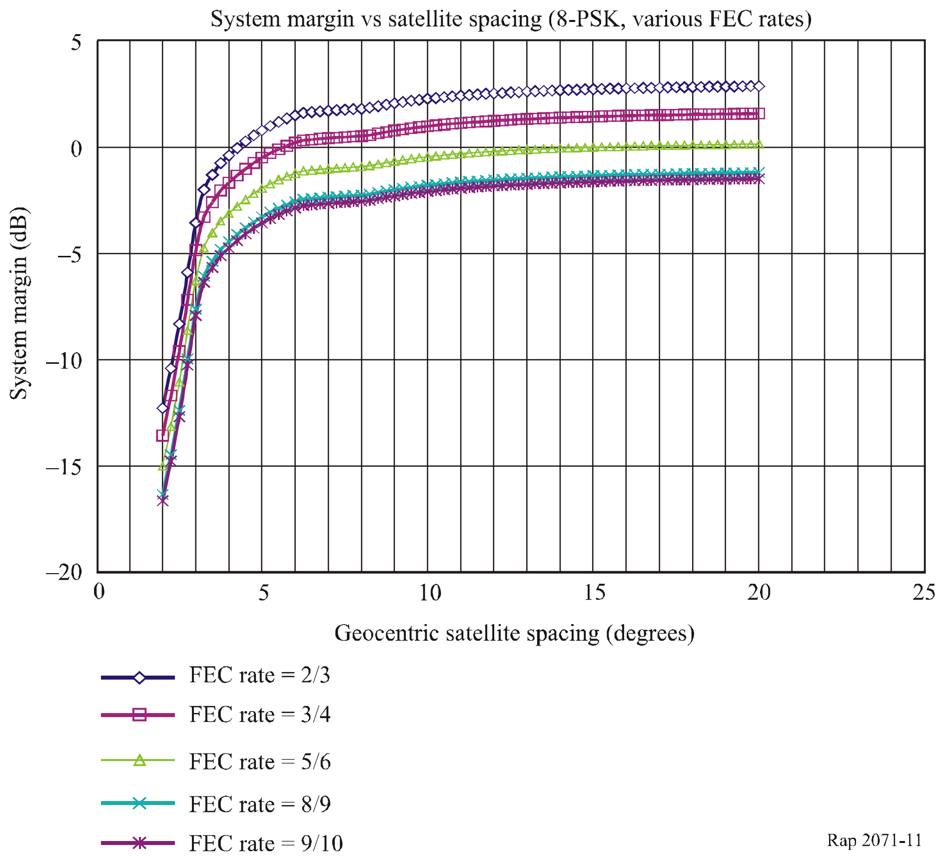

3.1.3 Case 3: using 16-APSK modulation

Analysis was also performed for systems using 16-APSK modulation and an FEC rate of 2/3. The $(C/N)_{threshold}$ of a 16-APSK system is 7.05 dB higher than that of the QPSK system therefore the uplink and downlink powers for the 16-APSK system were increased by this amount.

Figure 12 shows the relationship between system performance and satellite spacing for a system using 16-APSK modulation, and Fig. 13 shows the effect of FEC rate on the system performance.

From Fig. 13, it can be observed that for FEC rates of 5/6, 8/9 and 9/10, the system margin will always be less than 0 dB. Therefore, for FEC rates of 5/6, 8/9 and 9/10 additional increases of the feeder link and downlink e.i.r.p.s of 1.75 dB, 5.1 dB and 5.99 dB respectively are needed to achieve a 0 dB system margin at 20 degree satellite spacing.

FIGURE 12

System margin vs. satellite spacing for system using 16-APSK

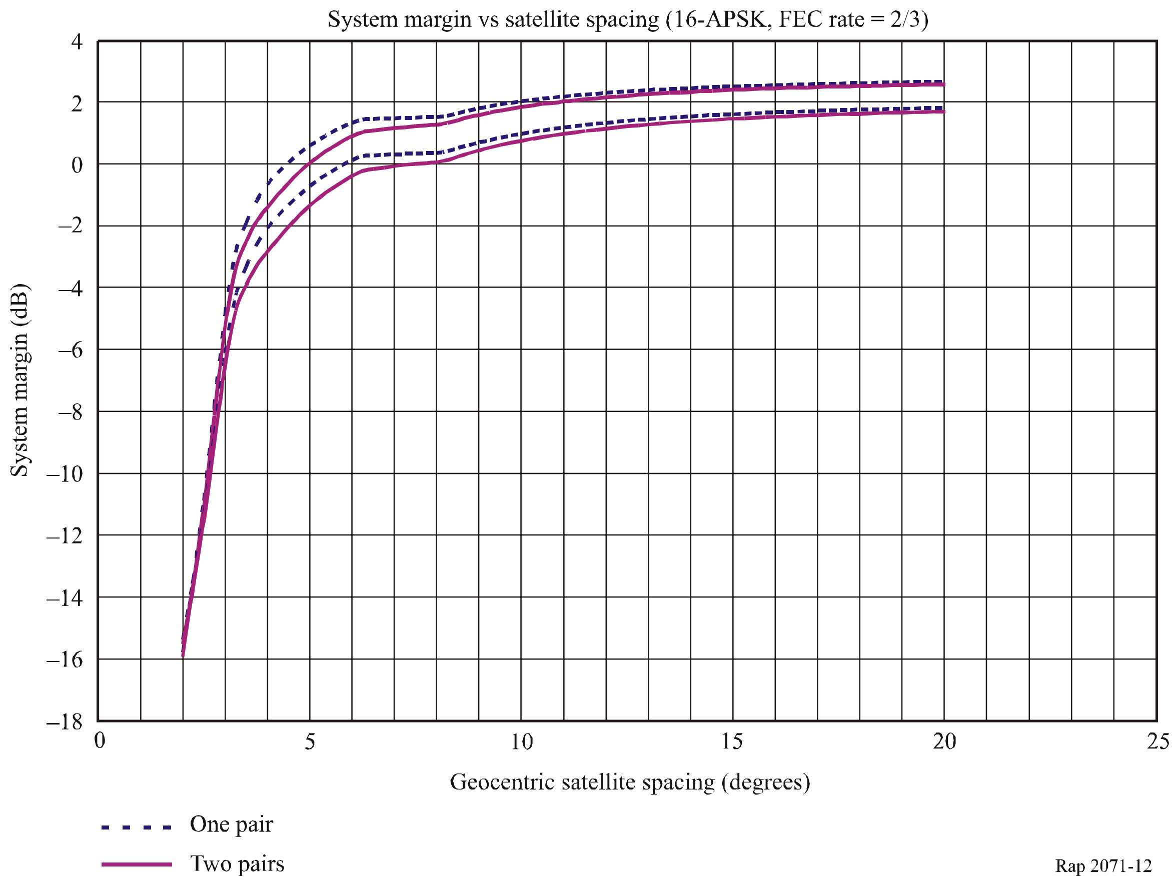

FIGURE 13

System margin vs. satellite spacing for various FEC rates

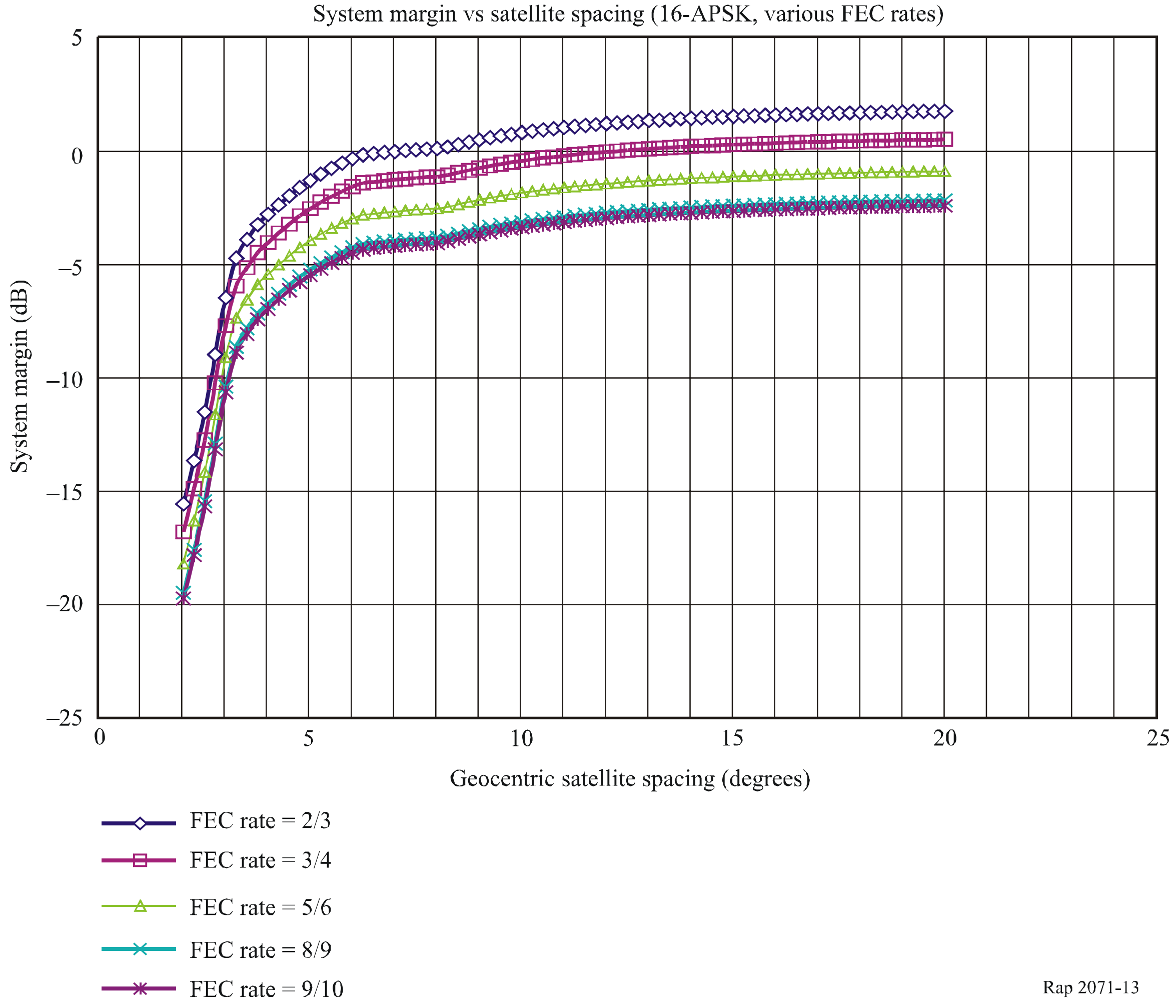

3.1.4 Case 4: using 32-APSK modulation

Similarly, analysis was performed for systems using 32-APSK modulation and an FEC rate of 3/4. However, in this case, it is impossible to achieve 0 dB system margin at 20° separation. As can be seen from Fig. 14, which plots the system $C/(N+I)$ versus uplink and downlink powers, the system $C/(N+I)$ curve is always less than the C/N threshold, even for transmit power increased by 50 dB. Thus, under the assumption of maintaining a fixed receive earth station performance 32-APSK modulation is not feasible. Although there are ways to improve the system $C/(N+I)$ to enable the operation of 32-APSK modulation, for example, improving receive earth station performance by increasing antenna size and/or lowering receiver noise temperature, decreasing the intra-system interference caused by rain depolarization by reducing the amount of frequency reuse, however these techniques go beyond the scope of this study.

FIGURE 14

C/(N + I) vs. uplink and downlink power for 32-APSK

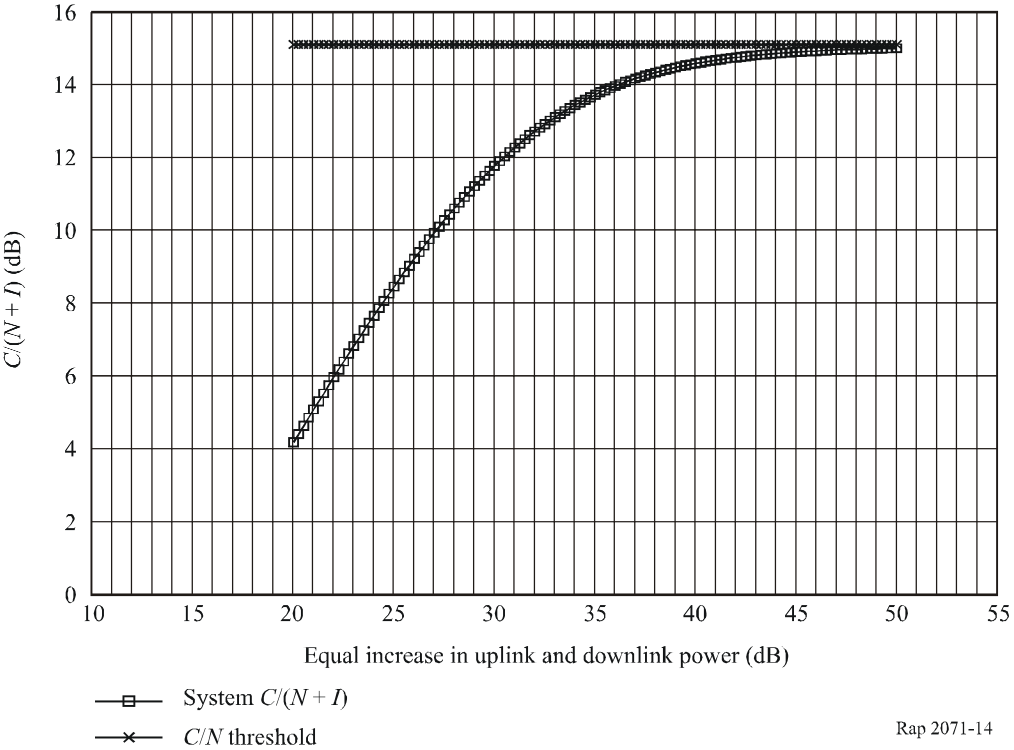

3.2 Inhomogeneous model for interfering system based on different modulation methods

To further study the effect of modulation method on the system performance, analyses were conducted for an inhomogeneous model involving systems using different modulation methods. Here, the interfering system uplink and downlink transmitting powers are referred to as interfering powers. From the point of view of the effect on the wanted satellite system, the result of changing the interfering system modulation is analogous to changing the transmit powers from the interfering systems. Thus the effect of using different modulation methods on the system performance can be examined by varying the interfering transmit powers and determining the required satellite spacing to achieve a 0 dB system margin. Again two adjacent pairs of interfering satellites are assumed.

The results of the analysis are presented in Figs. 15, 16 and 17. The y-axis is the required orbital spacing for a system margin of 0 dB, and the x-axis is the difference between the interfering and wanted transmit power levels. It is assumed that the wanted and interfering systems have the same characteristics as given in § 3.1. Also, for these cases, a maximum orbital spacing of 30° is assumed.

FIGURE 15

Required satellite spacing to achieve 0 dB system margin vs. interfering transmitted power for QPSK

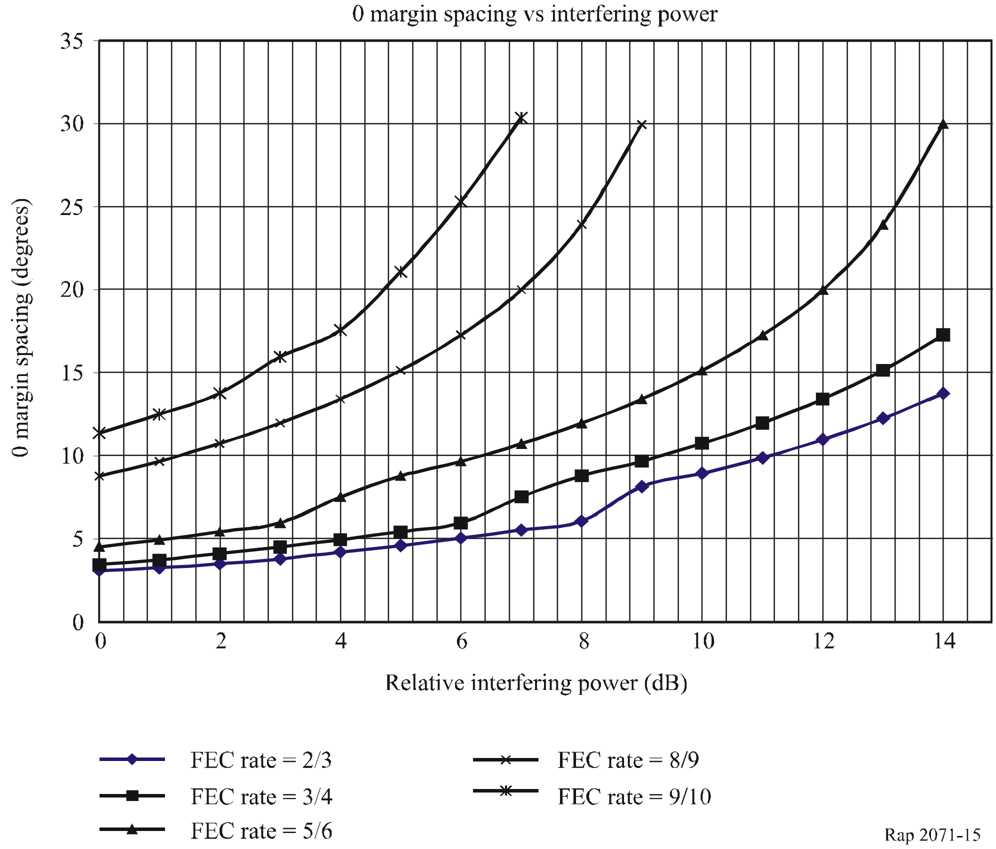

FIGURE 16

Required satellite spacing to achieve 0 dB system margin vs. interfering transmit power for 8-PSK

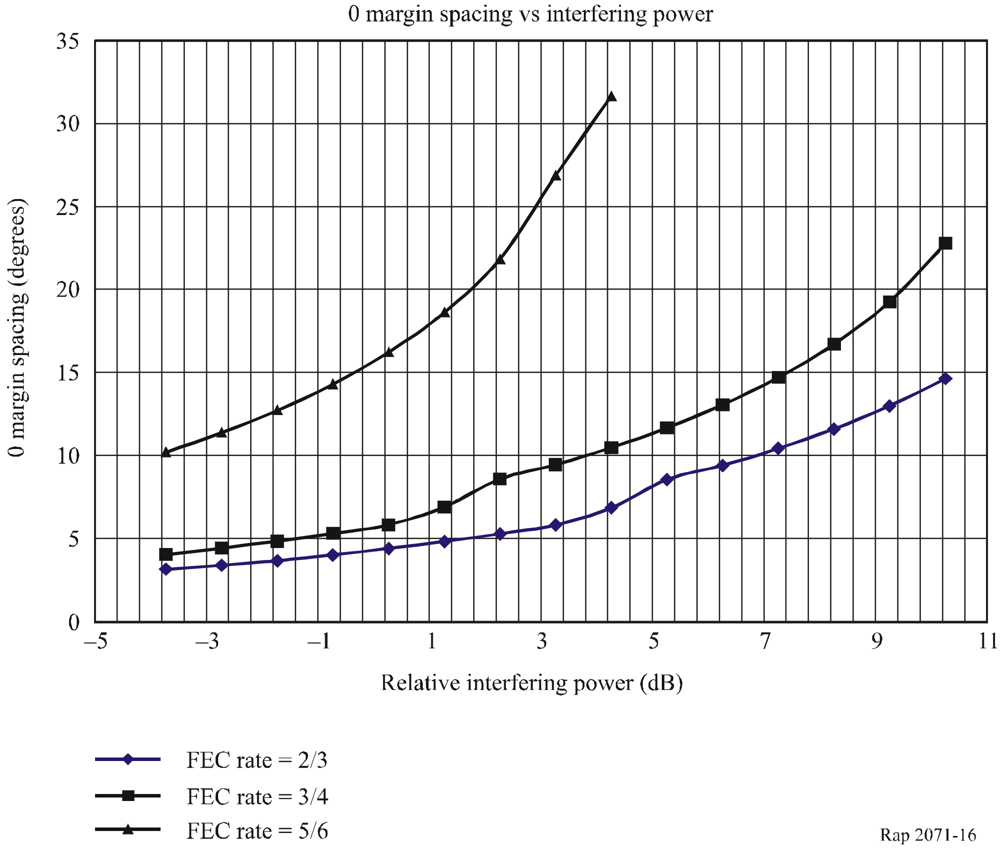

FIGURE 17

Required satellite spacing to achieve 0 dB system margin vs. interfering transmit power for 16-APSK

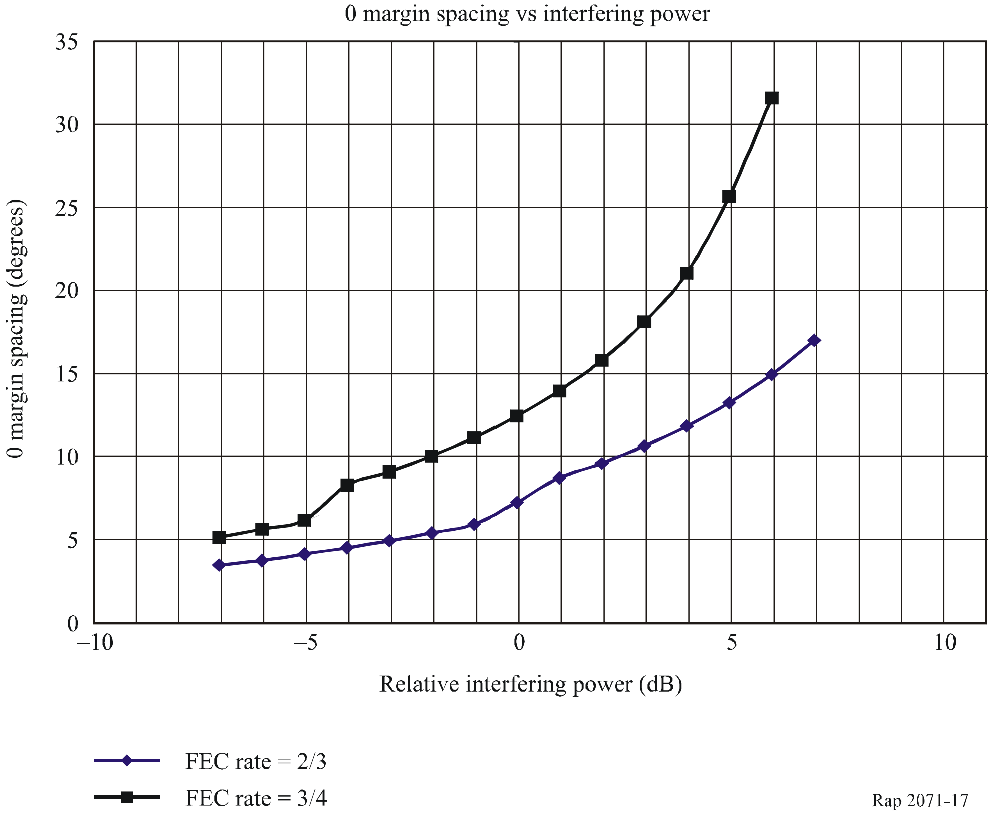

4 Conclusion

Using the system characteristics specified in the draft ETSI DVB-S.2 standard, this document studies the impact of satellite separation (intersystem interference) on system performance for BSS systems operating in the unplanned frequency band 17.3-17.8 GHz and associated 24.75-25.25 GHz feeder-link band. The results of the study are summarized in the following figures and tables.

It is recommended that the following text be included in the Report on system parameters for BSS systems in the unplanned 17.3-17.8 GHz and 24.75-25.25 GHz bands for future reference and review.

TABLE 4

Homogeneous interfering model

	Increase in uplink and downlink power (dB)	Satellite spacing to achieve 0 dB excess system margin (degrees)
QPSK		
FEC rate = 2/3	0	3.11
FEC rate = 3/4	0	3.47
FEC rate = 5/6	0	4.53
FEC rate = 8/9	0	8.80
FEC rate = 9/10	0	11.38
8-PSK		
FEC rate = 2/3	3.75	4.31
FEC rate = 3/4	3.75	5.69
FEC rate = 5/6	3.75	15.68
FEC rate = 8/9	5.49	20.00
FEC rate = 9/10	5.94	20.00
16-APSK		
FEC rate = 2/3	7.05	7.35
FEC rate = 3/4	7.05	12.50
FEC rate = 5/6	8.80	20.00
FEC rate = 8/9	12.15	20.00
FEC rate = 9/10	13.04	20.00

FIGURE 18

Case 1: Inhomogeneous interfering model: QPSK

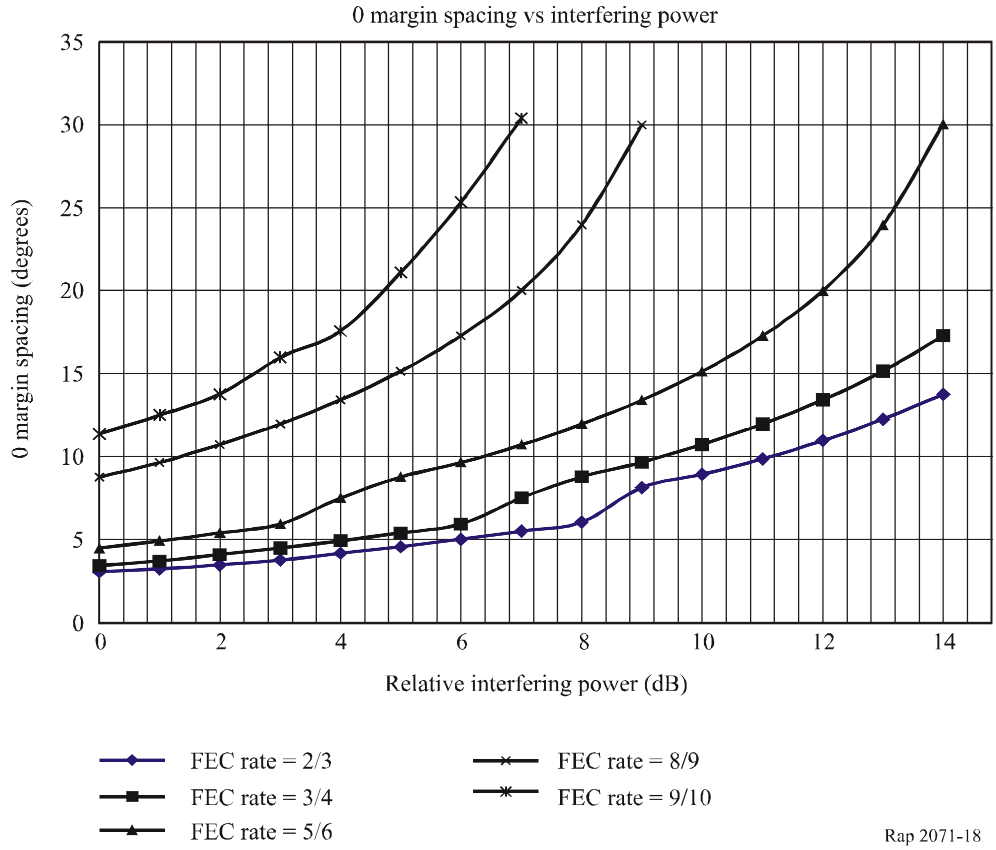

FIGURE 19

Case 2: Inhomogeneous interfering model: 8-PSK

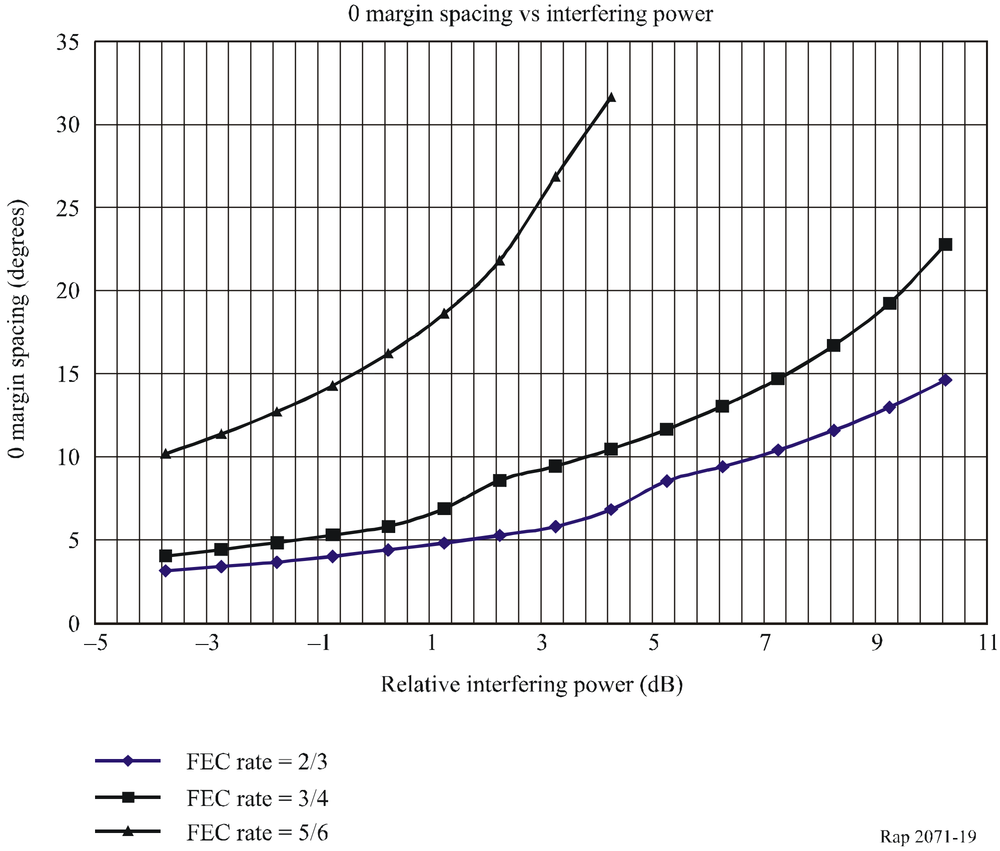

Rap 2071-19

FIGURE 20

Case 3: Inhomogeneous interfering model: 16-APSK

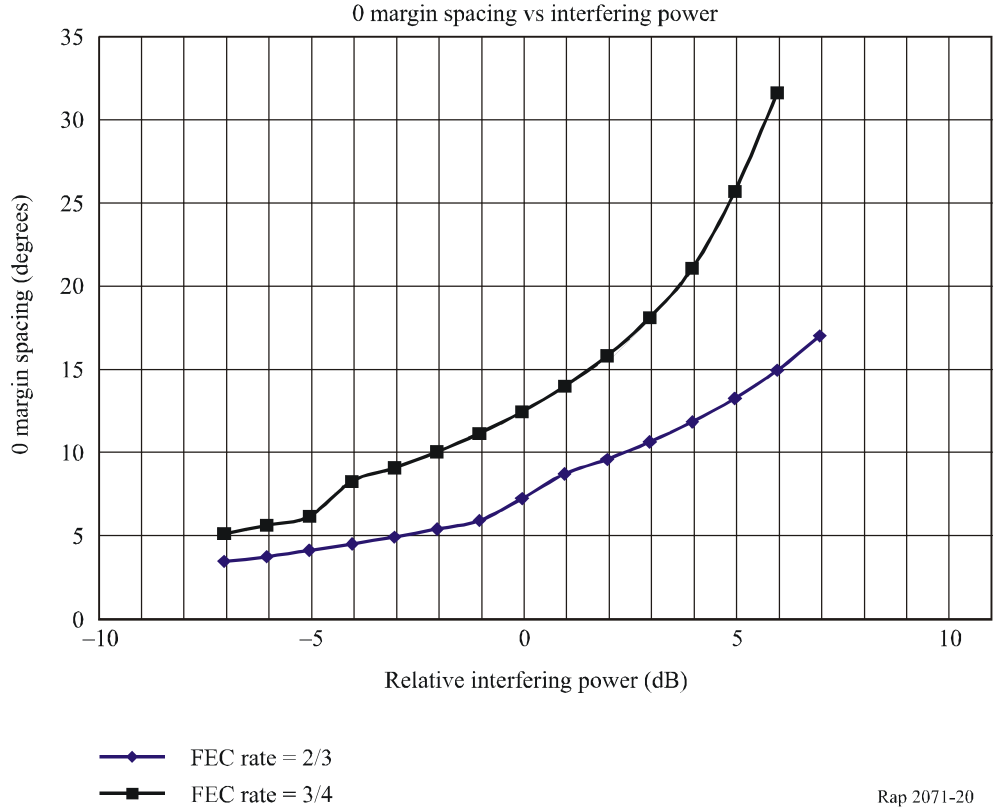

Attachment 1 to Appendix 3

TABLE 5

FEC coding parameters*

LDPC code	BCH uncoded block K_{bch}	BCH coded block N_{bch} LDPC uncoded block K_{ldpc}	BCH *t*-error correction	LDPC coded block n_{ldpc}
1/4	16 008	16 200	12	64 800
1/3	21 408	21 600	12	64 800
2/5	25 728	25 920	12	64 800
1/2	32 208	32 400	12	64 800
3/5	38 688	38 800	12	64 800
2/3	43 040	43 200	10	64 800
3/4	48 408	48 600	12	64 800
4/5	51 648	51 840	12	64 800
5/6	53 840	54 000	10	64 800
8/9	57 472	57 600	8	64 800
9/10	58 192	58 320	8	64 800

* Table 5a from ETSI standard draft ETSI EN 302 307 V1.1.1 (Digital Video Broadcasting (DVB); Second generation framing structure, channel coding and modulation systems for Broadcasting, Interactive services, News Gathering and other broadband satellite applications).

Attachment 2
to Appendix 3

TABLE 6

Error performance requirements*

Modulation	Inner code rate (FEC rate)	Ideal E_b/N_0 (dB)	Modem implementation margin (dB)	Required E_b/N_0 for BER = 10^{-7}	System C/N threshold (dB)
QPSK	2/3	1.8869	0.63	2.5169	2.61
	3/4	2.3055	0.63	2.9355	3.54
	5/6	2.9929	0.63	3.6229	4.69
	8/9	3.7290	0.63	4.3590	5.71
	9/10	3.8948	0.63	4.5248	5.93
8-PSK	2/3	3.6520	0.85	4.5020	6.36
	3/4	4.4306	0.85	5.2806	7.65
	5/6	5.4080	0.85	6.2580	9.09
	8/9	6.4641	0.85	7.3141	10.42
	9/10	6.6999	0.85	7.5499	10.71
16-APSK	2/3	4.7586	1.80	6.5586	9.66
	3/4	5.4872	1.80	7.2872	10.90
	5/6	6.4246	1.80	8.2246	12.30
	8/9	7.4207	1.80	9.2207	13.58
	9/10	7.6066	1.80	9.4066	13.82
32-APSK	3/4	7.0441	3.50	10.5441	15.13
	5/6	8.1315	3.50	11.6315	16.68
	8/9	9.2576	3.50	12.7576	18.08
	9/10	9.5634	3.50	13.0634	18.45

* Based on Table 13 and Table H.1.1 of ETSI standard draft ETSI EN 302 307 V1.1.1 (Digital Video Broadcasting (DVB); Second generation framing structure, channel coding and modulation systems for Broadcasting, Interactive services, News Gathering and other broadband satellite applications).

Annex 2

System parameters of BSS systems in frequency band 21.4-22.0 GHz and associated feeder links

1 Study items of 21 GHz band broadcasting satellites

The BSS systems in the band have the possibility to deliver wide-RF-band digital multiprogramme services, which may consist of HDTV, audio and data programmes. In the future, they also can be appropriate channels to accommodate higher bit-rate programmes, such as extremely high-resolution imagery whose number of lines is much larger than HDTV, three-dimensional TV and high bit-rate data programme.

On the other hand, the study of the technical parameters for the broadcasting-satellite service in the band 21.4-22 GHz in Regions 1 and 3 was included in WRC-07 agenda item 6, and the results of the studies by the ITU-R Study Groups may be reported to WRC-07 under WRC-07 agenda item 7.1 (Administrative Circular CA/128, 29 July 2003.)

The Recommendation – Mitigation techniques for rain attenuation for BSS systems in frequency bands between 17.3 GHz and 42.5 GHz was approved as Recommendation ITU-R BO.1659 (December 2003). Recommendation ITU-R BO.1659 includes the following techniques to mitigate the rain attenuation when considering facilitating the introduction of the BSS systems:

– increase in e.i.r.p.;

– hierarchical transmission;

– broadcasting system assuming storage in receiver.

The examples of study items necessary for the orderly spectrum usage in the 21 GHz band broadcasting-satellite services and the associated feeder-link systems are shown in Table 7 along with the corresponding ITU-R Recommendations. The system parameters might be different depending on the BSS systems.

It is encouraged that administrations submit contributions in order to progress the studies.

TABLE 7

Study items for the 21 GHz band broadcasting-satellite services and the associated feeder-link systems*

Study items	BSS systems with the mitigation technique of			Corresponding Recommendations ITU-R
	Increase in e.i.r.p.	Hierarchical transmission	Broadcasting system assuming storage in receiver	
1 Service availability	– Objective of availability against the fading caused by precipitation	– Objective of availability against the fading caused by precipitation	– Definition of service availability for non-real time broadcasting	
2 Attenuation caused by precipitation and other meteorological factors	– Relation between attenuation and time	– Fade dynamics (Frequency and duration of attenuation)	– Fade dynamics (Frequency and duration of attenuation)	P.618-8 P.1623

TABLE 7 (*end*)

Study items	BSS systems with the mitigation technique of			Corresponding Recommendations ITU-R
	Increase in e.i.r.p.	Hierarchical transmission	Broadcasting system assuming storage in receiver	
3 Downlink e.i.r.p. or pfd	– Derived by the required service availability and attenuation	– Derived by the required service availability and attenuation	– Derived by the required service availability and attenuation	
4 Channel coding	– Modulation scheme, interleave, etc.	– Modulation scheme, interleave, etc.	– Modulation scheme, interleave, etc.	BO.1211, BO.1408-1, BO.1516
5 Sharing criteria	– Protection ratios, pfd mask, $\Delta T / T$, C/I, EPM, I/N	– Protection ratios, pfd mask, $\Delta T / T$, C/I, EPM, I/N	– Protection ratios, pfd mask, $\Delta T / T$, C/I, EPM, I/N	BO.792, BO.1293-2, BO.1297
6 Methodology for interference calculation	– Including the satellite orbital spacing, satellite station keeping	– Including the satellite orbital spacing, satellite station keeping	– Including the satellite orbital spacing, satellite station keeping	BO.1212, BO.1293-2
7 Frequencies for feeder link	– 17.8-18.4 GHz, 24.75-25.25 GHz, 27.5-30 GHz			
8 Feeder-link e.i.r.p.	– site diversity -power control	– site diversity -power control	– site diversity -power control	
9 Receiving G/T	– NF	– NF	– NF	BO.790
10 Polarization	– LP, CP, or not specified			BO.791
11 Reference receive earth station antenna patterns	– Diameter, gain, reference pattern	– Diameter, gain, reference pattern	– Diameter, gain, reference pattern	BO.1213
12 Reference patterns for satellite transmitting antennas	– Range of gain control, description in Appendix 4	– Gain, off-axis radiation pattern	– Gain, off-axis radiation pattern	BO.652-1, BO.1445
13 Reference patterns for satellite receiving antennas	– Gain, off-axis radiation pattern	– Gain, off-axis radiation pattern	– Gain, off-axis radiation pattern	BO.1296
14 Reference transmit earth station antenna off-axis e.i.r.p. patterns	– e.i.r.p., reference pattern	– e.i.r.p., reference pattern	– e.i.r.p., reference pattern	BO.1295
15 Unwanted emission level	– Review of Recommendation ITU-R SM.1633 (Annex 12)			
16 Others				

* The issues described in this Table are examples of study items and not intended to confine the studies.

2 Downlink receiving earth station antenna patterns

In this section, measured downlink receiving earth station antenna patterns for the 21 GHz band broadcasting in Regions 1 and 3 are presented. More measured antenna patterns are needed in order the study to be completed. Administrations are further invited to submit measured downlink receiving earth station antenna patterns for the 21 GHz band BSS systems.

2.1 Conditions for the measurement

The conditions for the measurement of antenna patterns in the 21 GHz band are shown in Table 8.

TABLE 8

The conditions for the measurement

Antenna type	Reflector and feed horn	
Diameter of the reflector *D*	45 cm	60 cm
Focal length of the reflector *F*	20.8 cm	28.2 cm
Frequency *f*	21.7 GHz	
Polarization	Linear (horizontal, vertical)	
Beamwidth of the feed horn (co-pol.)	43° (E-plane), 46° (H-plane)	
XPD_{min} of the feed horn within 45°	37 dB (E-plane), 31 dB (H-plane)	
Planar angle of the antenna in the measurement	0° (horizontal)	

2.2 Measured antenna patterns

The summary of the measured antenna patterns in the 21 GHz band is given in Table 9. In Table 9, it is seen that the antenna gain of the 45 cm antenna is slightly high (the efficiency is 83.3%) while the usual antenna efficiency lies between 70-80%. One possible reason for the high antenna gain is that the antenna under test might receive a reflected wave in phase with the main signal, however, the efficiency value of 83.3% is considered within a measurement error.

TABLE 9

The summary of the measured antenna patterns

Diameter of the reflector *D*	45 cm		60 cm	
Antenna gain G_{max} Efficiency (Calculated)	39.4 dBi 83.3% (38.9 dBi, 75.6%)		41.8 dBi 81.4% (41.4 dBi, 75.6%)	
Polarization	H	V	H	V
Beamwidth (–3 dB)	2.2°	2.3°	1.6°	1.7°
XPD (minimum)	14.7 dB	18.7 dB	17.2 dB	18.5 dB

The individual antenna patterns are shown in Fig. 21 (45 cm), Fig. 22 (60 cm).

The antenna pattern masks in Figs. 21 and 22 are expressed as follows:

Co-polar

$G_{co}(\varphi) = 2.5 \times 10^{-3} \left(\frac{D}{\lambda}\varphi\right)^2$ for $0 \leq \varphi < \varphi_m$ where $\varphi_m = \frac{\lambda}{D}\sqrt{\frac{G_{max} - G_1}{0.0025}}$

$G_{co}(\varphi) = G_1 = 29 - 25 \log \varphi_r - G_{max}$ for $\varphi_m \leq \varphi < \varphi_r$ where $\varphi_r = 95\frac{\lambda}{D}$

$G_{co}(\varphi) = 29 - 25 \log \varphi - G_{max}$ for $\varphi_r \leq \varphi < \varphi_b$ where $\varphi_b = 10^{(34/25)}$

$G_{co}(\varphi) = -5 - G_{max}$ for $\varphi_b \leq \varphi < 70°$

$G_{co}(\varphi) = 0 - G_{max}$ for $70° \leq \varphi < 180°$

where $\varphi_0 = 2\frac{\lambda}{D}\sqrt{\frac{3}{0.0025}}$

= 3 dB beamwidth

Cross-polar

$G_{cross}(\varphi) = -25$ for $0 \leq \varphi < 0.25\ \varphi_0$

$G_{cross}(\varphi) = -25 + 8\left(\frac{\varphi - 0.25\varphi_0}{0.19\varphi_0}\right)$ for $0.25\ \varphi_0 \leq \varphi < 0.44\ \varphi_0$

$G_{cross}(\varphi) = -17$ for $0.44\ \varphi_0 \leq \varphi < \varphi_0$

$G_{cross}(\varphi) = -17 - 13.5625\left|\frac{\varphi - \varphi_0}{\varphi_1 - \varphi_0}\right|$ for $\varphi_0 \leq \varphi < \varphi_1$ where $\varphi_1 = \frac{\varphi_0}{2}\sqrt{10.1875}$

$G_{cross}(\varphi) = 21 - 25 \log \varphi - G_{max}$ for $\varphi_1 \leq \varphi < \varphi_2$ where $\varphi_2 = 10^{(26/25)}$

$G_{cross}(\varphi) = -5 - G_{max}$ for $\varphi_2 \leq \varphi < 70°$

$G_{cross}(\varphi) = 0 - G_{max}$ for $70 \leq \varphi < 180°$

It can be said in Figs. 21 and 22 that the measured antenna patterns agree well with the calculated ones. The measured patterns are mostly under the antenna pattern masks, which are derived from Recommendation ITU-R BO.1213 such that they are expressed with relative gain, given by the above equations. However, in the vicinity of the antenna boresight the cross-polar patterns in part exceed the antenna pattern masks. Further study is needed on this matter.

FIGURE 21-1-1a

Co-polar pattern (45 cm, H)
(measured vs. calculated)

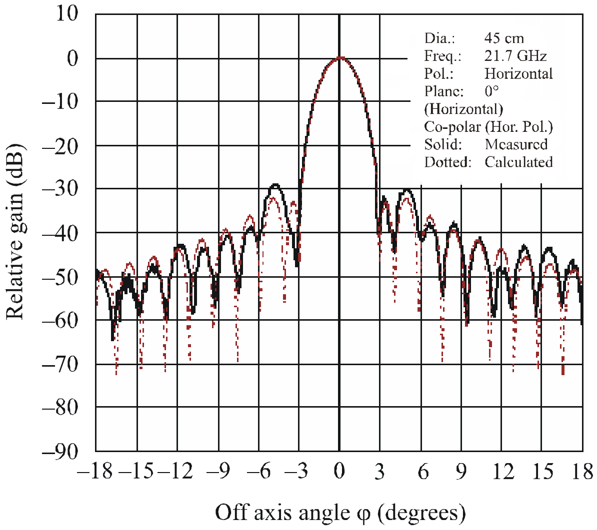

FIGURE 21-1-2a

Cross-polar pattern (45 cm, H)
(measured vs. calculated)

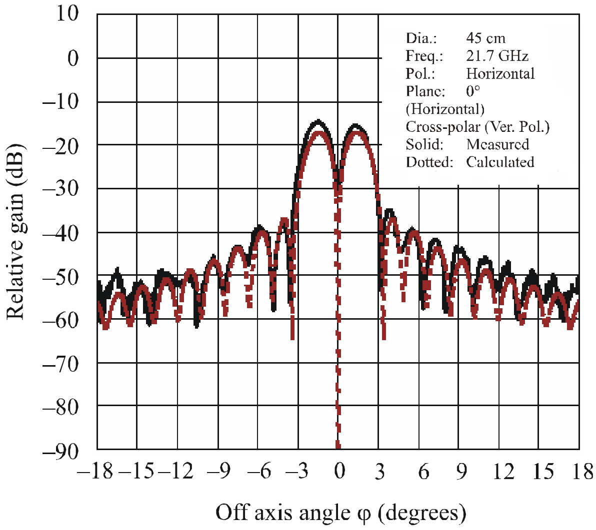

Rap 2071-2111a

FIGURE 21-1-1b

Co-polar pattern (45 cm, H)
(measured vs. BO.1213 mod.)

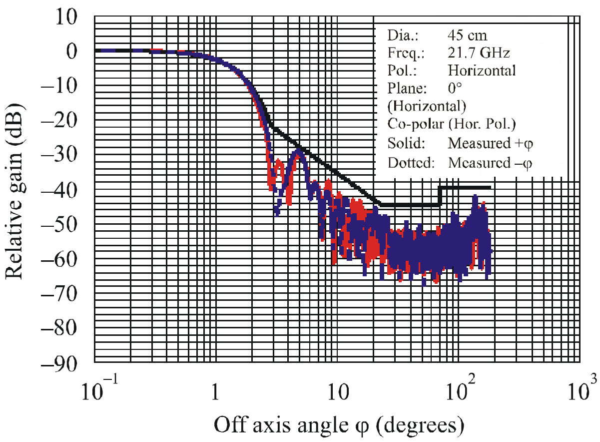

FIGURE 21-1-2b

Cross-polar pattern (45 cm, H)
(measured vs. BO.1213 mod.)

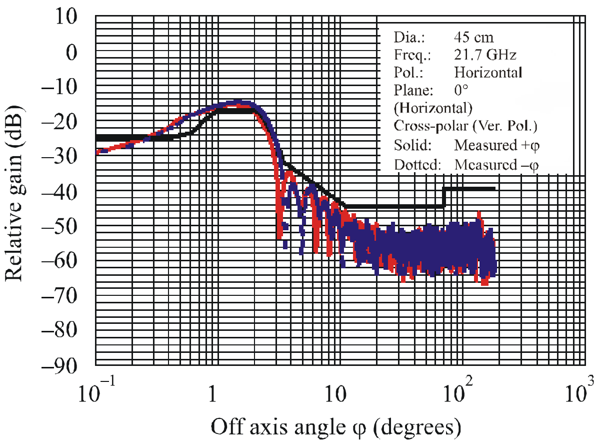

Rap 2071-2111b

FIGURE 21-2-1a

Co-polar pattern (45 cm, V)
(measured vs. calculated)

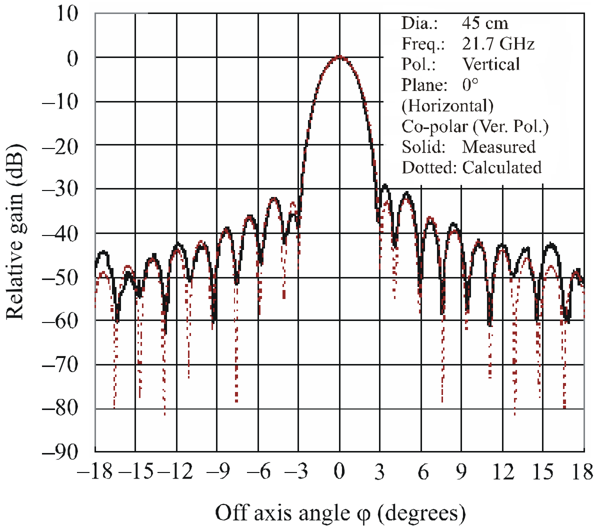

FIGURE 21-2-2a

Cross-polar pattern (45 cm, V)
(measured vs. calculated)

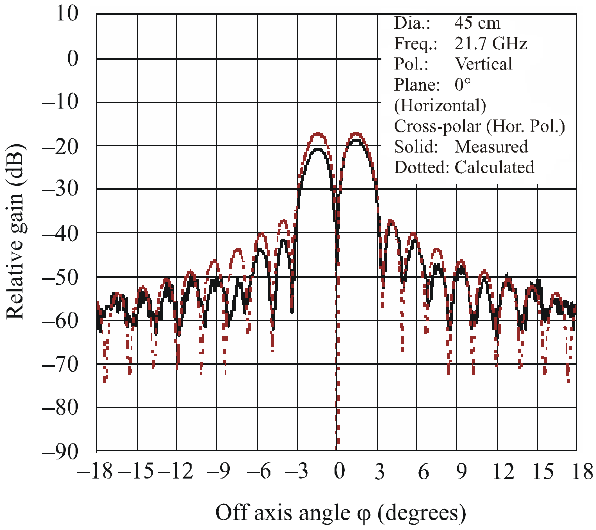

Rap 2071-2121a

FIGURE 21-2-1b

Co-polar pattern (45 cm, V)
(measured vs. BO.1213 mod.)

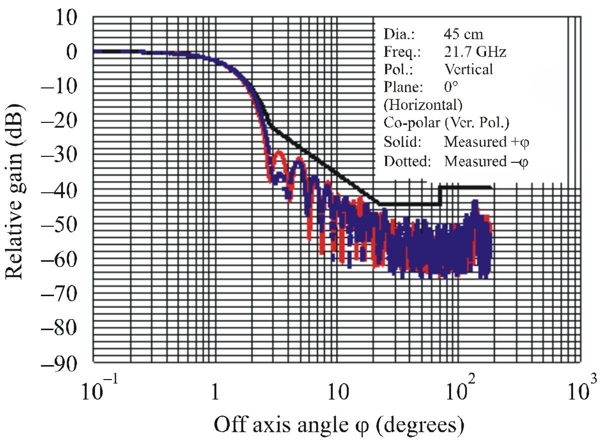

FIGURE 21-2-2b

Cross-polar pattern (45 cm, V)
(measured vs. BO.1213 mod.)

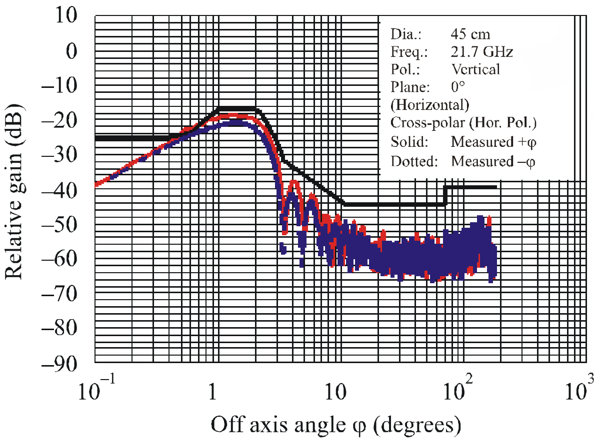

Rap 2071-2121b

FIGURE 22-1-1a

Co-polar pattern (60 cm, H)
(measured vs. calculated)

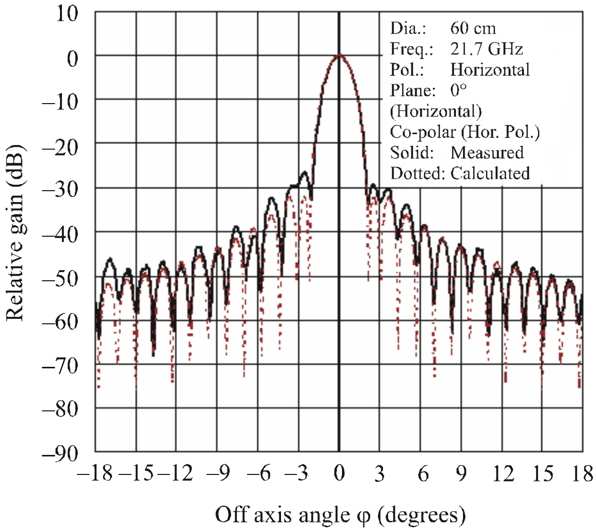

FIGURE 22-1-2a

Cross-polar pattern (60 cm, H)
(measured vs. calculated)

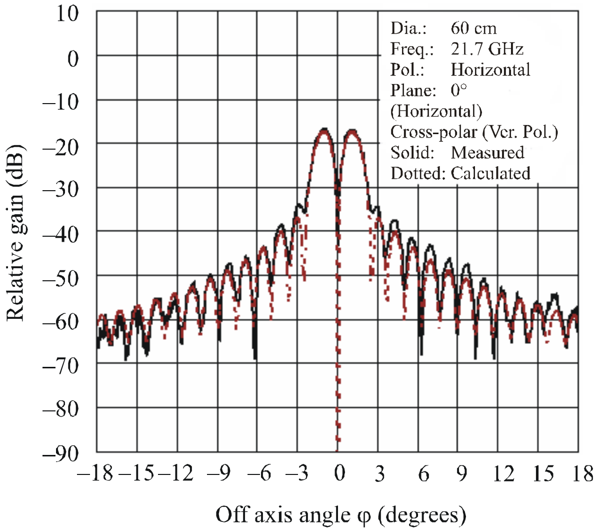

Rap 2071-2211a

FIGURE 22-1-1b

Co-polar pattern (60 cm, H)
(measured vs. BO.1213 mod.)

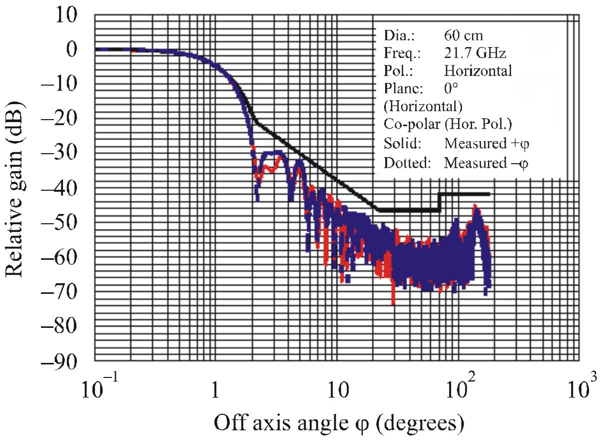

FIGURE 22-1-2b

Cross-polar pattern (60 cm, H)
(measured vs. BO.1213 mod.)

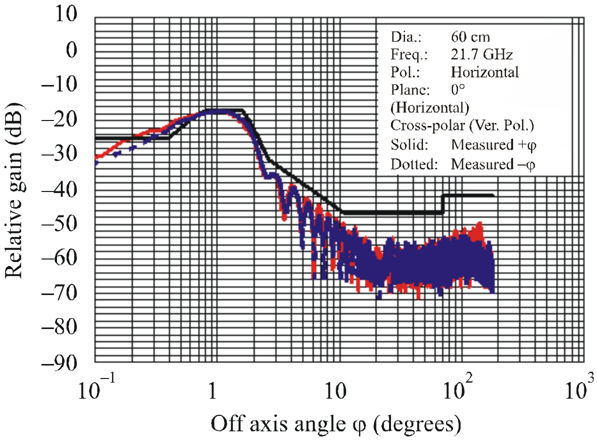

Rap 2071-2211b

FIGURE 22-2-1a

Co-polar pattern (60 cm, V)
(measured vs. calculated)

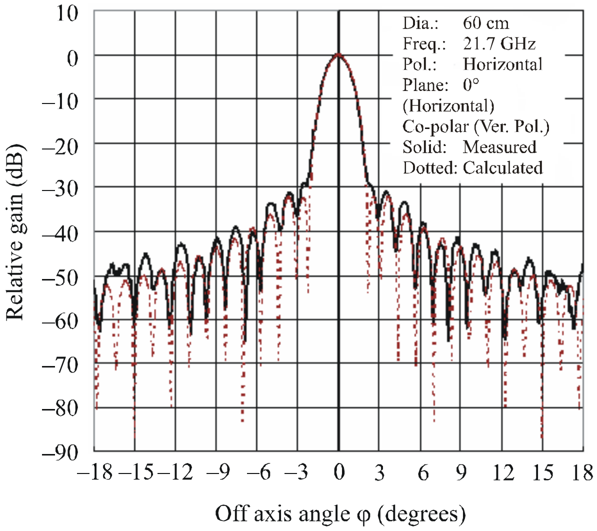

FIGURE 22-2-2a

Cross-polar pattern (60 cm, V)
(measured vs. calculated)

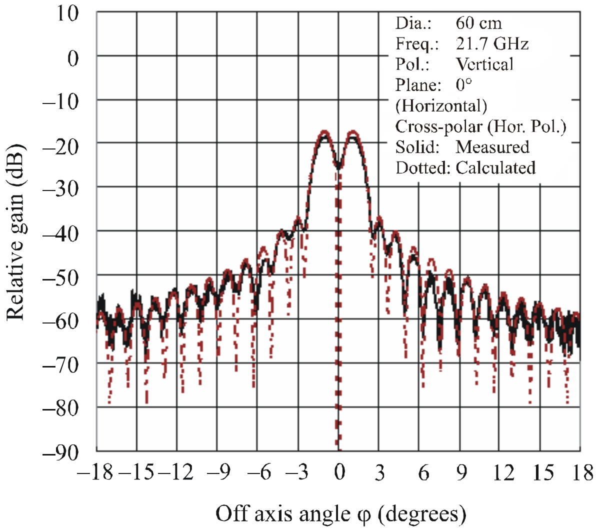

Rap 2071-2221a

FIGURE 22-2-1b

Co-polar pattern (60 cm, V)
(measured vs. BO.1213 mod.)

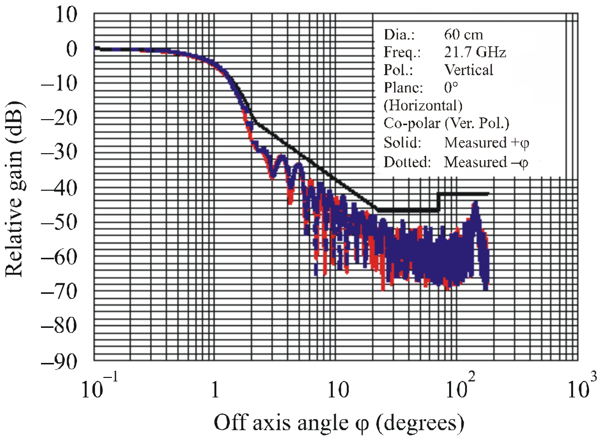

FIGURE 22-2-2b

Cross-polar pattern (60 cm, V)
(measured vs. BO.1213 mod.)

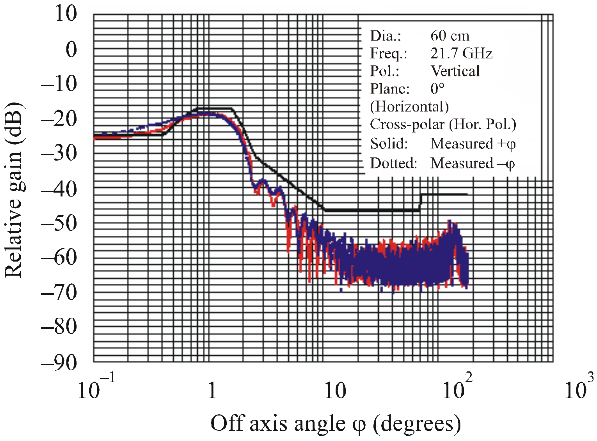

Rap 2071-2221b

3 Example of the 21 GHz band broadcasting satellites

This section deals with the following items for BSS systems with rain and other attenuation mitigation techniques by increase of satellite e.i.r.p.:

– service availability;
– attenuation caused by precipitation and other meteorological factors;
– downlink e.i.r.p. or pfd;
– channel coding.

This section also presents examples of the 21 GHz band BSS utilizing the locally-variable e.i.r.p. system (see Recommendation ITU-R BO.1659) and shows required pfd values to overcome the large rain attenuation. The locally-variable e.i.r.p. system can significantly reduce the necessary total RF power compared to conventional systems.

3.1 A promising satellite transmitting antenna technique to achieve the locally-variable e.i.r.p. system

An array-fed phased-reflector antenna employing miniature TWTs is considered as one of the promising satellite transmitting antenna techniques to achieve the locally-variable e.i.r.p. system (see Recommendation ITU-R BO.1659).

3.2 Service availability for the BSS with the increase in e.i.r.p. in the band 21.4-22 GHz

The downlink service availability of the 21 GHz band BSS is desired to be achieved at that of the 12 GHz band. Therefore, a service availability of 99.7-99.9% in a year or more is required for the 21 GHz band BSS to carry out real-time broadcasting.

3.3 Attenuation caused by precipitation and other meteorological factors in the band 21.4-22 GHz

The rain attenuations and atmospheric absorptions for some major cities in Regions 1 and 3 are tabulated in the § 5 of Appendix 1 to Annex 3 of Recommendation ITU-R BO.1659. An example of time percentage of rain attenuation calculated by Recommendation ITU-R P.618-8 is depicted in Fig. 23. The rain attenuations at 0.3% and 0.1% of time are 6.1 dB and 11.1 dB, respectively. The gaseous attenuation is 1.7 dB, the attenuation due to clouds is 1.12 dB, and the attenuation due to tropospheric scintillation is 0.42 dB. By using the equation (46) in § 2.5 of Recommendation ITU-R P.618-8, the total attenuations at 0.3% and 0.1% of time become 9.0 dB and 13.9 dB, respectively.

3.4 Downlink e.i.r.p. or pfd in the band 21.4-22 GHz

The example in Tables 10a and 10b shows the necessary pfd values to overcome the rain attenuation of 11.1 dB and 6.1 dB, which corresponds to the service availability of 99.9% and 99.7% in the case of Fig. 23 respectively, for various channel codings. The required *C*/*N* in this Table include some degradations by actual hardware such as non-linear effects of satellite transponder, etc. The peak pfd ranges from −97.2 dB(W/(m^2 · MHz)) to −110.7 dB(W/(m^2 · MHz)) for the rain attenuation of 11.1 dB, and from −102.5 dB(W/(m^2 · MHz)) to −116.0 dB(W/(m^2 · MHz)) for the rain attenuation of 6.1 dB.

The downlink e.i.r.p. can be derived from the pfd value in Table 10 and the bandwidth. The detail is discussed in the next section.

FIGURE 23

Example of rain attenuation at 21.7 GHz calculated by Recommendation ITU-R P.618-8

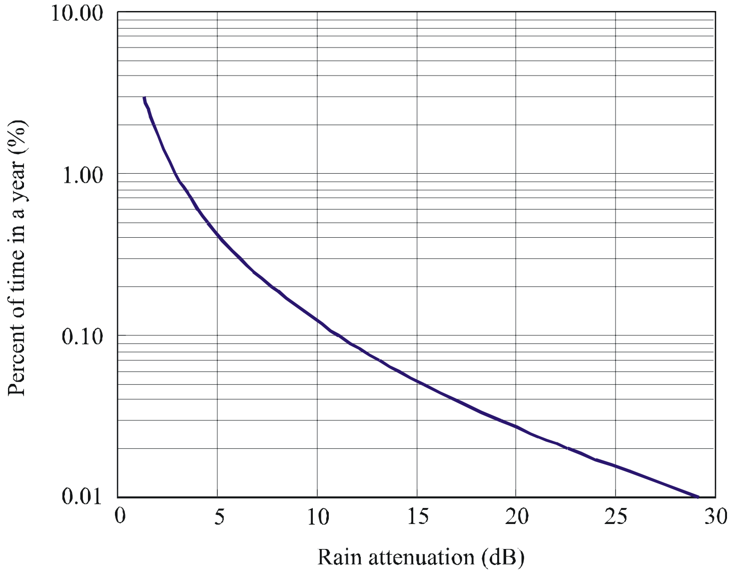

21.7 GHz
P.618-8 *R*0.01% = 56.3 mm/h
Location (135.53E, 34.65N)
Circular pol. El. = 41° El. = 220°

Rap 2071-23

TABLE 10a

The pfd values for overcoming the rain attenuation of 11.1 dB (overall propagation loss is 13.9 dB)

Modulation	Required *C*/*N*	Edge (–3 dB)	Peak
QPSK1/2	4.4 dB	–113.7 dB(W/(m^2 · MHz))	–110.7 dB(W/(m^2 · MHz))
QPSK3/4	7.5 dB	–110.6 dB(W/(m^2 · MHz))	–107.6 dB(W/(m^2 · MHz))
TC8-PSK	10.7 dB	–107.3 dB(W/(m^2 · MHz))	–104.3 dB(W/(m^2 · MHz))
16-QAM3/4	17.0 dB	–100.2 dB(W/(m^2 · MHz))	–97.2 dB(W/(m^2 · MHz))

TABLE 10b

The pfd values for overcoming the rain attenuation of 6.1 dB (overall propagation loss is 9.0 dB)

Modulation	Required *C*/*N*	Edge (–3 dB)	Peak
QPSK1/2	4.4 dB	–118.9 dB(W/(m^2 · MHz))	–116.0 dB(W/(m^2 · MHz))
QPSK3/4	7.5 dB	–115.8 dB(W/(m^2 · MHz))	–112.9 dB(W/(m^2 · MHz))
TC8-PSK	10.7 dB	–112.5 dB(W/(m^2 · MHz))	–109.5 dB(W/(m^2 · MHz))
16-QAM3/4	17.0 dB	–105.4 dB(W/(m^2 · MHz))	–102.5 dB(W/(m^2 · MHz))

3.5 Examples of BSS utilizing the locally-variable e.i.r.p. system in the band 21.4-22 GHz

Examples of BSS parameters utilizing a locally-variable e.i.r.p. system are given in the Appendix to § 3 of Annex 2. The required RF powers for these examples are shown in Table 11. In these examples, required RF powers per 1 MHz are presented. Some examples of transmitting antenna gain patterns concerning each Table as follows can be referred to the following Appendix.

TABLE 11a

Required RF power for overcoming the rain attenuation of 11.1 dB

	Locally-variable e.i.r.p. system			**Uniform**
Boosted beam diameter (% vs. nationwide beam)	200 km (2%)	300 km (5%)	400 km (7%)	–
Boosted beam gain (–3 dB)	47.5 dBi	47.3 dBi	46.7 dBi	–
Nationwide antenna gain	38.8 dBi	38.8 dBi	38.0 dBi	40.2 dBi
	Required specific RF power per MHz			
QPSK1/2	1.1 W/MHz	1.2 W/MHz	1.4 W/MHz	6.1 W/MHz
QPSK3/4	2.3 W/MHz	2.4 W/MHz	2.8 W/MHz	12.5 W/MHz
TC8-PSK	5.0 W/MHz	5.2 W/MHz	6.0 W/MHz	26.8 W/MHz
16-QAM2/3	25.3 W/MHz	26.5 W/MHz	30.4 W/MHz	135.9 W/MHz

TABLE 11b

Required RF power for overcoming the rain attenuation of 6.1 dB

	Locally-variable e.i.r.p. system			**Uniform**
Boosted beam diameter (% vs. nationwide beam)	200 km (2%)	300 km (5%)	400 km (7%)	–
Boosted beam gain (−3 dB)	44.7 dBi	45.1 dBi	44.0 dBi	–
Nationwide antenna gain	39.6 dBi	39.5 dBi	39.2 dBi	40.2 dBi
	Required specific RF power per MHz			
QPSK1/2	0.6 W/MHz	0.6 W/MHz	0.8 W/MHz	1.8 W/MHz
QPSK3/4	1.3 W/MHz	1.2 W/MHz	1.6 W/MHz	3.8 W/MHz
TC8-PSK	2.9 W/MHz	2.6 W/MHz	3.4 W/MHz	8.1 W/MHz
16-QAM2/3	14.5 W/MHz	13.3 W/MHz	17.1 W/MHz	41.0 W/MHz

It can be said from Table 11 that by employing a locally-variable e.i.r.p. system, the transmitting power can be reduced by about 7 dB or 4 dB. It should be noted that in the locally-variable e.i.r.p. system, the pfd values of the nationwide beam are significantly lower than the peak value. These lower pfd values should be taken into account in the sharing study.

3.6 Conclusion

This Report presents the relation between pfd values and the service availability values for various channel codings. In order to overcome the large rain attenuation of 11.1 dB or 6.1 dB, which corresponds to the service availability of 99.9 or 99.7% in a year, the peak pfd ranges between −97.2 dB(W/(m^2 · MHz)) and −116.0 dB(W/(m^2 · MHz)). It was also shown that by employing a locally-variable e.i.r.p. system, the transmitting RF power can be reduced by 7 dB or 4 dB compared to the uniform beam system. For the locally-variable e.i.r.p. system, the minimum pfd values should be taken into account in the sharing study.

Appendix to § 3 of Annex 2

Examples of BSS parameters utilizing a locally-variable e.i.r.p. system

Examples of BSS parameters utilizing a locally-variable e.i.r.p. are given in this Appendix for various parameters.

– The service availability: 99.7%, 99.9% of a year

– The rain attenuation: 6.1 dB for 99.7%, 11.1 dB for 99.9% of service availability

– The diameter of a boosted beam: 200 km (2%), 300 km (5%), 400 km (7%) (% compared to the nationwide beam)

– Modulation: QPSK1/2, QPSK3/4, TC8-PSK, 16-QAM3/4.

The diameter of onboard antenna is 4 m and the number of feed elements is 188. The radiation patterns are given in Fig. 24 (uniform beam), Fig. 25 (boosted beam has about 9 dB higher gain) and Fig. 26 (boosted beam has about 4 dB higher gain). Figure 28 shows an example of experimental feed array consisting of 7 mini-TWTs, and each TWT has about 10 W RF output power.

BSS system parameters, especially total RF power, are given for three cases as follows:

Case 1 – The diameter of the boosted beam is about 200 km. (Table 12)

Case 2 – The diameter of the boosted beam is about 300 km. (Table 13)

Case 3 – The diameter of the boosted beam is about 400 km. (Table 14)

In these examples, the required total RF powers for transmitting about 40 Mbit/s of information bit rate are given.

For example, the necessary peak pfd values are derived for TC8-PSK as follows:

– for 11.1 dB (99.9% of service availability): –104.5 dB(W/(m^2 · MHz))

– for 6.1 dB (99.7% of service availability): –109.5 dB(W/(m^2 · MHz))

It is interesting to compare the necessary RF power for the uniform beam system (Fig. 24) and the locally-variable e.i.r.p. system (e.g. Fig. 25a). The antenna gain of the former is 40.2 dBi and the latter is 47.5 dBi and the difference between the two is about 7 dB. That means the necessary RF power differs by 7 dB for attaining the same service availability.

The difference in the antenna gain between the uniform beam system (40.2 dBi in Fig. 24) and the nationwide beam (38.8 dBi in Fig. 25a) is 1.4 dB. It can be said that by adding 1.4 dB more RF power to the uniform beam, 11.1 dB of rain attenuation can be overcome (the 99.9% of service availability can be achieved).

TABLE 12

Examples of 21 GHz band BSS parameters utilizing a locally-variable e.i.r.p. system

(The diameter of the boosted beam is 200 km and the information rate is about 40 Mbit/s)

Link parameters				
Uplink $C/(N+I)$	24 dB			
Tx antenna diameter	4 m			
No. of feed horns	188			
Receiving antenna	Dia. = 45 cm, Effic. = 70%, NF = 1.5 dB			
Information bit rate	About 40 Mbit/s			
Modulation	**QPSK1/2**	**QPSK3/4**	**TC8-PSK**	**16-QAM3/4**
Required C/N	4.4 dB	7.5 dB	10.7 dB	17.0 dB
Channel bandwidth (99%)	54.2 MHz	35.4 MHz	26.4 MHz	17.4 MHz
Symbol rate	45.2 MBd	29.6 MBd	22 MBd	14.6 MBd
Required pfd (dB(W/(m^2 · MHz)))[(1)]	−126.6	−123.4	−120.1	−113.1
Case 1				
Service availability in a year by boosted beam	99.9% (Rain attenuation: 11.1 dB total attenuation: 13.9 dB)			
Antenna gain (Fig. 25a)	Boosted beam (−3 dB): 47.5 dBi Nationwide beam (min.): 38.8 dBi			
Total RF power (Fig. 27)	57.6 W	77.8 W	126 W	418 W
e.i.r.p. nationwide	56.4 dBW	57.7 dBW	59.8 dBW	65.0 dBW
e.i.r.p. boosted beam(–3 dB)	65.1 dBW	66.4 dBW	68.5 dBW	73.7 dBW
Peak pfd (dB(W/(m^2 · MHz)))	−111.0	−107.8	−104.5	−97.5
Boosted beam pfd (dB(W/(m^2 · MHz)))	−114.0	−110.8	−107.5	−100.5
Nationwide beam pfd (dB(W/(m^2 · MHz)))	−122.7	−119.5	−116.2	−109.2
Case 2				
Service availability in a year by boosted beam	99.7% (Rain attenuation: 6.1 dB total attenuation: 9.0 dB)			
Antenna gain (Fig. 26a)	Boosted beam (−3 dB): 44.7 dBi Nationwide beam (min.): 39.6 dBi			
Total RF power (Fig. 27)	35.6 W	48.0 W	76.0 W	258 W
e.i.r.p. nationwide	55.1 dBW	56.4 dBW	58.4 dBW	63.7 dBW
e.i.r.p. boosted beam(–3 dB)	60.2 dBW	61.5 dBW	63.5 dBW	68.8 dBW
Peak pfd (dB(W/(m^2 · MHz)))	−115.9	−112.8	−109.5	−102.4
Boosted beam pfd (dB(W/(m^2 · MHz)))	−118.9	−115.8	−112.5	−105.4
Nationwide beam pfd (dB(W/(m^2 · MHz)))	−124.0	−120.9	−117.6	−110.5

(1) The required pfd overcomes attenuation including propagation losses due to clouds, gas and tropospheric scintillation.

TABLE 13

Examples of 21 GHz band BSS parameters utilizing a locally-variable e.i.r.p. system

(The diameter of the boosted beam is 300 km and the information rate is about 40 Mbit/s)

Link parameters				
Uplink $C/(N+I)$	24 dB			
Tx antenna diameter	4 m			
No. of feed horns	188			
Receiving antenna	Dia. = 45 cm, Effic. = 70%, NF = 1.5 dB			
Information bit rate	About 40 Mbit/s			
Modulation	**QPSK1/2**	**QPSK3/4**	**TC8-PSK**	**16-QAM3/4**
Required C/N	4.4 dB	7.5 dB	10.7 dB	17.0 dB
Channel bandwidth (99%)	54.2 MHz	35.4 MHz	26.4 MHz	17.4 MHz
Symbol rate	45.2 MBd	29.6 MBd	22 MBd	14.6 MBd
Required pfd (dB(W/(m^2 · MHz)))(1)	−126.6	−123.4	−120.1	−113.1
Case 1				
Service availability in a year by boosted beam	99.9% (Rain attenuation: 11.1 dB total attenuation: 13.9 dB)			
Antenna gain (Fig. 25b)	Boosted beam (3 dB): 47.3 dBi Nationwide beam (min.): 38.8 dBi			
Total RF power (Fig. 27)	60.4 W	81.4 W	132 W	438 W
e.i.r.p. nationwide	56.6 dBW	57.9 dBW	60.0 dBW	65.2 dBW
e.i.r.p. boosted beam (–3 dB)	65.1 dBW	66.4 dBW	68.5 dBW	73.7 dBW
Peak pfd (dB(W/(m^2 · MHz)))	−111.0	−107.8	−104.5	−97.5
Boosted beam pfd (dB(W/(m^2 · MHz)))	−114.0	−110.8	−107.5	−100.5
Nationwide beam pfd (dB(W/(m^2 · MHz)))	−122.5	−119.3	−116.0	−109.0
Case 2				
Service availability in a year by boosted beam	99.7% (Rain attenuation: 6.1 dB total attenuation: 9.0 dB)			
Antenna gain (Fig. 26b)	Boosted beam (–3 dB): 45.1 dBi Nationwide beam (min.): 39.5 dBi			
Total RF power (Fig. 27)	32.4 W	43.8 W	69.4 W	235 W
e.i.r.p. nationwide	54.6 dBW	65.9 dBW	57.9 dBW	63.2 dBW
e.i.r.p. boosted beam (–3 dB)	60.2 dBW	61.5 dBW	63.5 dBW	68.8 dBW
Peak pfd (dB(W/(m^2 · MHz)))	−115.9	−112.8	−109.5	−102.4
Boosted beam pfd (dB(W/(m^2 · MHz)))	−118.9	−115.8	−112.5	−105.4
Nationwide beam pfd (dB(W/(m^2 · MHz)))	−124.5	−121.4	−118.1	−111.0

(1) The required pfd overcomes attenuation including propagation losses due to clouds, gas and tropospheric scintillation.

TABLE 14

Examples of 21 GHz band BSS parameters utilizing a locally-variable e.i.r.p. system

(The diameter of the boosted beam is 400 km and the information rate is about 40 Mbit/s)

Link parameters				
Uplink $C/(N+I)$	24 dB			
Tx antenna diameter	4 m			
No. of feed horns	188			
Receiving antenna	Dia. = 45 cm, Effic. = 70%, NF = 1.5 dB			
Information bit rate	About 40 Mbit/s			
Modulation	**QPSK1/2**	**QPSK3/4**	**TC8-PSK**	**16-QAM3/4**
Required C/N	4.4 dB	7.5 dB	10.7 dB	17.0 dB
Channel bandwidth (99%)	54.2 MHz	35.4 MHz	26.4 MHz	17.4 MHz
Symbol rate	45.2 MBd	29.6 MBd	22 MBd	14.6 MBd
Required pfd (dB(W/(m^2 · MHz)))(1)	−126.6	−123.4	−120.1	−113.1
Case 1				
Service availability in a year (Boosted beam)	99.9% (Rain attenuation: 11.1 dB total attenuation: 13.9 dB)			
Antenna gain	Boosted beam (–3 dB): 46.7 dBi Nationwide beam (min.): 38.0 dBi			
Total RF power (Fig. 27)	69.4 W	93.6 W	152 W	502 W
e.i.r.p. nationwide	56.4 dBW	57.7 dBW	59.8 dBW	65.0 dBW
e.i.r.p. boosted beam(–3 dB)	65.1 dBW	67.4 dBW	67.5 dBW	73.7 dBW
Peak pfd (dB(W/(m^2 · MHz)))	−111.0	−107.8	−104.5	−97.5
Boosted beam pfd (dB(W/(m^2 · MHz)))	−114.0	−110.8	−107.5	−100.5
Nationwide beam pfd (dB(W/(m^2 · MHz)))	−122.7	−119.5	−116.2	−109.2
Case 2				
Service availability in a year (Boosted beam)	99.7% (Rain attenuation: 6.1 dB total attenuation: 9.0 dB)			
Antenna gain	Boosted beam (–3 dB): 44.0 dBi Nationwide beam (min.): 39.2 dBi			
Total RF power (Fig. 27)	41.8 W	56.4 W	89.4 W	303 W
e.i.r.p. nationwide	65.4 dBW	56.9 dBW	58.7 dBW	64.0 dBW
e.i.r.p. boosted beam (–3 dB)	60.2 dBW	61.5 dBW	63.5 dBW	67.8 dBW
Peak pfd (dB(W/(m^2 · MHz)))	−115.9	−112.8	−109.5	−102.4
Boosted beam pfd (dB(W/(m^2 · MHz)))	−118.9	−115.8	−112.5	−105.4
Nationwide beam pfd (dB(W/(m^2 · MHz)))	−123.7	−120.6	−117.3	−110.2

(1) The required pfd overcomes attenuation including propagation losses due to clouds, gas and tropospheric scintillation.

FIGURE 24

Gain contour of onboard satellite antenna (uniform beam)

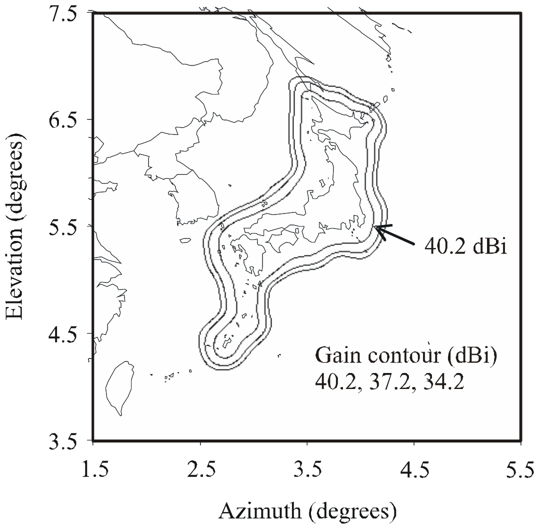

FIGURE 25a

200 km boosted and nationwide beam for service availability of 99.9%

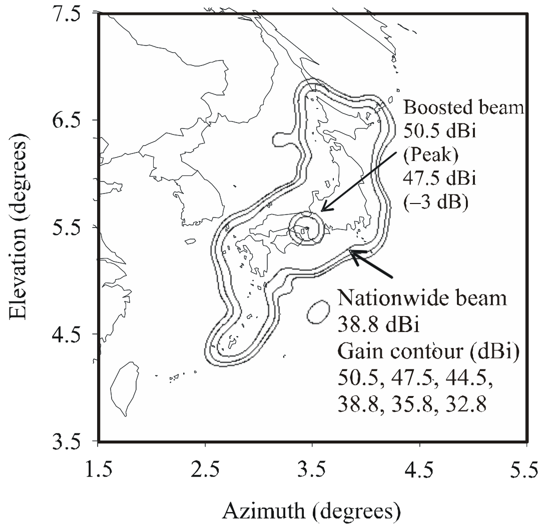

Rap 2071-2425a

FIGURE 25b

300 km boosted and nationwide beam for service availability of 99.9%

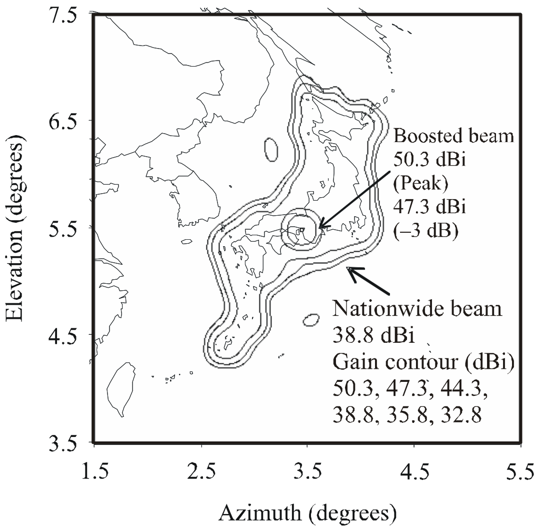

FIGURE 25c

400 km boosted and nationwide beam for service availability of 99.9%

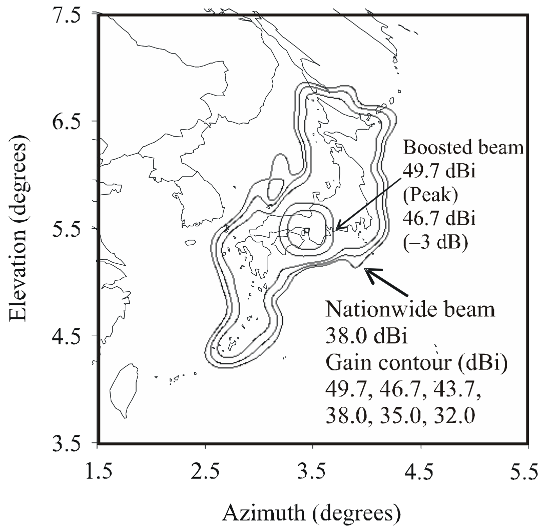

Rap 2071-25b25c

FIGURE 26a

200 km boosted and nationwide beam for service availability of 99.7%

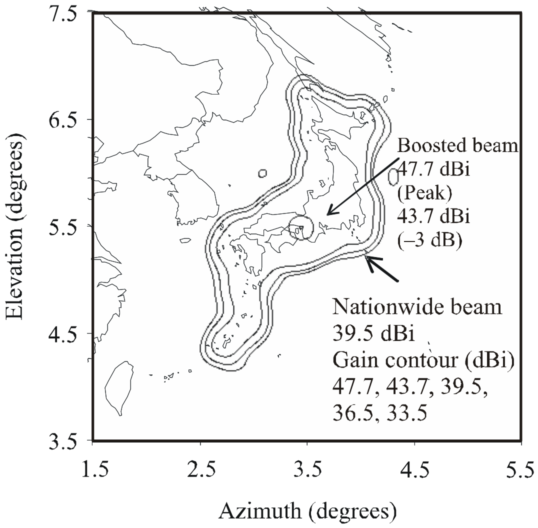

FIGURE 26b

300 km boosted and nationwide beam for service availability of 99.7%

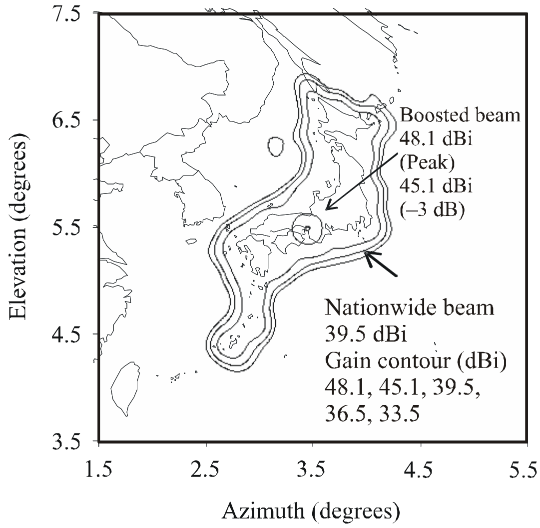

Rap 2071-26a26b

FIGURE 26c

400 km boosted and nationwide beam for service availability of 99.7%

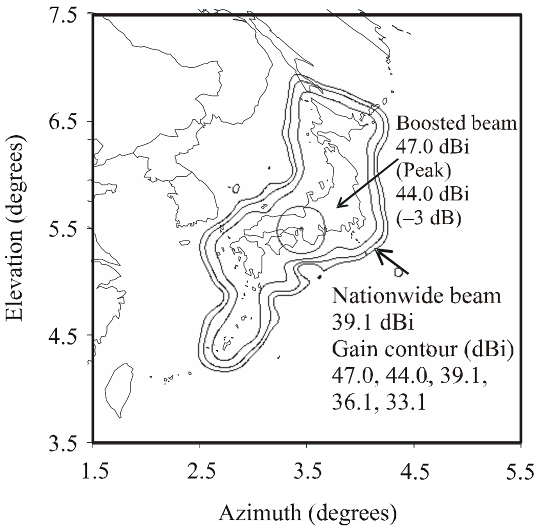

FIGURE 27

Distribution of RF power in the feed array

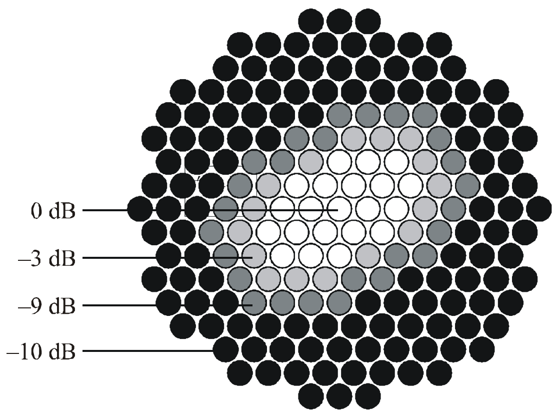

Rap 2071-26c27

FIGURE 28

Example of amplifier consisting of 7 mini-TWTs (experimental model)

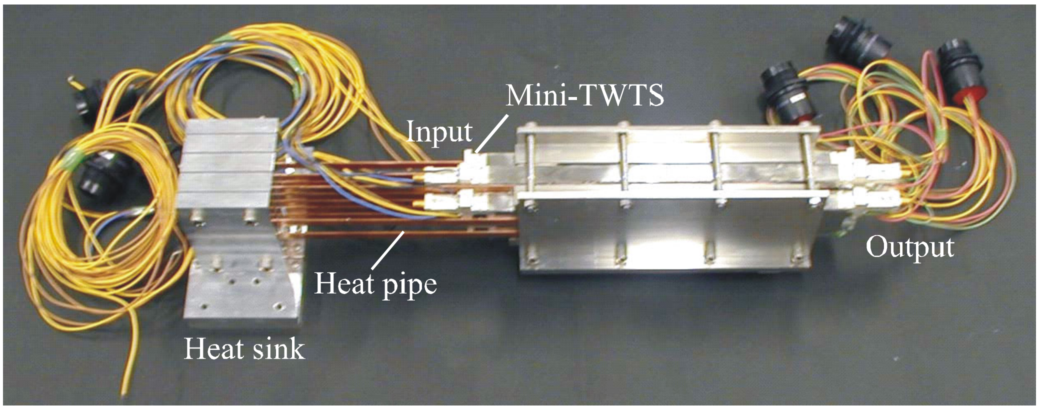

Rap 2071-28

4 A study of antenna radiation pattern of a variable e.i.r.p. broadcasting-satellite system in the 21 GHz band

4.1 Introduction

Sidelobe characteristics of satellite transmitting antenna are evaluated to reflect a rain attenuation compensating system with a phased array antenna in the Plan of BSS in the 21 GHz band. To evaluate the characteristics, grid points are set in countries surrounding Japan and the maximum sidelobe level and its location are detected for each country. Furthermore, a radiation pattern that can appear on a cut plane between the location of maximum sidelobe level and the centre of planned beam for Japan used for the Plan of BSS in the 12 GHz band is calculated for each country surrounding Japan.

4.2 Simulation of radiation pattern design

The satellite orbital location is assumed 110E. The shape of nationwide beam is approximated like the shape of Japanese territory. Grid points are set in countries surrounding Japan and the maximum sidelobe level and its location are detected for each country. Figure 29 shows constraint points used for the design of radiation pattern of satellite transmitting antenna and cities in Japan where a boosted beam is formed. Figure 30 shows the gain evaluation points to detect sidelobe level. In this simulation, the normal vector to define a zero point for each azimuth and elevation direction points the centre of Earth on the line between the satellite orbital location and the centre of Earth.

FIGURE 29

Constraint points to design the radiation pattern and cities in Japan where a boosted beam is formed

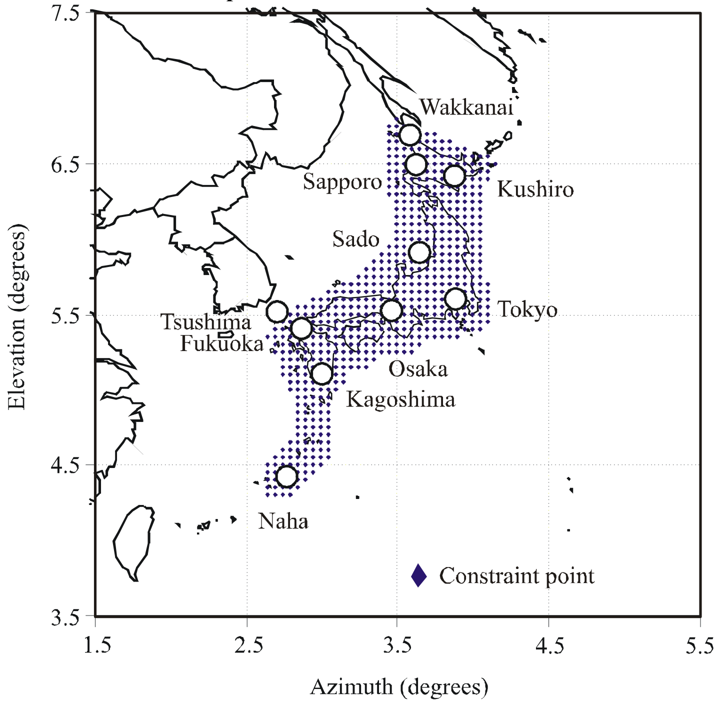

Rap 2071-29

FIGURE 30

Gain evaluation points to detect sidelobe level

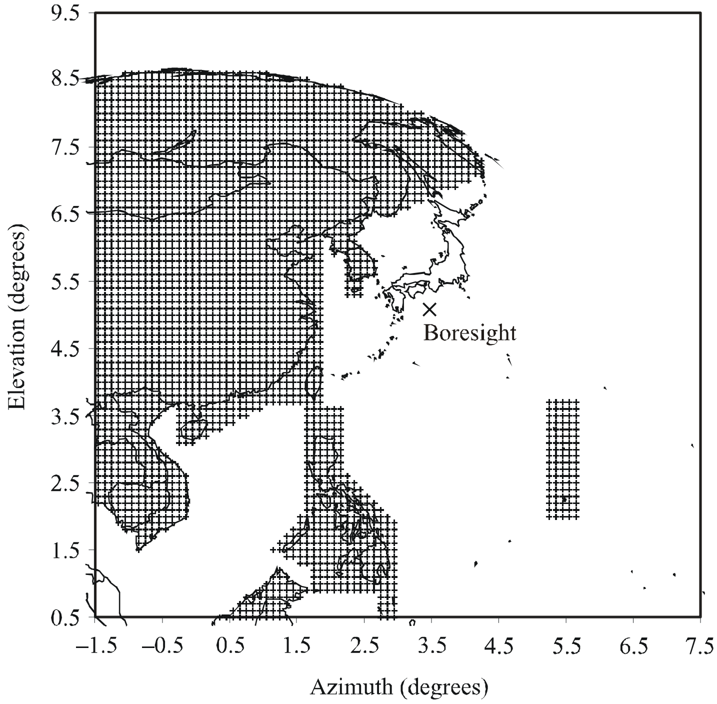

Rap 2071-30

The comparison of the pattern mask in the 12 GHz band and the radiation patterns at a cut plane in this study is conducted in the way prescribed as follows:

a) The gain of radiation pattern of cut plane is corrected to keep the antenna gain for a boosted beam generated for Wakkanai city below the antenna mask level for main beam.

b) The angle for horizontal axis is normalized by a half angle width of the planned beam.

Figure 31 shows the evaluation results. From this figure, it is found that the radiation pattern does not exceed the antenna mask.

FIGURE 31

Radiation pattern at a cut plane between the location of maximum sidelobe level and the centre of planned beam for Japan

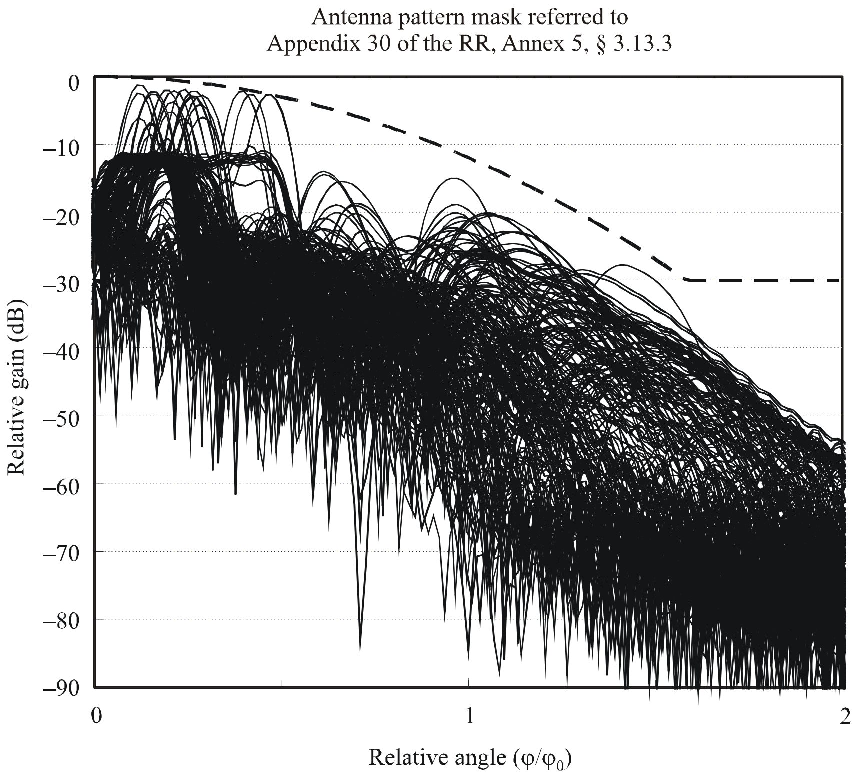

4.3 Conclusion

Sidelobe characteristics of satellite transmitting antenna are evaluated by computer simulations to reflect a rain attenuation compensating system with a phased array antenna in the Plan of BSS in the 21 GHz band. It is found that the radiation pattern for variable e.i.r.p. BSS in the 21 GHz band does not exceed the antenna mask that is shown in § 3.13.3 of Annex 5 of Appendix 30 of the RR.

5 *C*/(*N* + *I*) margins in the sharing situations for BSS in the 21 GHz band

5.1 Introduction

This section presents a study on the frequency sharing situation of BSS systems in the frequency band 21.4-22.0 GHz and associated feeder links. In this section, some calculated results of *C*/(*N* + *I*) at a receiving earth station are presented when locally-variable e.i.r.p. satellite systems are introduced. It is pointed out that, from a viewpoint of *C*/(*N* + *I*) criterion, a 6° geocentric orbital separation might allow frequency sharing between two 21 GHz BSS systems employing locally-variable e.i.r.p. with some margin over the required *C*/*N* for various channel codings. Further study is needed to evaluate the impact of *C*/(*N* + *I*) degradation on the link availability and develop a suitable sharing criteria for the 21 GHz band BSS systems.

5.2 Assumed interfering situation

Figure 32 depicts the assumed interfering situation. In this figure, satellite A is an interfered-with conventional satellite and satellite B is a locally-variable e.i.r.p. satellite as an interferer. Both satellites cover the same service area with the same polarization and the receiving earth stations for both satellites are located at the same ground area. These satellites are separated by θ_g° (geocentric) from each other. Satellite B and the transmitting earth station B cause interference to the reception at receiving earth station A that receives wanted signals from the satellite A. Satellite B is assumed to employ the locally-variable e.i.r.p. satellite system and emits radiowaves to the earth receiving station B on the ground where the receiving earth station A is also located.

FIGURE 32

Assumed interfering situation

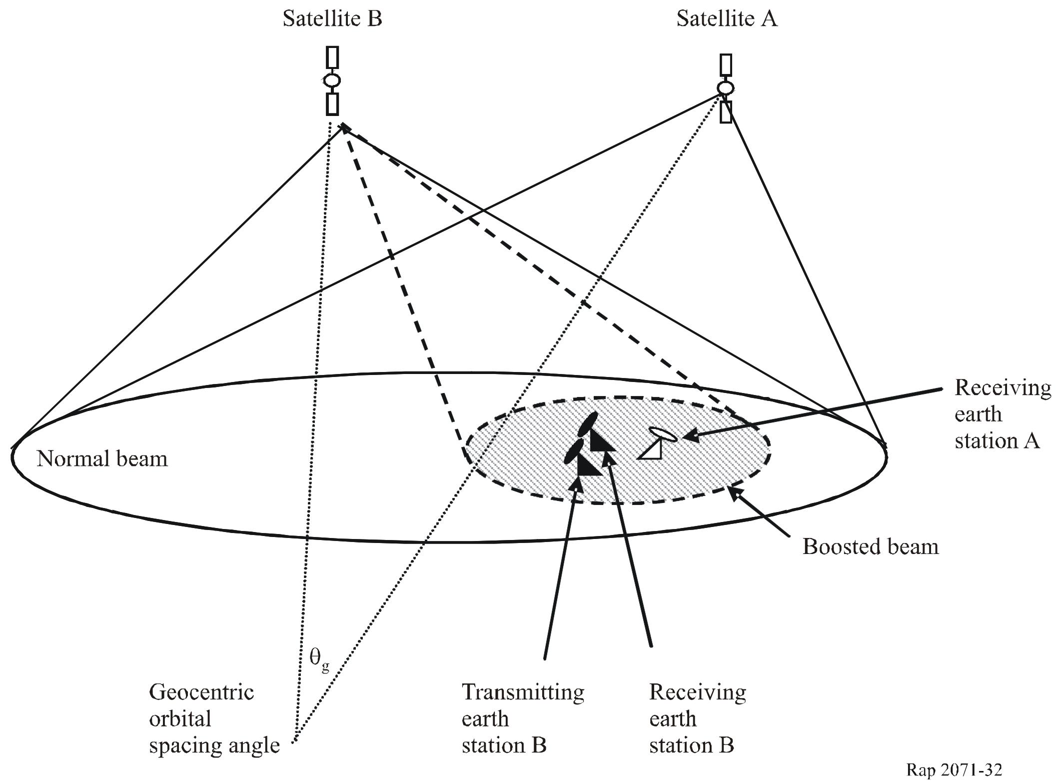

5.3 An example of BSS system parameters for this study

An example of BSS system parameters for this study is shown in Table 15. The boosted beam antenna gain and the normal beam antenna gain are cited in Table 11a. The modulation schemes and their required *C*/*N* are also referred to in Table 10a.

TABLE 15

System parameters for BSS

Item	Symbol	Unit	Value (as an example)	Remarks
Transponder power of satellite A	p_S	W/MHz	5.0 for TC8-PSK 2.3 for QPSK3/4 1.1 for QPSK1/2	Wanted satellite
Transmitting antenna gain of satellite A	G_S	dBi	38.8	Normal beam
Receiving antenna gain of earth station A toward satellite A	G_{E_max}	dBi	38.8	45 cm diameter parabolic antenna with efficiency of 65%
Transponder power of satellite B	p'_S	W/MHz	5.0 for TC8-PSK 2.3 for QPSK3/4 1.1 for QPSK1/2	Interfering satellite Variable e.i.r.p. system
Transmitting antenna gain of satellite B	G'_S	dBi	50.5	Boosted beam
Receiving antenna gain of earth station A toward satellite B	$G_E(\theta)$	dBi	BO.1213 applied to 21 GHz band satellite B	45 cm diameter parabolic antenna with efficiency of 65% θ is topocentric
Frequency	f	GHz	21.7	
System noise temperature	T_{System}	K	269.1	Gaseous absorption of 1.71 dB and received ground emission antenna noise temperature of 55 K is assumed
Latitude of the earth station	ξ	Degrees	34.65 N	
Difference in longitude between the satellite A and the earth station A	β	Degrees	25.53	
Propagation loss	L_{Prop}	dB	2.1	Gaseous absorption and Scintillation predicted by P.618-8

The power flux-density (pfd) produced by the boosted beam and the normal beam for each modulation scheme is shown in Table 16. Note that in this example, the difference of the pfd values between the boosted beam and the normal beam with same modulation is 11.7 dB and the maximum difference of the pfd values between the boosted beam (TC8-PSK) and the normal beam (QPSK1/2) is 18.3 dB.

TABLE 16

Power flux-density on the ground (pfd) by the boosted beam and the normal beam

Modulation scheme	Peak pfd by boosted beam (dB(W/(m^2 · MHz))	pfd by normal beam (dB(W/(m^2 · MHz))
TC8-PSK	–105.0	–116.7
QPSK3/4	–108.4	–120.1
QPSK1/2	–111.6	–123.3

5.4 Applied methodologies

The formula to calculate the $C/(N + I)$ is described as follows:

$$\left(\frac{C}{N+I}\right) = \frac{\dfrac{p_S \cdot G_S \cdot G_{E\_max}}{\left(\dfrac{4\pi l_S}{\lambda}\right)^2 \cdot L_{prop}}}{k \cdot T_{system} + \dfrac{p'_S \cdot G'_S \cdot G_E(\theta)}{\left(\dfrac{4\pi l'_S}{\lambda}\right)^2 \cdot L_{prop}}}$$

where k is Boltzmann's constant and λ is wavelength. l_S and l'_S are propagation lengths between each satellite and each receiving earth station and they are calculated by using ξ and β in Table 15. All parameters in this formula are numeric values. Other symbols in this formula are referred to in Table 15. Note that the bandwidths for C, N and I are the same and they are omitted in the above equation.

5.5 Summary of calculation results of *C*/(*N* + *I*)

5.5.1 *C*/(*N* + *I*) in the case of using same modulation scheme for the locally-variable e.i.r.p. satellite

Figure 33 shows the result of $C/(N + I)$ in the case of using the same modulation scheme between the two satellites. In this example, the pfd value of the interferer is 11.7 dB higher than that of the wanted satellite.

In the 12 GHz BSS Plan for Regions 1 and 3, many orbital position assignments are separated by an orbital spacing of 6°. Therefore, it is interesting to calculate the system margin, which is the difference between $C/(N + I)$ and the required C/N, at the orbital spacing of 6°. From Fig. 33, the system margin at the orbital spacing of 6° is obtained for each modulation scheme as in Table 17.

FIGURE 33

$C/(N+I)$ in the case of using the same modulation scheme

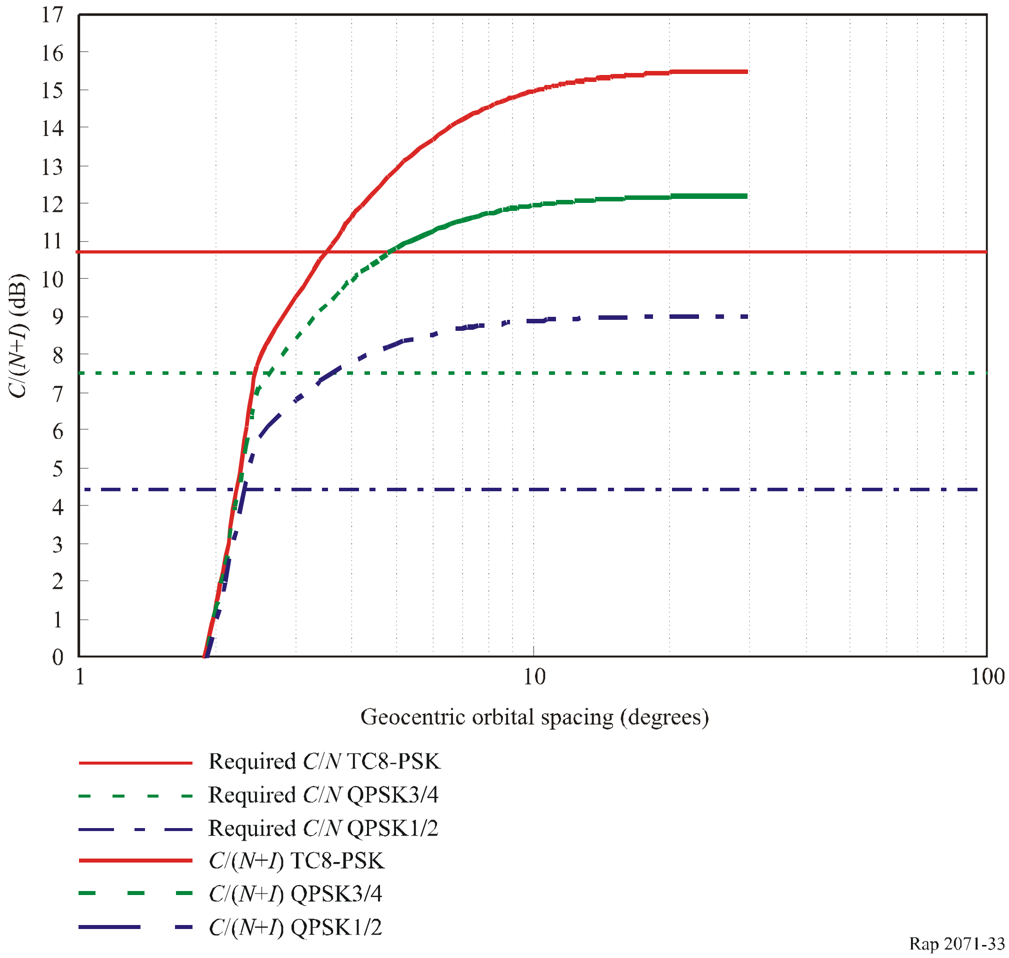

TABLE 17

System margin at the orbital spacing of 6°

Modulation scheme	**System margin at the orbital spacing of 6° (dB)**
TC8-PSK	3.0
QPSK3/4	3.8
QPSK1/2	4.1

5.5.2 *C*/(*N* + *I*) in the case of using different modulation schemes for the locally-variable e.i.r.p. satellite

Figures 34 and 35 show the result of *C*/(*N* + *I*) in the case of using different modulation schemes between the wanted and one (Fig. 34) or two (Fig. 35) interfering satellites when using a 45 cm antenna. In this evaluation, it is assumed that satellite B always uses TC8-PSK as its modulation scheme with a boosted beam. The maximum difference of the pfd values between the boosted beam is 18.3 dB when satellite A uses QPSK1/2.

FIGURE 34

***C*/(*N* + *I*) in the case of using different modulation schemes (1 interfering satellite, 45 cm antenna)**

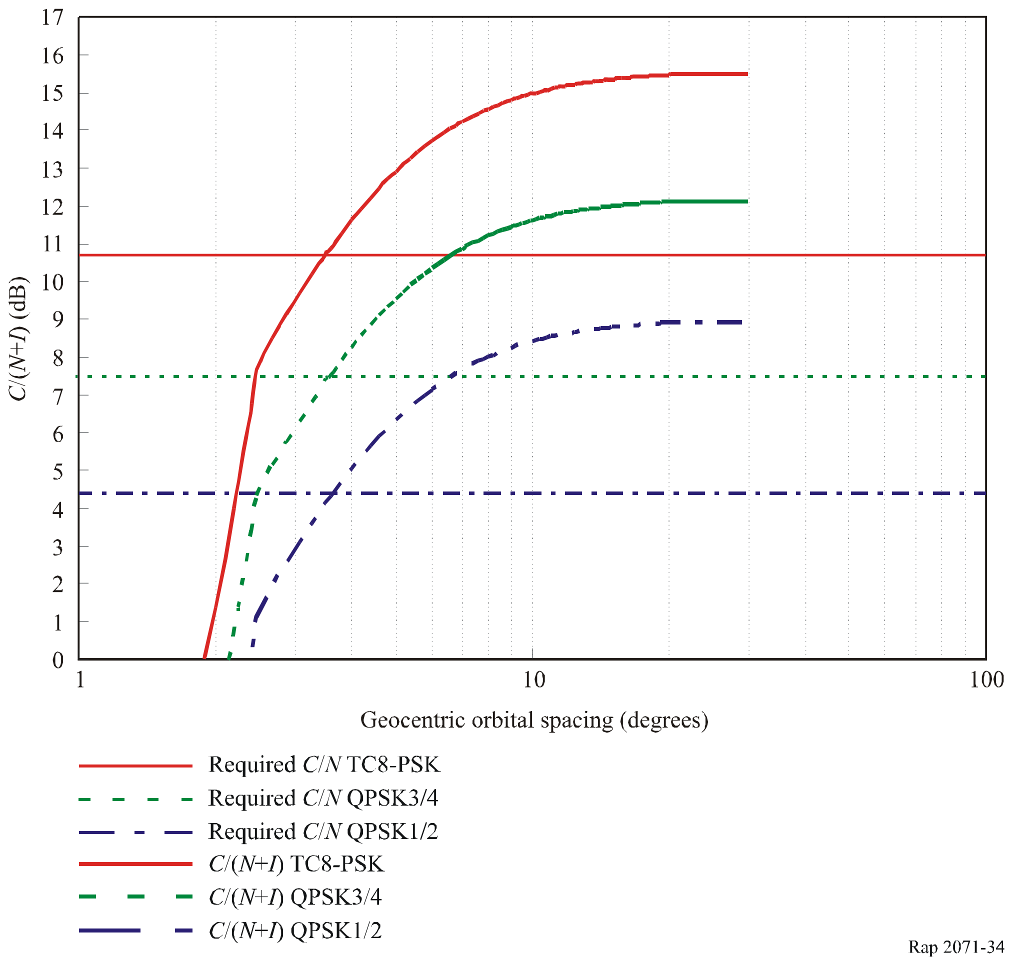

Rap 2071-34

FIGURE 35

C/(N + I) in the case of using different modulation schemes (2 interfering satellites, 45 cm antenna)

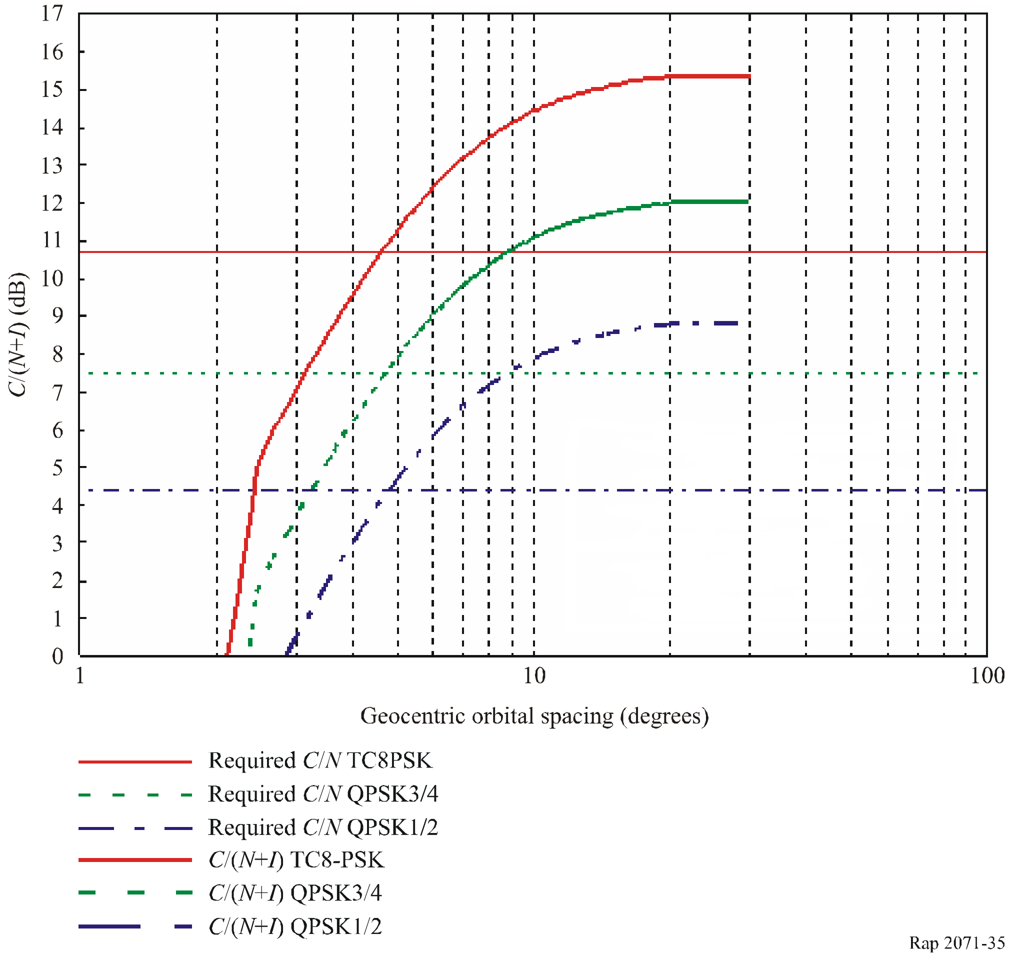

Rap 2071-35

From Figs. 34 and 35, the system margin at the orbital spacing of 6° is obtained for each modulation scheme as in Table 18 when a 45 cm antenna is used.

TABLE 18

System margin at the orbital spacing of 6° (45 cm antenna)

Modulation scheme	System margin at the orbital spacing of 6° (dB) (1 interfering satellite)	System margin at the orbital spacing of 6° (dB) (2 interfering satellite)
TC8-PSK	3.0	1.7
QPSK3/4	2.8	1.5
QPSK1/2	2.7	1.4

Table 19 shows the system margin at the orbital spacing of 6° when a 60 cm antenna is used.

TABLE 19

System margin at the orbital spacing of 6° (60 cm antenna)

Modulation scheme	System margin at the orbital spacing of 6° (dB) (1 interfering satellite)	System margin at the orbital spacing of 6° (dB) (2 interfering satellites)
TC8-PSK	5.5	4.2
QPSK3/4	5.3	4.0
QPSK1/2	5.2	3.9

5.5.3 Consideration of the worst case of $C/(N+I)$ margin for the receiving earth station A and its duration of interference

From Table 18, it is shown that there is $C/(N+I)$ margin of about 3 dB for the receiving earth station A in the shaded area in Fig. 32 even though satellite B has a boosted beam in the same area. This margin is considered as the worst case of $C/(N+I)$ margin for the receiving earth station A because the $C/(N+I)$ margin can be increased if satellite A also employs the same locally-variable e.i.r.p. system and increases its e.i.r.p. for the shaded area when rain attenuation in the area becomes large. Furthermore, the high e.i.r.p. interference from satellite B will not last for a long time. The aggregate duration of the worst case of $C/(N+I)$ margin is same as the duration of the highest e.i.r.p. situation and such duration seems to be a few percentages of time in a year.

5.5.4 $C/(N+I)$ when using conventional BSS

As a reference, the same calculation of $C/(N+I)$ at a receiving earth station when using conventional BSS that do not employ locally-variable e.i.r.p. satellite systems are presented in the Appendix.

5.6 Conclusion

The results of this study show the system margins in terms of $C/(N+I)$ at the orbital spacing of 6° for several modulation schemes. The $C/(N+I)$ margin is about 3 dB or 1.4 dB respectively for one or two interfering variable e.i.r.p. satellites at the 6° separations in the normal beam area of the conventional BSS systems when using 45 cm antennas. The $C/(N+I)$ margin is about 5 dB or 4 dB respectively for one or two interfering variable e.i.r.p. satellites at the 6° separations in the normal beam area of the conventional BSS systems when using 60 cm antennas. These margins are the worst case and these values can not become worse, if the conventional satellites also employ the same locally-variable e.i.r.p. system and increase its e.i.r.p. when rain attenuation in the area becomes large.

Appendix to § 5 of Annex 2

Summary of calculation results of $C/(N + I)$ when using conventional BSS

1 $C/(N + I)$ in the case of using same modulation scheme

Figure 36 shows the result of $C/(N + I)$ in the case of using the same modulation scheme between two satellites that are conventional BSS. In this example the pfd value of the interferer is equal to that of the wanted satellite.

FIGURE 36

$C/(N+ I)$ in the case of using the same modulation scheme

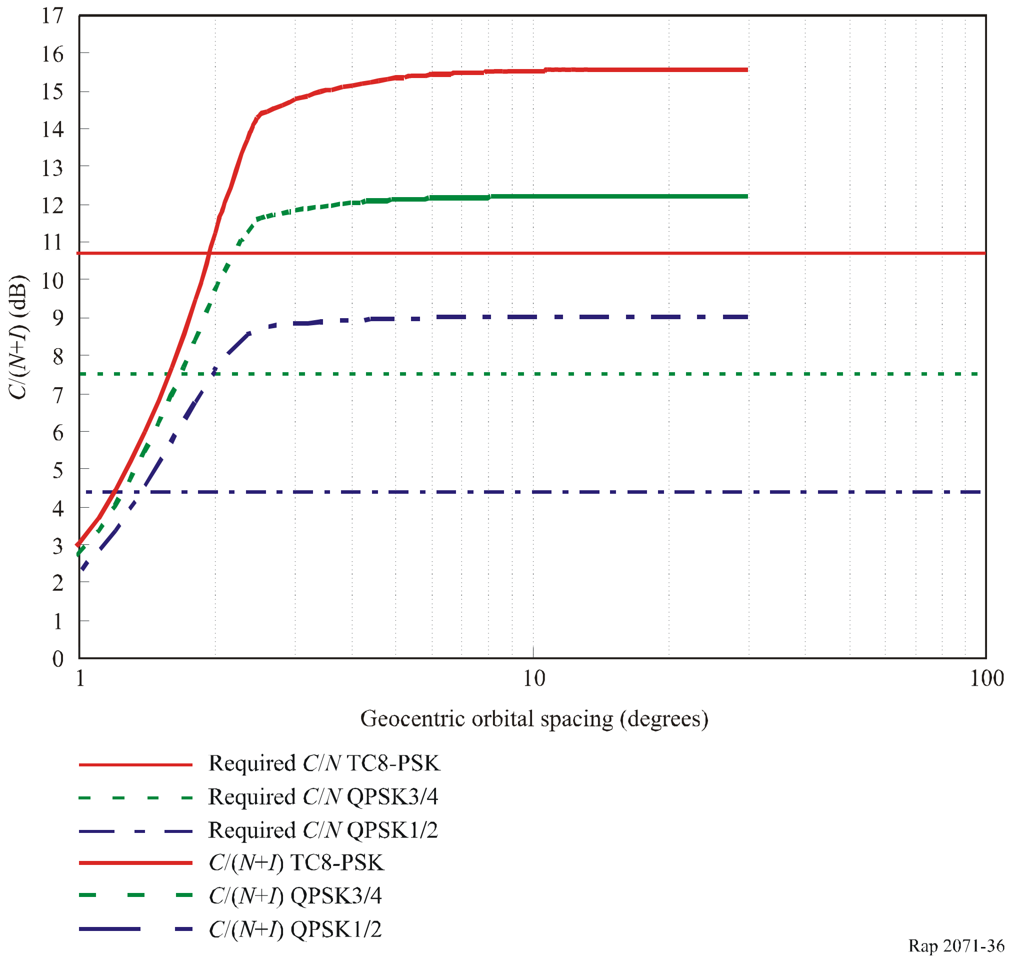

From Fig. 36, the system margin at the orbital spacing of 6° is obtained for each modulation scheme as in Table 20.

TABLE 20

System margin at the orbital spacing of 6°

Modulation scheme	System margin at the orbital spacing of 6 ° (dB)
TC8-PSK	4.7
QPSK3/4	4.6
QPSK1/2	4.6

2 *C*/(*N* + *I*) in the case of using different modulation schemes

Figure 37 shows the result of *C*/(*N* + *I*) in the case of using different modulation schemes between the two satellites. In this evaluation, it is assumed that satellite B always uses TC8-PSK as its modulation scheme. The maximum difference of the pfd is 6.6 dB when satellite A uses QPSK1/2.

FIGURE 37

***C*/(*N* + *I*) in the case of using different modulation schemes**

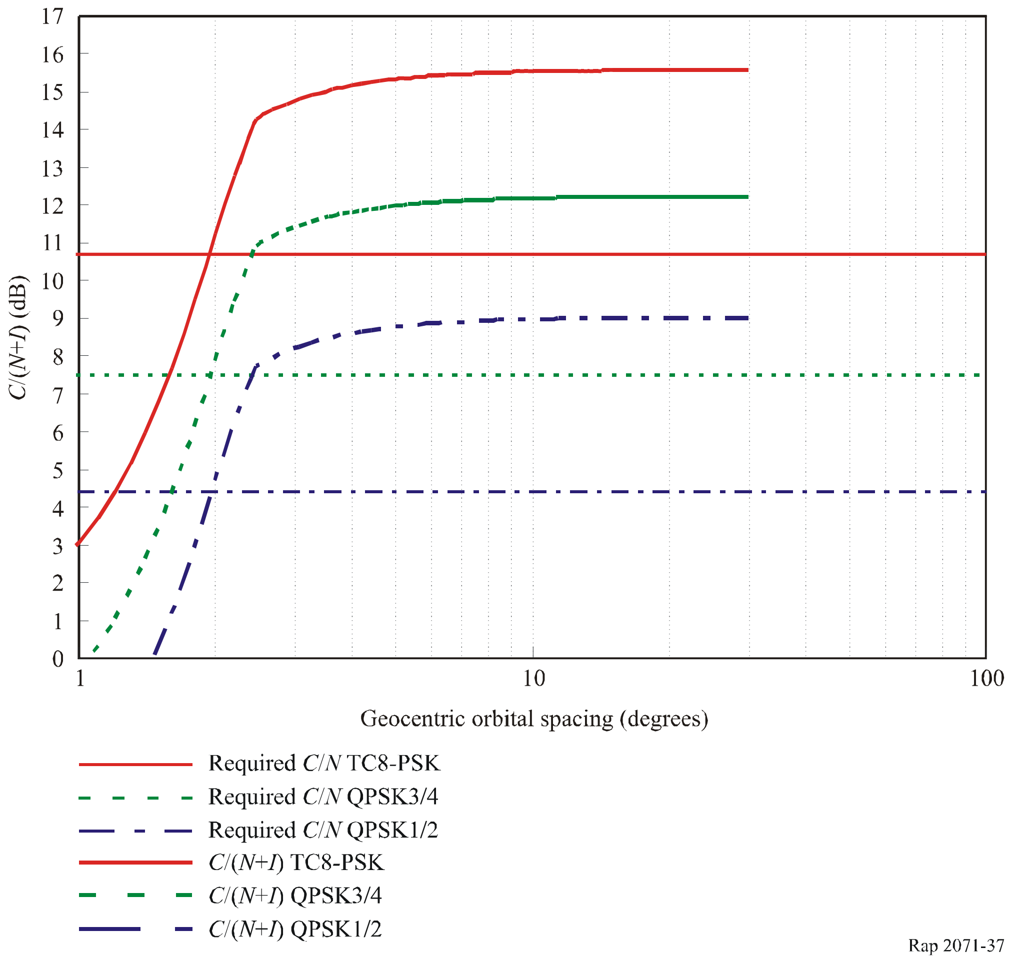

From Fig. 37, the system margin at the orbital spacing of 6° is obtained for each modulation scheme as in Table 21.

TABLE 21

System margin at the orbital spacing of 6°

Modulation scheme	System margin at the orbital spacing of 6° (dB)
TC8-PSK	4.7
QPSK3/4	4.6
QPSK1/2	4.5

6 Methodology to estimate unwanted emissions from BSS (21.4-22.0 GHz)

6.1 Introduction

This section contains a methodology to estimate unwanted emission from BSS (21.4-22.0 GHz) falling into the RAS band (22.21-22.5 GHz) and presents study results.

6.2 Methodology

6.2.1 Technical items in regard to unwanted emissions

Technical items to be studied to estimate unwanted emissions are as follows:

BSS system parameters:

1 transmission characteristics: modulation, symbol rate, bandwidth, centre frequency, rolloff factor, etc.;

2 downlink e.i.r.p. (or pfd);

3 other parameters.

Sources of unwanted emissions (RR 1.146):

1 spectral regrowth of digital-modulated signals due to non-linearity of satellite transponders;

2 uplink spectral regrowth due to non-linearity of uplink transmitter;

3 thermal noise from satellite receivers ;

4 noise originating from high power TWT amplifier;

5 intermodulation products (in the case of multicarrier transponders);

6 other sources.

The spectral power density of unwanted emissions in the RAS band will be derived from these parameters. The power of unwanted emissions with an arbitrary reference bandwidth is to be calculated from the integration of the spectral density over the span, which is in line with the methodology in Annex 1 to Recommendation ITU-R SM.1633.

6.2.2 Example of analysis of unwanted emissions falling into the RAS band

The power flux-density of unwanted emissions due to the aforementioned sources falling into the RAS band is expressed in the function of frequency as:

$$P(f) = 10\ \log\left[\sum_{n=1}^{N} 10^{\,PFD^{n}/10} \times \left[\frac{1}{10^{\,P_R^n/10}} + \frac{1}{10^{\,P_T^n/10}} + \frac{1}{10^{\,P_{UR}^n/10}} + \frac{1}{10^{\,P_{UN}^n/10}} + \frac{1}{10^{\,IM^{n}/10}}\right]\right] \quad \text{dB}$$

$$P_R^n = P_{reg}^n(f) + F_{OMUX}^n(f) \qquad \text{dB}$$

$$P_T^n = P_{TWT}^n(f) + F_{OMUX}^n(f) \qquad \text{dB}$$

$$P_{UR}^n = P_{Up-R}^n(f) + F_{OMUX}^n(f) + F_{IMUX}^n(f) \qquad \text{dB}$$

$$P_{UN}^n = P_{Up-N}^n(f) + F_{OMUX}^n(f) + F_{IMUX}^n(f) \qquad \text{dB}$$

$$IM^{n} = \sum_{m=1, m\neq n}^{N} IM_m^n(f) + F_{OUT}^n(f) \qquad \text{dB}$$

where:

$P(f)$: power flux-density of unwanted emissions (dB(W/(m^2 · Hz)))

PFD^n: maximum power flux density of n-th channel transmission signals (dB(W/(m^2 · Hz)))

$P_{reg}^n(f)$: level of regrowth due to satellite transponder relative to the PFD^n (dB)

$P_{TWT}^n(f)$: level of TWT noise relative to the PFD^n (dB)

$P_{Up-R}^n(f)$: level of uplink regrowth relative to the PFD^n (dB)

$P_{Up-N}^n(f)$: uplink noise relative to the PFD^n (dB)

IM_m^n: intermodulation products relative to the PFD^n between n-th channel signal and other any m-th channel signals for a multicarrier transmission transponder (dB)

$F_{OMUX}^n(f), F_{IMUX}^n(f)$: out-mux, or in-mux filter rejection value (dB)

$F_{OUT}^n(f)$: output filter rejection value for a multicarrier transmission transponder (dB)

f: frequency

N: maximum number of broadcasting channels.

The interference power of an arbitrary reference bandwidth can be expressed in integral form;

$$I = \int_{f_1}^{f_2} P(f)\mathrm{d}f$$

where:

I: interference power within reference bandwidth (dB(W/m^2))

f_1, f_2: lower and upper frequency of reference band.

Unwanted emissions were estimated based on this methodology.

Thermal noise and intermodulation products were considered in Document 10-11S/151 (12 May 1999), on which the figures in Annex 12 to Recommendation ITU-R SM.1633 are based. However, the transponders of BSS satellites are usually operated at near saturation, and each channel is occupied by a single carrier. In this case, the spectral regrowth of a modulated signal close to the BSS upper band edge may fall into the RAS band.

6.3 Estimation of spectral regrowth of digital modulated signal due to transponder non-linearity and TWT noise falling into RAS band

The spectral regrowth from multiple broadcasting channel signals as well as noise generated from transponder components, especially travelling wave tube amplifiers (TWTA) into the RAS band (22.21-22.5 GHz) were estimated. TWTAs are widely used as final stage amplifiers of a BSS satellite because of their high efficiency and high output power capability in spite of relatively noisy characteristics.

6.3.1 Assumption of transmission parameters for BSS system and block diagram of simulation

Parameters in Table 22 were chosen for computer simulation. The impact of the non-linearity of satellite transponder on spectral regrowth was evaluated using the simulation block diagram in Fig. 38. This includes TWTA block, which is a dominant cause of regrowth, and the input/output multiplexer (I/OMUX) filters with parameters listed in Table 22. Figure 39 illustrates the power transfer and the phase shift characteristics of the TWTA. Figure 40 corresponds to the I/OMUX frequency response.

Although the rejection of filter designed on an elliptic function is not large in the out-of-band, the amplitude and phase distortions can be small within the in-band. Therefore, it is possible to transmit high bit-rate signals for the assigned bandwidth with less transmission impairment.

TABLE 22

Parameters used in analysis

Number of channels	6
Centre frequencies (GHz)	21.942/21.845/21.748/21.651/21.554/21.458
99% power bandwidth (MHz) per channel	87.1
Symbol rate per channel (MBd)	73
Channel separation (MHz)	97
Modulation	PSK
Roll-off factor	0.35 with aperture compensation
TWTA non-linear characteristics	See Fig. 39
I/OMUX filter design	Unloaded *Q* factor: 6 800 Filter type: elliptic function Order of filter: 6th (IMUX), 4th (OMUX) Frequency response: See Fig. 40

FIGURE 38

Simulation block diagram

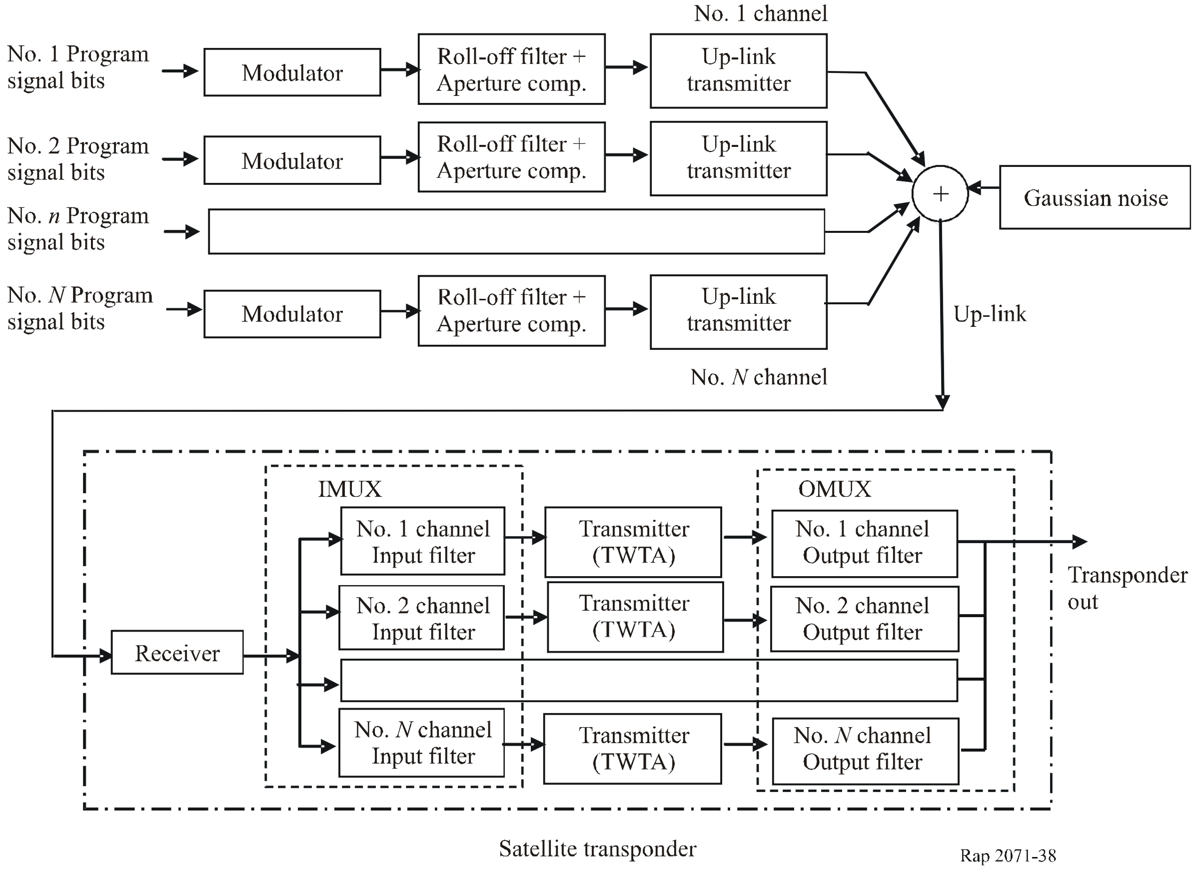

Rap 2071-38

FIGURE 39

TWTA non-linear characteristics

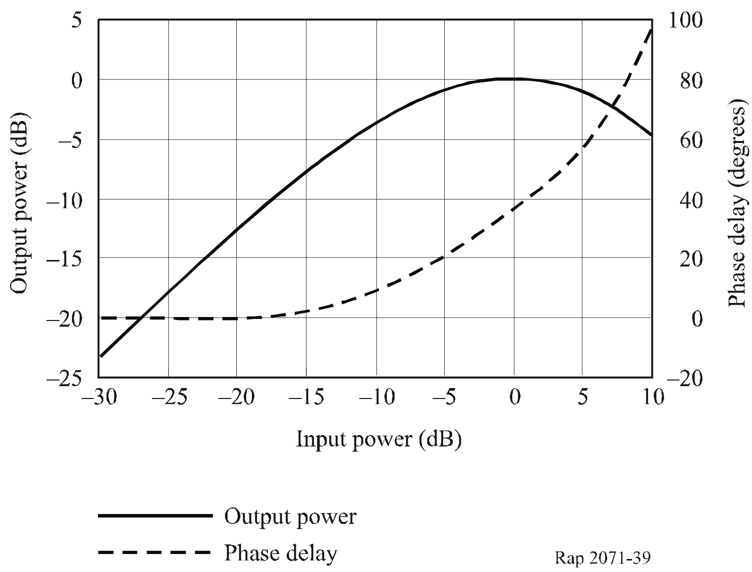

Rap 2071-39

FIGURE 40

I/OMUX frequency response

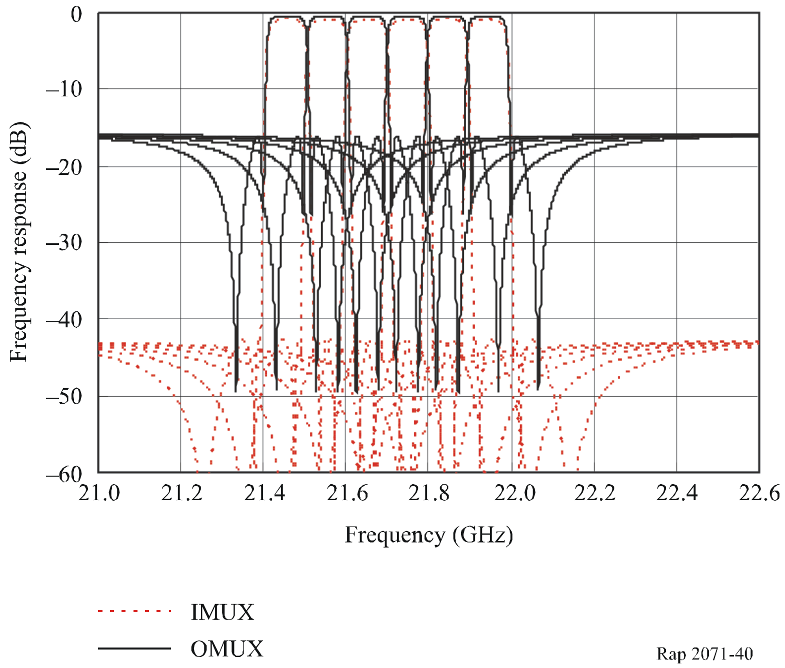

6.3.2 Spectral regrowth for PSK signal

Simulation was carried out at a TWTA output back-off of 0 dB. The normalized output power spectra of the PSK signals are plotted in Fig. 41. The bold solid line indicates the spectrum envelope of transponder output signal. The fine solid line indicates the spectrum immediately after the TWTA, which is the raw spectrum of regrowth due to non-linear amplification. The broken lines indicate each channel's output of the transponder.

FIGURE 41

Output power spectrum

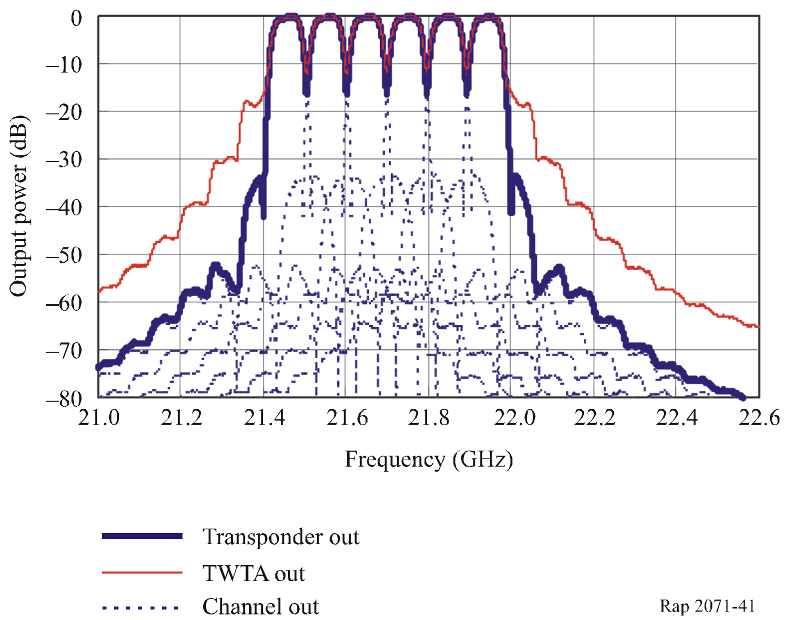

6.3.3 Estimation of noise originating from TWTA

Carrier level vs. noise ratio (*C*/*N*) at the TWTA output terminal can be evaluated as follows:

$$(C/N) = C - 10\ \log(B) - 10\ \log(T_0) - F - k \qquad \text{dB}$$

where:

- C: carrier power level converted into the input terminal of TWTA (dBW)
- B: signal bandwidth (Hz)
- T_0: temperature at input terminal (K)
- F: noise figure referred to input terminal of TWTA (dB), it might be assumed to be larger than 10 dB
- k: Boltzmann's constant –228.6 (dBJ/K)
- N: noise power converted into the input terminal originating from TWTA (dBW).

Assuming that TWTA is operated under parameters tabulated in Table 23, (*C*/*N*) can be estimated as $P_{TWT}^{n}(f)$ in the equation of § 6.2.2.

TABLE 23

Example of TWT operating parameters

C (dBW)	−30
B (MHz)	87.1[(1)]
T_0 (K)	290
F (dB)	32.5
(C/N) (dB)	62.1

(1) This value is the bandwidth listed in Table 22.

The impact of adding the noise of TWTA in the BSS transmission condition is illustrated in Fig. 42. This shows the relative power in the RAS band increased slightly in comparison with that in Fig. 41.

FIGURE 42

Output power spectrum including TWT noise

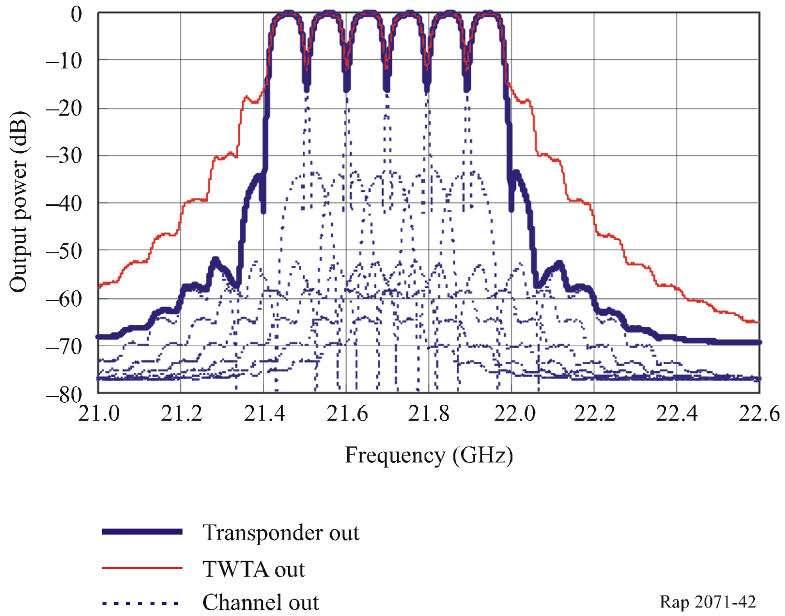

6.3.4 Improvement in the out-of-band rejection of filters

Out-of-band rejection of filters can be improved by the modification of the parameters in the elliptic filter design technique. Figure 43 shows the improvement result of OMUX filter, which has slightly moved the rejection pole position in outside of band edge.

According to the filter design, this leads to relaxing the cut-off characteristics of the filter. However, in the case of the slight modifications, the OMUX filter can be used without any significant deterioration in the 21 GHz transmission.

FIGURE 43

Improvement in the out of band rejection in the OMUX

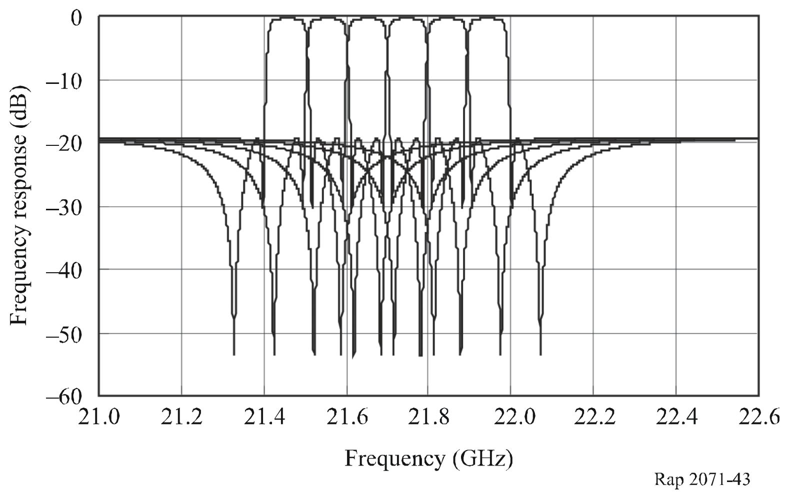

The unwanted emissions assuming the OMUX filter characteristics are illustrated in Fig. 44.

FIGURE 44

Unwanted emissions assuming the improved OMUX

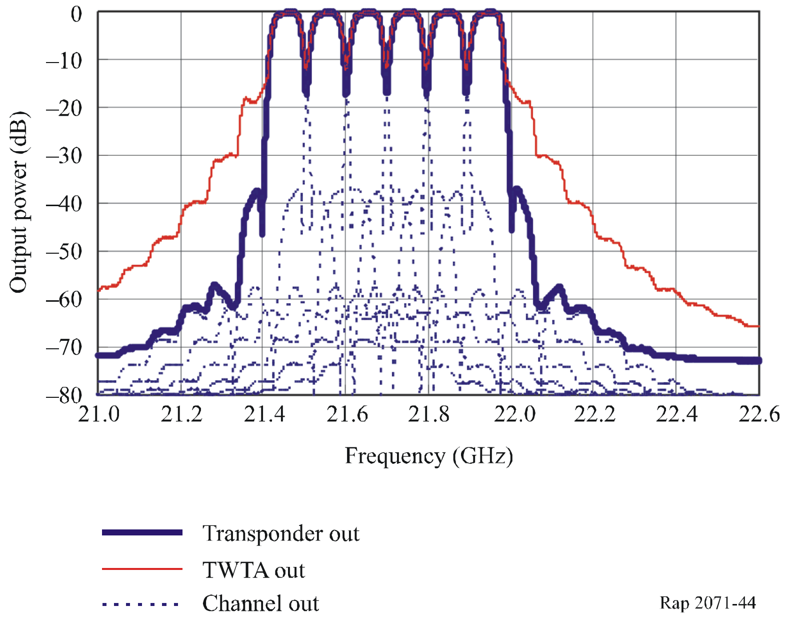

6.3.5 Unwanted emissions in the RAS band from the BSS system

Unwanted emission power density can be derived from the simulated output power spectra in Fig. 44. The integral over the RAS bandwidth of 290 MHz and the maximum calculated unwanted emission power with the reference bandwidth of 250 kHz within the band are listed in Table 24 as power ratios to in-band emission per 290 MHz and 250 kHz, respectively. The maximum emission in the 250 kHz was observed at the lower end of the RAS band. These values include a deviation margin of 2 dB for the OMUX filter rejection level.

Unwanted emission levels into the RAS band from a six-channel BSS system were calculated, as shown in Fig. 44. It was found that the narrower bandwidth of a BSS channel resulted in less unwanted emissions into the RAS band when compared with Figs. 4.5 and 4.6 in Attachment 2 of Annex 4 to Document 6S/94 (April 2005, WP 6S Chairman's Report).

TABLE 24

Calculated relative unwanted emissions in RAS band (22.21-22.5 GHz) from the BSS system

Power ratio between unwanted emission in the 290 MHz bandwidth (22.21-22.5 GHz) and in-band emission in a 290 MHz bandwidth (dB)	**Power ratio between maximum unwanted emission in a 250 kHz bandwidth within 22.21-22.5 GHz and in-band emission in a 250 kHz bandwidth (dB)**
−68.6	−64.9

Referring to Table 24, the maximum pfd level in 21 GHz band that meets all RAS threshold pfd levels shown in Recommendation ITU-R RA.769 is given in Table 25.

TABLE 6.4

Study results on maximum pfd level in the 21 GHz to meet Recommendation ITU-R RA.769 RAS threshold pfd levels

Type of observation	Continuum observations	Spectral line observations	VLBI observations
Reference bandwidth	290 MHz	250 kHz	250 kHz
Recommendation ITU-R RA.769 RAS threshold pfd levels (dB(W/m^2))	–146.0	–162.0	–128.0
Maximum pfd level in the 21 GHz band to meet ITU-R RA.769 threshold level (dB(W/(m^2 · MHz))) for each observation type	–102	–91.1	–57.1
Maximum pfd level in the 21 GHz band to meet ITU-R RA.769 threshold level (dB(W/(m^2 · MHz)))	–102 (Minimum value for the three observation types)		

In the compliance for threshold pfd levels stated in Recommendation ITU-R RA.769, as a case study, the maximum pfd level of BSS in the 21 GHz band is calculated as −102 dB(W/(m^2 · MHz)) which is the minimum value for the three observation types shown in Table 25, where the parameters shown in Table 22 and the OMUX filter characteristics depicted in the Figure are assumed.

The maximum pfd level depends very much on the channel bandwidth and the filter characteristics, and the non-linear characteristics of the transponder.

On the other hand, according to Resolution 525 (Rev.WRC-03), the threshold pfd value of BSS in the 21 GHz band is stated as –105 dB(W/(m^2 · MHz)) for angles of arrival between 25° and 90° above the horizontal plane. In the case of adhering to this threshold pfd, the margin of at least 3 dB can be attained for the threshold pfd value in Recommendation ITU-R RA.769.

The regulation in regard to the maximum pfd for BSS in the 21 GHz band is going to be discussed more in detail with treatment of Resolution 525 (Rev.WRC-03) in Study Group 6. Compatibility between RAS and BSS in the 21 GHz band is one of the important elements for determination of the maximum pfd for the BSS.

6.4 Conclusion

Compatibility studies were made to estimate unwanted emissions in the RAS band (22.21-22.5 GHz) from the BSS band (21.4-22.0 GHz).

For a 21 GHz band BSS system shown in this section, the study results shows that the maximum pfd level of −102 dB(W/(m^2 · MHz)) meets the requirement to avoid excess interference to the RAS defined in Recommendation ITU-R RA.769. These results can be used to update Table 32 in Annex 12 to Recommendation ITU-R SM.1633.

7 Transmission schemes for satellite broadcasting utilizing the receiver with a storage function

This section deals with the satellite broadcasting system assuming a storage device in the receiver. The parity-symbols time differential (PTD) transmission scheme is presented. The PTD transmission scheme aims for a non-real-time broadcasting system and an improved transmission scheme of long block-length data interleaving (see Annex 3 of Recommendation ITU-R BO.1659). The mitigation effect against the rain attenuation is simulated using the measured rain attenuation data. The simulation results for the PTD is shown and compared with the time diversity (TD), in other word repetitive transmission, in terms of the delay time, which affects the storage capacity to process signals.

7.1 Parity-symbols time differential (PTD) transmission scheme

The features of the PTD transmission scheme are as follows:

– The PTD transmission scheme allows viewers to watch the programme in real time with possible short time signal interruption caused by heavy rain attenuation.

– The parity data is produced from long block-length interleaved original data, and the parity data is transmitted after the original data with a certain time of delay.

– If the data loss occurred in the propagation path by the rain attenuation, the original data can be retrieved by correcting the received data using parity bits of an error correction code.

– The viewers can enjoy the programme without any signal interruption after a certain time from receiving the original programme data.

In this section the following items are studied from a view point of the delay time:

– suitable modulation scheme for PTD;

– comparison of PTD with TD and real-time transmission;

– dependence on the rain attenuation margin, in other words, the relation between the outage duration, frequency and the delay time, which somewhat simulates the different rain zone case.

Figure 45 shows the block diagram for PTD transmission scheme. Note that the PTD part is only the left side of Fig. 45 and it is added to the real-time satellite broadcasting transmission part, which is the right side of Fig. 45, i.e. from RS(204,188) encode to RS(204,188) decode.

Figure 46 shows a frame structure of the PTD transmission scheme. The definitions of abbreviations appeared in Fig. 45 and Fig. 46 and their example values are given in Table 26.

FIGURE 45

Block diagram for PTD transmission scheme

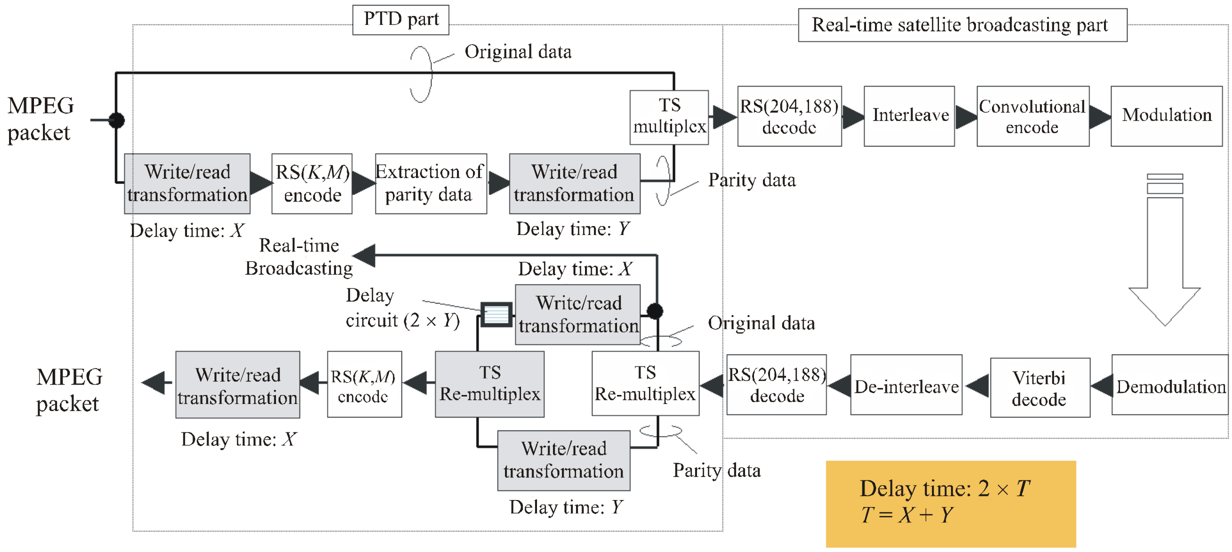

T:	Storage time (= *X* + *Y*)
TS:	Transport stream
RS[*K*,*M*]...*K*:	Block length
M:	Data length

Rap 2071-45

FIGURE 46

Frame structure in the PTD part in Fig. 45

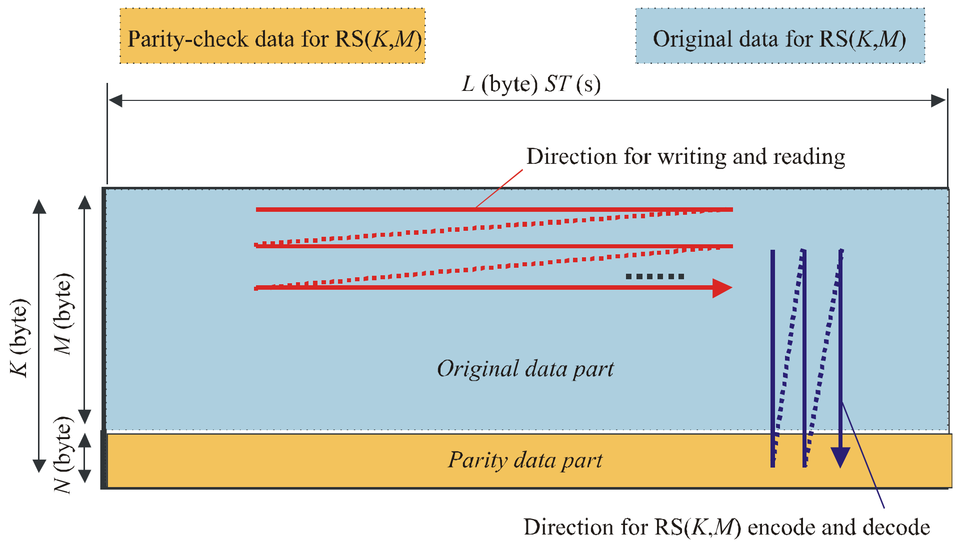

Rap 2071-46

FIGURE 47

Time differential transmission for the parity symbols in PTD transmission scheme (when observed at the TS multiplex block in the PTD part in Fig. 45)

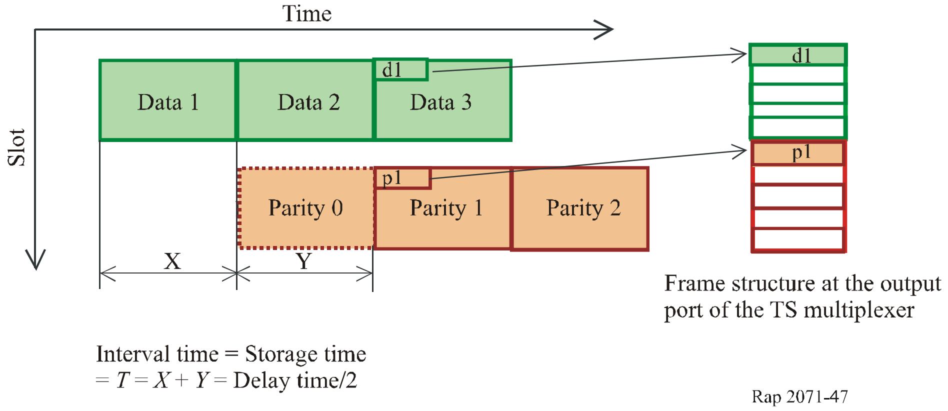

TABLE 26

Definitions of abbreviations in Fig. 45 and Fig. 46 and their example values

Abbreviation	Definition	Example value
T	Storage time $K \times ST = X + Y$ $X = M \times ST$, $Y = N \times ST$	$T = 4$ h $X = Y = 2$ h
RS(K, M)	Reed-Solomon parity code for PTD K: block length, M: data length	$K = 200$ (byte) $M = 100$ (byte)
N	Parity code length: $N = K - M$	100 (byte)
R	Transmission rate of input MPEG packet = speed of writing data to a storage	90 (Mbit/s)
	Transmission rate at the output of TS multiplex for TC8PSK	About 180 (Mbit/s)
	Nyquist bandwidth	97.7 (MHz)
ST	Time of writing data L in a row of a PTD frame $ST = T/K = L/R$	72 (s)
L	The number of bytes in a row of a PTD frame $L = R \times ST$	810 (Mbyte)

The write/read transformation block in the left upper side of Fig. 45 writes the original data to a row direction of which length is L byte in a ST time duration. Then the parity check code is calculated to a column direction and added to the bottom at the RS(K, M) encode block. The parity data is read to a row direction and sent to the TS multiplex block.

In this document, the delay time is defined as the time difference between the start of the real-time broadcasting programme and the start of the non-real-time broadcasting programme at the receiver. Fig. 47 depicts the frame sequence when observed at the entrance of the TS (transport stream) multiplex block in Fig. 45. In the Fig. 47 case, the size of each "data" frame is same as the size of each "parity" frame. The storage device is located at the 5 "write/read transformation" blocks in Fig. 45. At the "write/read transformation" block the writing and reading is carried out in the row direction and the RS(K, M) encoding and decoding is carried out in the column direction as shown in Fig. 46. Since the speed to write data to a storage device R, which is equal to the transmission rate of the input MPEG packet, is much smaller than the speed to read data from a storage device and the other processing time can be neglected, the delay time is determined dominantly by the time to write data (in other word, storage time). The storage time is X for each original data frame and Y for each parity-check data frame, and the total storage time T is $X + Y$. The storage time T is equal to the time difference between the start of the original data and the corresponding parity data. The transmission rate at the output of TS multiplex in Fig. 45 is approximated to $R/(M/K)$, since the data packets and the parity packets are multiplexed and sent the real-time satellite broadcasting part. For example, with the parameters in Table 26, the transmission rate at the output of TS multiplex is approximated to $2 \times R$.

The storage time T is needed at the transmission side and the reception side, therefore the delay time becomes $2 \times T$. Note that the L (or ST) and K are variables and determine the delay time, however, in this document for the simplicity, K is fixed at 200 bytes and the delay time $2 \times T$ is varied by changing the L (or ST).

The time difference between the start of the original data and the corresponding parity data entering into the TS multiplex block in Fig. 45 is called the interval time in this document. For the PTD structure in Fig. 45, the interval time is approximated to the storage time, which is the time to write data to storage devices, and is equal to T as shown in Fig. 47. In order to align the original data (e.g. Data 1) and the corresponding parity data (e.g. Parity 1) at the RS(K, M) block in the receiver, a delay circuit with the delay time of $2 \times Y$ is inserted in the original data path as shown in Fig. 45. Note that the Data 1 has arrived at the TS de-multiplex earlier than the Parity 1 by T, and has been written to the write/read transmission on the original data path for the duration of X when the Parity 1 arrives at the TS de-multiplex, and the time difference between them becomes Y. The Data 1 has to further wait for the Parity 1 being written to the write/read transmission on the parity data path for the duration of Y.

The interval time can be analytically increased or decreased. The effect of the various interval time is studied in the following Appendix and is shown that the PTD transmission scheme with the interval time T is good from the viewpoints of the delay time and the equivalent outage time.

7.2 Method of simulation using the measured rain attenuation data

In a non-real-time broadcasting system, the mitigation effect against the rain attenuation is evaluated by simulation using the measured rain attenuation data with respect to the equivalent outage time in an average year or the amount of remaining incorrect data.

The rain attenuation data used in the simulation was measured every 1 second at Tokyo using satellite broadcasting wave in the 12 GHz band for almost three years (from May 2000 to December 2002). Fig. 48 shows an example of the measured rain attenuation profile. In this case, it was observed the rain attenuation of more than 12 dB. The rain attenuation margins in Fig. 48 are derived from the link budget when assuming an e.i.r.p. of 43.6 dB(W/MHz) and the receiving G/T of 12.2 dB. The rain attenuation margin of 4.9 dB and 10.6 dB corresponds to the TC8-PSK and the QPSK1/2 modulations, respectively.

Table 27 shows an example of the total outage time, which was averaged for about three years and expressed as the average value in a year, for the different modulation schemes. The maximum outage durations are also given in Table 27.

To investigate the mitigation effect of the outage time by using non-real-time transmission schemes, in the simulation, the start time of the data transmission was varied 1 s by 1 s on the time series of the rain attenuation data in order to avoid the dependence of the results on the specific rain attenuation profiles. The outage times were obtained by averaging the all results of the outage time. Since the rain attenuation data was measured with 1 s interval, the outage time was accumulated with 1 s interval.

In this section, in order to compare the mitigation effect of the outage time among various transmission schemes, the MPEG packet rate is fixed at 90 Mbit/s in the Nyquist bandwidth of 97.7 MHz (see Table 28 for example).

The mitigation effect of the non-real-time transmission scheme is evaluated by the delay time when the equivalent service outage time is zero, that means the all stored data is correct.

7.3 Simulation results of non-real-time transmission schemes

7.3.1 Modulation for PTD

By comparing some modulation parameters, it was found that the QPSK7/8 modulation gave the minimum delay time for the specific measured rain attenuation data used in this simulation. For example, the simulation result of the equivalent service outage time for QPSK3/4 and TC8-PSK are shown in Fig. 49 and the parameters are given in Table 28. From Fig. 49 it can be said that the PTD with QPSK7/8 reaches the equivalent service outage time of zero at the delay time of about 220 min, while the PTD with TC8-PSK does not approaches to zero over the delay time of 240 min.

The QPSK7/8 modulation is used for the PTD transmission scheme in the remaining part of this document.

7.3.2 Comparison of PTD with TD and real-time transmission

The PTD transmission scheme is compared with the time diversity (TD), in other words repetitive transmission, and the real-time transmission scheme QPSK1/2 under the condition that the MPEG packet rate is fixed at 90 Mbit/s in the Nyquist bandwidth of 97.7 MHz. For the TD, TC8-PSK is employed and the original data is retransmitted with an interval time, which is defined as the delay time. The parameters are given in Table 29 and the simulation result is shown in Fig. 50.

From Fig. 50 it can be said that the PTD with QPSK7/8 reaches the equivalent service outage time of zero at the delay time of about 220 min, while the TD with 8-PSK does not approaches to zero over the delay time of 600 min.

7.3.3 Dependence on the rain attenuation margin

So far the rain attenuation margin was 5.9 dB for QPSK7/8. It is interesting to see the mitigation effect with respect to the delay time. Fig. 51 and Fig. 52 show the relation between the delay time and the equivalent service outage time with the rain attenuation margin of 9 dB and 3 dB for QPSK7/8, respectively. In the larger margin case (9 dB) as well as 5.9 dB case, the PTD transmission scheme with QPSK7/8 reaches the equivalent service outage time of zero, while the equivalent service outage time of the TD transmission scheme does not always stay at zero. In the lower margin case (3 dB), the TD transmission scheme gives better performance than the PTD transmission scheme, however, it takes about 32 hours to reach zero equivalent outage time.

7.4 Conclusion

This section presents the parity-symbols time differential (PTD) transmission scheme and the time diversity (TD), in other words repetitive transmission for non-real-time broadcasting systems as mitigation techniques against the heavy rain attenuation. These transmission schemes also allow viewers to watch the programme in real time with a few outages caused by heavy rain attenuation. Suitable transmission scheme, modulation parameters and the delay time may be determined depending on the transmission rate, the rain attenuation margin, or the rain attenuation profile.

In this section, simulations were carried out under the following conditions:

– MPEG packet rate (information rate) is 90 Mbit/s in the Nyquist bandwidth of 97.7 MHz;

– the rain attenuation data was measured every 1 s at Tokyo using satellite broadcasting wave in the 12 GHz band for almost three years (from May 2000 to December 2002).

The results of the simulation are as follows:

– Suitable modulation parameter for PTD transmission scheme is the QPSK7/8 compared to other modulation parameters such as TC8-PSK or QPSK3/4.

– Comparison of PTD transmission scheme with TD transmission scheme and real-time transmission was carried out for various rain attenuation margins. With a large rain attenuation margin, the PTD with QPSK7/8 reaches the equivalent service outage time of zero, while the equivalent service outage time of the TD does not always stay at zero. With a small rain attenuation margin, the TD gives better performance than the PTD, however, it takes a lot of time (for example, about 32 h) to reach zero equivalent outage time.

This study was done with a specific rain attenuation profile for about three years. Further study is left for simulating the mitigation effect of the outage time using other rain attenuation data.

FIGURE 48

An example of rain attenuation profile in the 12 GHz band

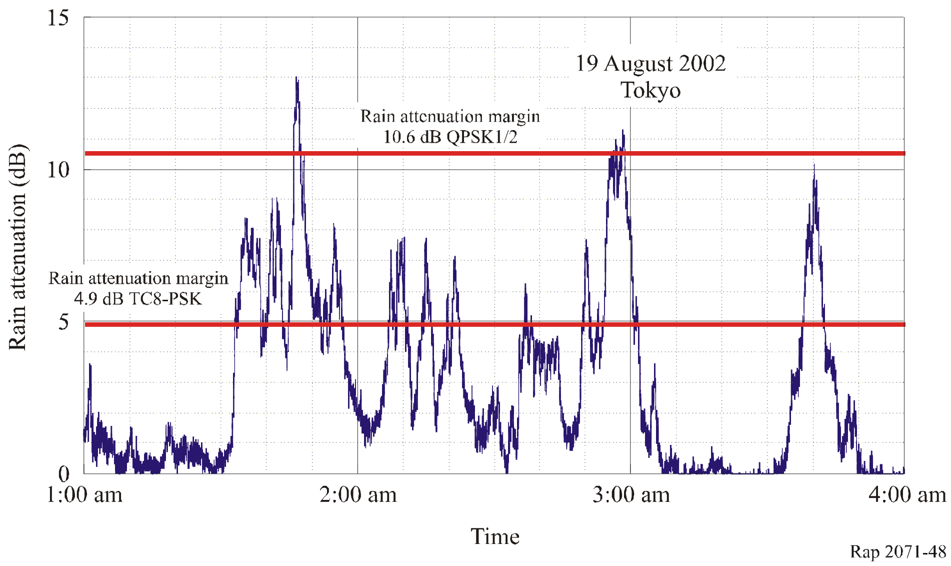

TABLE 27

Example of outage time for different modulation schemes

Modulation	TC8-PSK	QPSK1/2
Required *C*/*N*	10.7 dB	4.4 dB
Rain attenuation margin	4.9 dB	10.6 dB
Total outage time in an average year	526 min.	210 min.
Maximum outage duration	47 min.	26 min.
Duration of observation	From May 2000 to December 2002	
Interval of observation	1 s	

TABLE 28

Comparison of QPSK3/4, QPSK7/8 and TC8-PSK

Modulation	QPSK3/4	QPSK7/8	TC8-PSK
Required *C*/*N*	7.5 dB	9.5 dB	10.7 dB
Rain attenuation margin	7.7 dB	5.9 dB	4.9 dB
RS(*K*, *M*)	RS(200, 133)	RS(200, 114)	RS(200, 100)
MPEG packet rate	90 Mbit/s in the Nyquist bandwidth of 97.7 MHz		

TABLE 29

Parameters for comparison of PTD with TD and real-time transmission

Service	**Non-real-time**		**Real-time**
Transmission	PTD	TD	
Modulation	QPSK7/8, RS(200, 114)	TC8-PSK	QPSK1/2
Rain attenuation margin	5.9 dB	4.9 dB	10.6 dB
MPEG packet rate	90 Mbit/s in the Nyquist bandwidth of 97.7 MHz		

FIGURE 49

Comparison of modulations for PTD transmission scheme
(MPEG packet rate is 90 Mbit/s in the Nyquist bandwidth of 97.7 MHz.
Rain att. data for three years at Tokyo)

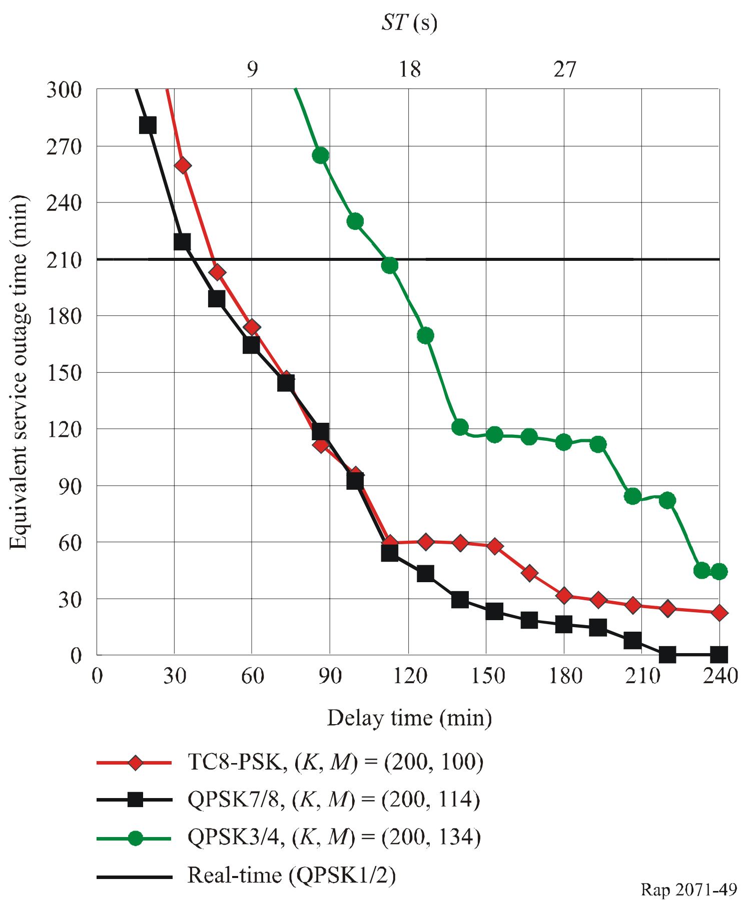

FIGURE 50

Comparison of PTD(QPSK7/8) (rain attenuation margin 5.9 dB) with TD(8-PSK) and real-time transmission (QPSK1/2) (MPEG packet rate is 90 Mbit/s in the Nyquist bandwidth of 97.7 MHz. Rain att. data for three years at Tokyo)

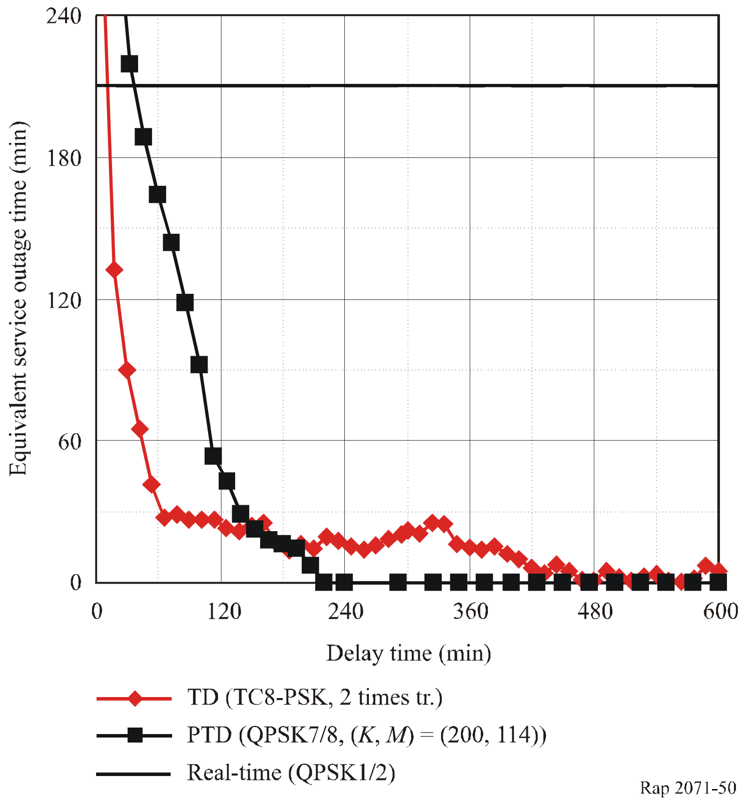

FIGURE 51

Comparison of PTD(QPSK7/8) (rain attenuation margin 9 dB) with TD(8-PSK) and real-time transmission (QPSK1/2) (MPEG packet rate is 90 Mbit/s in the Nyquist bandwidth of 97.7 MHz. Rain att. data for three years at Tokyo)

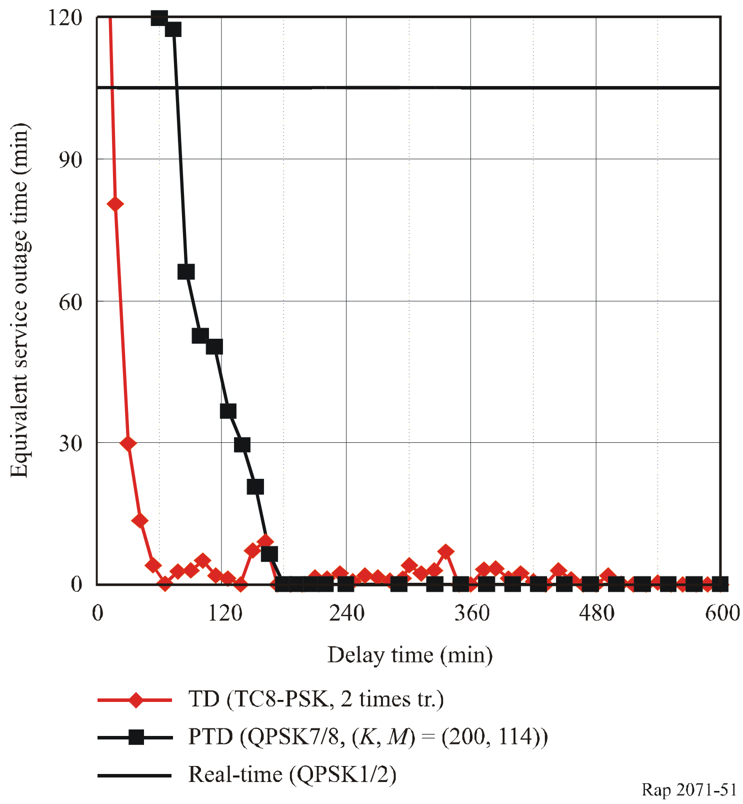

FIGURE 52

Comparison of PTD(QPSK7/8) (rain attenuation margin 3 dB) with TD(8-PSK) and real-time transmission (QPSK1/2) (MPEG packet rate is 90 Mbit/s in the Nyquist bandwidth of 97.7 MHz. Rain att. data for three years at Tokyo)

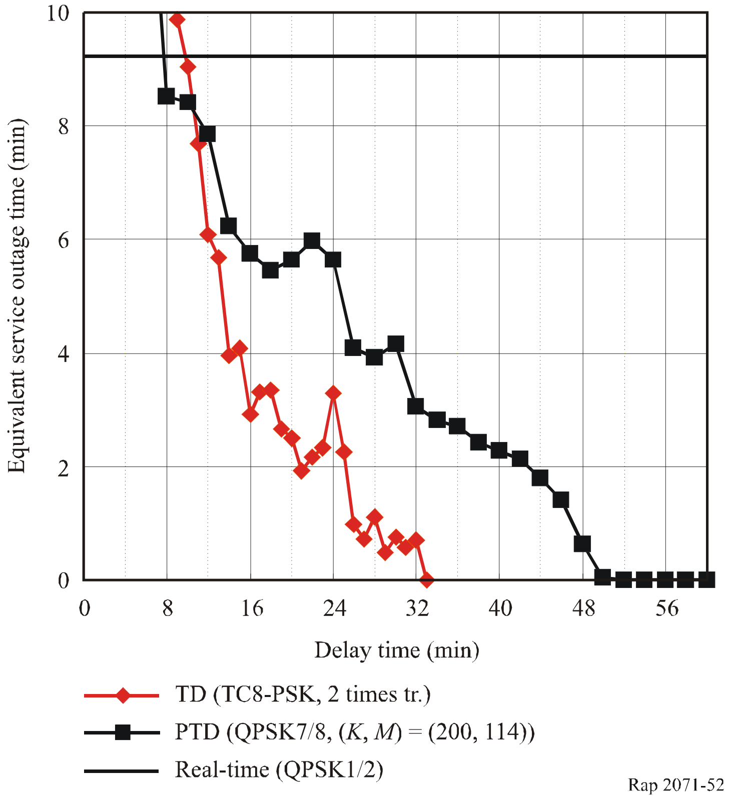

Appendix to § 7 of Annex 2

Dependence of interval time

The interval time (time difference between the start of the original data and the corresponding parity data entering into the TS multiplex block, see Fig. 47) may affect the mitigation effect. The interval time can be analytically increased or decreased. Fig. 53 shows the equivalent service outage time with respect to the interval time for QPSK7/8, of which parameters are same as in Table 28. In this case the *ST* is 18 s and the reference interval time is T (= X + Y = 1 h). For decreasing the interval time a delay circuit is inserted before the input port of the original data at the TS multiplex block and for increasing the interval time a delay circuit is inserted before the input port of the parity data. The zero interval time in Fig. 50 indicates that the original data is delayed by T at the input port of the TS multiplex block in Fig. 45, that is, the original data and the corresponding parity data enter into the TS multiplex block at the same time.

It can be seen from Fig. 53 that the interval time significantly affects only when it is below 1 h and the PTD transmission scheme with the interval time T is good from the viewpoints of the delay time and the equivalent outage time.

FIGURE 53

Relation between the interval time and the equivalent service outage time for QPSK7/8 in PTD transmission scheme (MPEG packet rate is 90 Mbit/s in the Nyquist bandwidth of 97.7 MHz. Rain att. data for three years at Tokyo)